2011

RESISTANCE FACTORS FOR ECCENTRICALLY BRACED STEEL FRAMES PROPORTIONED USING CAPACITY DESIGN

Jaya Prakash Vemuri

RESISTANCE FACTORS FOR ECCENTRICALLY BRACED STEEL FRAMES PROPORTIONED USING CAPACITY DESIGN

(Spine Title: Resistance Factors for Eccentrically Braced Steel Frames)

(Thesis format: Monograph)

by

Jaya Prakash Vemuri

Graduate Program in Engineering Science
Department of Civil and Environmental Engineering

A thesis submitted in partial fulfillment
of the requirements for the degree of
Master of Engineering Science

The School of Graduate and Postdoctoral Studies
The University of Western Ontario
London, Ontario, Canada

July 2011

THE UNIVERSITY OF WESTERN ONTARIO
School of Graduate and Postdoctoral Studies

CERTIFICATE OF EXAMINATION

Supervisor	Examiners
Dr. F. Michael Bartlett	Dr. Maged Youssef
	Dr.Wenxing Zhou
	Dr.Robert Klassen

The thesis by

Jaya Prakash Vemuri

titled

Resistance Factors for Eccentrically Braced Steel Frames Proportioned using Capacity Design

is accepted in partial fulfilment of the
requirements for the degree of

Master of Engineering Science

Date_____

_____
Chair of the Thesis Examination Board

ABSTRACT

Components proportioned using Capacity-Based Design have resistances that exceed the forces that can be generated by adjacent elements, particularly ductile elements in seismic-load-resisting systems. This thesis investigates the reliability indices for compression braces in Eccentrically Braced Frames (EBF) proportioned using Capacity-Based Design. The primary research objectives are: (1) to develop statistical models for link overstrength due to strain hardening and probable yield strengths; (2) to examine, using these models, the reliability indices obtained using the current Capacity-Based Design provisions for EBFs in CSA S16-09 (CSA, 2009); and (3) to calibrate the resistance factor for a proposed new overstrength model to replace the link overstrength criteria in CSA S16-09. The statistical models for link overstrength account for the effect of the normalized link length, the plastic link rotation, the ratio of ultimate to yield strength and the normalized web stiffener spacing and are determined using a database of 77 EBF tests performed by others.

The statistical model for higher-than-nominal yield strength is determined using a database of 7717 tests of coupons from Class 1 sections presented by Schmidt (2000). Reliability indices, β, are computed using the First Order Second Moment (FOSM) method. The reliability indices for the current code provisions vary from 1.30 to values above 5.0 for typical ranges of link parameters. A new design equation is proposed that provides much more uniform reliability. Compression braces designed using the proposed design equation require the resistance factor ϕ be decreased to 0.75 from the current value of 0.9 to achieve acceptable reliability levels.

Keywords: resistance factor, Capacity-Based Design, link length, over strength, eccentrically braced frame, calibration, first order second moment method

ACKNOWLEDGEMENTS

I sincerely thank my advisor, Dr. Michael Bartlett for his guidance, supervision and great patience during the course of this research. He has helped me in developing the skills of critical thinking and scholarly writing. However this thesis was submitted for oral examination without Dr. Bartlett's approval. While I have been grateful that Dr. Bartlett has reviewed the thesis after the successful oral defense, he should not be held accountable for any errors that it may contain.

I am also grateful for the financial support provided by the Canadian Institute of Steel Construction (CISC) for my graduate studies.

My parents encouraged me to go to graduate school and I thank them for their love, support and advice through this period.

I acknowledge the support from my friends at Western- especially Dr.Prabhakar Sharma, Dr.Manoj Tripathi, Dr.Luis Orta, Kshitij Kumar Singh, Rajeev Nagotra, Anil Jhawar, Gaurav Goel, Chaitan Sandhu and Saeed Ahmed: they made my stay at Western very enjoyable.

TABLE OF CONTENTS

PAGE

Certificate of Examination ii
Abstract and Keywords iii
Acknowledgements iv
Table of Contents v
List of Tables vii
List of Figures viii
List of Notations ix

Chapter 1: Introduction 1
1.1: Background 1
1.2: Capacity-Based Design 2
1.3: Eccentrically Braced Frame 3
1.4: Research Objectives and Scope 5
1.5: Thesis Outline 6

Chapter 2: Literature Review 8
2.1: Introduction 8
2.2: Undesired Collapse Mechanisms 9
2.3: Statics of an EBF 12
2.4: Kinematics of an EBF 15
2.4.1: Effect of Frame Geometry 17
2.5: Link Behaviour 17
2.5.1: Link Beam 22
2.6: EBF Design in CSA S16-09 23
2.7: Overstrength in Links 24
2.7.1: Strain Hardening 25
2.7.2: Higher-than-Specified-Minimum Yield Strengths 28
2.7.3: Other Factors 29
2.8: Summary 30

Chapter 3: Statistical Parameters for Demand 32
3.1: Introduction 32
3.2: Experimental Data on Overstrength due to Strain Hardening 33
3.2.1: Link Rotation Capacity and Loading Protocol 35
3.2.2: Link Failure Modes 38
3.3: Overstrength due to Strain Hardening 39
3.3.1: Identification of Key Parameters 39
3.3.2: Regression Analysis 46
3.3.3: Residual Analysis 50
3.3.4: Coefficient of Variation of R_{str} for Reliability Analysis 51

3.4 Overstrength due to Higher Yield Strengths 51
3.4.1 Plots of R_y versus Various Parameters 54
3.5: Summary 56

Chapter 4: Reliability Analysis and Calibration of Resistance Factor 59
4.1: Introduction 59
4.1.1: Objectives 61
4.2: Statistical Parameters for Demand 61
4.2.1: Overstrength due to Strain Hardening 62
4.2.2: Summary of Statistical Parameters for Demand 64
4.3: Statistical Parameters for Resistance 66
4.3.1: Resistance Statistical Parameters using CSA S16-09 68
4.3.2: Resistance Statistical Parameters using Proposed Design Equation 68
4.3.3: Summary of Statistical Parameters for Resistance 70
4.4: Example Calculation of EBF Reliability Indices 70
4.5: Reliability of W-shape Braces 74
4.5.1: Reliability Indices for CSA S16-09 75
4.5.2: Reliability Indices using the Proposed Design Equation 78
4.6: Low Values of Reliability Index 84
4.7: Summary 84

Chapter 5: Summary and Conclusions 86
5.1: Summary 86
5.2: Conclusions 88
5.3: Future Research 89

References 91

Appendix A-1 Experimental Link Data to Model Strain Hardening 97
Appendix A-2 AISC Link data from Richards (2006) 99
Appendix A-3 Geometric data of test specimens 101
Appendix A-4 Graphs for Stiffener Spacing 103
Appendix A-5 Reliability Indices versus λ 104

Curriculum Vitae 105

LIST OF TABLES

PAGE

Table 2.1 Comparison of overstrength factors for EBF in various codes 24

Table 3.1 W-shape link data tabulated by Richards (2002) 34
Table 3.2 Results from the regression analysis for the generic model..... 47
Table 3.3 Results from the regression analysis for the proposed design equation 48
Table 3.3 Tensile properties for various grades of structural steel (Dexter et al. 2002) .. 53
Table 3.4 Classification of coupon data 54

Table 4.1 Statistical parameters for demand 65
Table 4.2 Statistical parameters for brace resistance 69

LIST OF FIGURES

PAGE

Figure 1.1 Members in a K-braced EBF. 4

Figure 2.1 Block diagram for Capacity-Based Design of EBF compression braces 8
Figure 2.2 Type A mechanisms and Type B mechanisms in an EBF 10
Figure 2.3 Possible collapse mechanisms in a 5-storey EBF 11
Figure 2.4 Undesirable collapse mechanisms due to yielding of non-fuse elements 12
Figure 2.5 Statics of an EBF a) Shear force in a link b) Free body diagram....13
Figure 2.6 Rigid-plastic mechanism in a K-braced frame 16
Figure 2.7 Moment, shear and axial force diagrams: a) Link b) Link beam and c) Brace 21
Figure 2.8 Hysteric loops for link 26
Figure 2.9 Overstrength in links 27
Figure 2.10 Hysteric behaviour of a) Un-stiffened and b) Stiffened link....30

Figure 3.1 (a) Obtaining backbone curve and (b) Computing inelastic rotation capacity 36
Figure 3.2 Shear capacity of link versus link rotation (modified from Richards, 2006) ..36
Figure 3.3 Design inelastic rotation capacity, γ_p, as per CSA S16-09 37
Figure 3.4 Plot showing a variation of link overstrength with link length 39
Figure 3.5 Overstrength versus plastic link rotation....40
Figure 3.6 Overstrength versus section depth, d 41
Figure 3.7 Overstrength versus stiffener spacing, a/a_o 42
Figure 3.8 $(M_p/ V_p d)$ versus d/b ratio 43
Figure 3.9 Peak link rotation versus normalized link length 44
Figure 3.10 Plastic link rotation versus normalized link length 44
Figure 3.11 Ratio of γ_{ult}/γ_p versus normalized link length 45
Figure 3.12 Fit between tests and predicted results (Equation [3.3]) 47
Figure 3.13 Fit between predicted and actual overstrength values (Equation [3.4]) 49
Figure 3.14 Residuals of Equation [3.3] versus $e/(M_p/V_p)$ and γ_{ult} 50
Figure 3.15 Residuals of Equation [3.4] versus F_u/F_y and link rotation, γ_p 51
Figure 3.16 R_y versus mass of W-shape (kg/m) 55

Figure 4.1 Example Eccentrically Braced Frame 71
Figure 4.2 S16-09 Design Method: Variation of reliability index with F_u/F_y 76
Figure 4.3 S16-09 Design Method: Variation of reliability index with link length 77
Figure 4.4 S16-09 Design Method: Variation in reliability index with peak rotation....78
Figure 4.5 Proposed Design Method: Variation of the reliability index with F_u/F_y 80
Figure 4.6 Proposed Design Method: Variation of the reliability index with link length 81
Figure 4.7 Proposed Design Method: Variation of the CoV with the link length....81
Figure 4.8 Variation in reliability index with stiffener spacing....82
Figure 4.9 Variation in reliability index with plastic link rotation 83

LIST OF NOTATIONS

a	stiffener spacing or length of link beam
a_o	stiffener spacing normalizing constant = 25.4 centimetres
a_1	length of the link beam on the left side of an unsymmetric frame
a_2	length of the link beam on the right side of an unsymmetric frame
A	gross area of the link
b	flange width
C_λ	factor accounting for reduced strength of a slender column
CoV	coefficient of variation
d	overall depth of the cross section
D	discretization factor
e	link length
E	Young's modulus of steel
F_u	ultimate tensile strength of steel
F_y	specified minimum steel yield strength
$\frac{F_u}{F_y}$	ratio of ultimate strength to yield strength of steel
$\overline{\frac{F_u}{F_y}}$	mean value of the ratio of ultimate strength to yield strength of steel
F_{ya}	actual yield strength
F_{yn}	nominal yield strength
G	geometric factor
h	height of storey

h_1	column height (left-side) of an unsymmetric frame
h_2	column height(right-side) of an unsymmetric frame
K	geometric factor that converts link shear to brace axial force
k	effective length factor
L	span length, length of compression member
L_{br}	brace member length
m	mass(kg/m) of the W-shape
m_R	mean value of resistance
$m_{R_{min}}$	mean value of demand
m_S	mean value of total load effect
M	material factor, bending moment
M_b	moment transferred to the link beam
M_{br}	moment transferred to the brace
M_e	total moment at the end of the link
M_p	plastic moment capacity
$M_p{}'$	Plastic moment capacity accounting for presence of axial force
n	number of specimens tested, fitting parameter in column strength equation
p	p-value, probability of observed outcome occurring by chance
P	professional factor
P_b	axial force in the link beam
P_{br}	axial force in brace (tensile or compressive)
P_{bru}	axial forces in brace immediately above the current storey
P_c	axial force in column

P_{cu}	axial forces in column immediately above the current storey
P_f	axial force in link (tensile or compressive)
r	radius of gyration
R^2	coefficient of determination
R_d	design resistance
R_{min}	expected capacity of fuse element
$\overline{R_{min}}$	mean value of the expected capacity of fuse element
R_n	nominal resistance
R_{str}	overstrength due to strain hardening
$\overline{R_{str}}$	mean value of overstrength due to strain hardening
R_y	overstrength due to higher yield strength
$\overline{R_y}$	mean value of overstrength due to higher yield strength
S_i	nominal load effect for applied load type *i*
t	flange thickness
V	maximum value of link shear
V_c	factored horizontal storey shear force
V_b	shear force in link beam
V_f	shear force in link
V_m	link resistance
V_p	plastic shear capacity
V_p'	plastic shear capacity accounting for presence of axial force
V_{ult}	ultimate shear force in link

V_y	yield shear force of link
w	web width
w_c	coupon thickness
Z_w	indicator variable, equal to 1 if test coupon obtained from the web or 0 if obtained from the flange.

GREEK SYMBOLS

α	angle between brace and beam
α_i	load factor for applied load type *i*
β	reliability index
γ	link rotation
γ_p	plastic link rotation
γ_{ult}	peak link rotation
$\widehat{\gamma_{ult}}$	predicted value of peak link rotation
ν_A	coefficient of variation of area of section
ν_d	coefficient of variation of section depth
ν_D	coefficient of variation of discretization
ν_P	coefficient of variation of professional factor
ν_M	coefficient of variation of material factor
$\nu_{R_{min}}$	coefficient of variation of demand
$\nu_{R_{str}}$	coefficient of variation of overstrength due to strain hardening
ν_{R_y}	coefficient of variation of overstrength due to higher yield strength
ν_w	coefficient of variation of section width

ν_R	coefficient of variation of resistance
υ_S	coefficient of variation of the total load effect
δ	bias coefficient, frame drift
δ_1	vertical link beam deflection at left end of the link
δ_2	vertical link beam deflection at right end of the link
δ_A	bias coefficient of area of section
δ_d	bias coefficient of section depth
δ_D	bias coefficient of discretization factor
δ_P	bias coefficient of professional factor
δ_M	bias coefficient of material factor
ε	regression model error
θ	link rotation angle
θ_1	rigid-body rotation of left side of the unsymmetric frame
θ_2	rigid-body rotation of right side of the unsymmetric frame
λ	slenderness parameter
ν	coefficient of variation
${\sigma_{\gamma_{ult}}}^2$	variance of the peak link rotation values
${\sigma_{\frac{F_u}{F_y}}}^2$	variance of the $\frac{F_u}{F_y}$ values for A992 steel
${\sigma_\varepsilon}^2$	mean square error of the linear regression fit
ϕ	resistance factor

CHAPTER 1: INTRODUCTION

1.1 BACKGROUND

Components or connections proportioned using "Capacity Design" principles are designed to be stronger than the member to which they are connected. Capacity-Based Design to resist seismic loads in accordance with Clause 27 of CSA S16-09 (CSA, 2009) requires the designer to identify "specific elements or mechanisms designed to dissipate energy" and to ensure "all other elements are sufficiently strong for this energy dissipation to be achieved" (Bartlett, 2007). CSA S16-09 specifies expected, not guaranteed minimum, material properties and strain-hardening factors on the demand side, and minimum specified material properties and the normal resistance or phi (ϕ) factors on the resistance side. In other words, these non-fuse elements, including connections, are proportioned using minimum specified yield strengths and conventional resistance factors to be stronger than the energy-dissipating elements, accounting for the probable yield strength and strain hardening of the energy-dissipating elements.

Hence, for capacity-based design, the limit states design equation is not the conventional equation:

$$\phi R \geq \Sigma \alpha_i S_i \qquad [1.1]$$

where ϕ is the resistance factor, R is the nominal resistance, and α_i is the load factor and S_i is the nominal load effect for applied load type i, respectively. Instead it is:

$$\phi R \geq R_{min} \qquad [1.2]$$

where R_{min} represents the minimum acceptable resistance as defined by the expected capacity of the elements intended by the designer to dissipate energy. The impact of the different right hand sides in Equations [1.1] and [1.2] has not been considered from a reliability perspective, and hence, adopting the existing methodology "may result in needlessly uneconomical designs… ...In some cases, the current approach can also lead to design requirements that are very difficult, and sometimes impossible to satisfy." (Engelhardt, 2006)

Generally loads, be they live, wind, snow or earthquake loads (e.g., Bartlett et al., 2003) are much more variable than resistances (e.g., Schmidt and Bartlett, 2002a; 2002b), so it may be possible to use larger resistance factors to reduce the perceived conservatism of Capacity-Based Design.

Thus, these Capacity-Based Design requirements must be re-evaluated using a reliability based approach, preferably using the First Order Second Moment (FOSM) based approach (Schmidt and Bartlett, 2002b), which is the basis of the load and resistance factors in CSA S16-09 (CSA, 2009) and the AISC 341-05 (AISC, 2005).

1.2 CAPACITY-BASED DESIGN

The Capacity-Based Design method was developed in the late 1960s in New Zealand (El Damatty, 2006). The method enables the designer to identify fuse elements where the inelastic response should occur, since inelastic action is recognized to be unavoidable in severe earthquakes. In other words, "Capacity-Based" methods have been developed to ensure that the members or connections attached to these fuses do not fail prematurely

(e.g. by yielding, local buckling or member instability) and so ensure that the desired energy dissipation occurs at the fuses. Examples of fuses in steel structures are:

a) plastic hinges in Moment-Resisting Frames;

b) diagonals in Concentrically Braced Frames; and,

c) links in Eccentrically Braced Frames.

These energy-dissipating elements allow only limited forces to be transferred to the connecting members, which are designed to have greater capacities than the maximum force effect transferred from the fuse. It has been proven in many strong earthquakes in the past that structures behave satisfactorily and possesses adequate seismic resistance when designed by the Capacity-Based Design method (Wangsadinata, 1999). Most seismic codes around the world adopt the Capacity-Based Design concept as a normative requirement (Wangsadinata, 1999).

1.3 ECCENTRICALLY BRACED FRAMES

The Seismic Load Resisting System chosen for the current research is the Eccentrically Braced Frame (EBF), a lateral-load-resisting system which combines high stiffness with ductility and energy-dissipation capacity (Engelhardt and Popov, 1987). The EBF was first introduced in 1970s and has been extensively adopted in construction. Figure 1.1 shows the key members of a K-braced EBF: the link, which is the fuse element; and the link beam, the brace and the column, which are the non-fuse elements. The mechanics and kinematics of EBFs are well established (e.g., Engelhardt and Popov, 1989).

Links are typically Class-1 W-shapes and are designed to respond inelastically during the seismic event. Typically, the link strain hardens and reaches its ultimate shear (or flexural) capacity, which is higher than the nominal plastic shear (or flexural) capacity based on the nominal (or even actual) yield strength. The non-fuse elements are intended to behave elastically during a seismic event and so are proportioned using Capacity-Based Design for the maximum capacity of the link. However, they could fail by premature yielding in cases where the links have unusually high reserve strengths. A statistical model is therefore needed to predict the link overstrength with reasonable accuracy. Once such a model is available, it can be used to calibrate the resistance factor, currently 0.9 for non-fuse elements in Eccentrically Braced Frames proportioned by Capacity-Based Design.

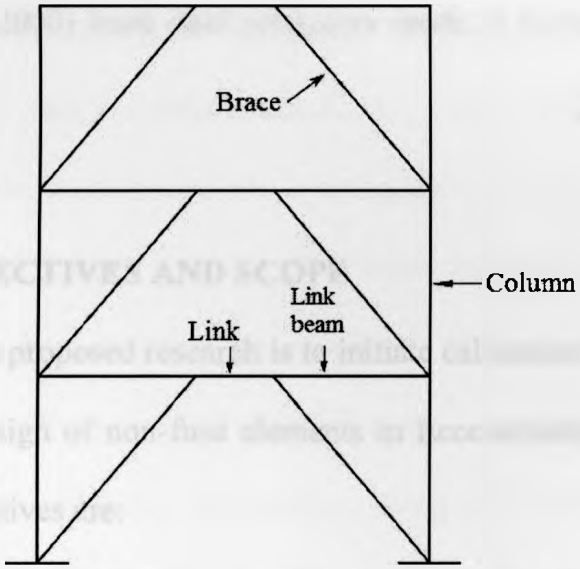

Fig.1.1: Members in a K-braced EBF

In 1980, Popov stated that "the shear links played the key role in maintaining the integrity of the frame and their capacity in the inelastic stage must be carefully

determined and implemented in design". Since then, several researchers have conducted experimental and analytical studies to determine the capacity of links. The current Canadian code (CSA, 2009) specifies an overstrength factor of 1.3 to account for strain hardening of the link. However, experimental tests on links have demonstrated markedly different link overstrengths. Several short links have failed at very high overstrength values while some long links have failed at overstrength factors that are much lower than 1.3. Leslie et al. (2009) have also suggested that the use of a single overstrength factor cannot predict member yielding with uniform probability in all cases. Hence there is a clear need to develop an approach for overstrength assessment for W-shape links.

Similarly, the actual yield strength of steel has a high likelihood of exceeding the specified minimum yield strength and so also affects overstrength of links. CSA S16-09 (CSA, 2009) specifies a factor of 1.1 to account for this. Steel coupon data previously collected by Schmidt (2000) from steel producers needs to be re-analyzed to assess the accuracy of this value.

1.4 RESEARCH OBJECTIVES AND SCOPE

The objective of the proposed research is to initiate calibration of the resistance factor for Capacity-Based Design of non-fuse elements in Eccentrically Braced Steel Frames. The specific main objectives are:

a) Propose statistical models for link overstrength and higher-than-nominal yield strengths.

b) Using these models, examine the reliability indices obtained using the current Capacity-Based Design provisions for Eccentrically Braced Frames in CSA S16-09.

c) Determine a target value of reliability index β and conduct a sensitivity analysis to observe the variation of the reliability index with various parameters.

d) Calibrate the resistance factor as may be necessary and propose suitable recommendations for design.

1.5 THESIS OUTLINE

Chapter 2 presents a literature review of the behaviour of EBFs and discusses the reasons for the uncertainty of link overstrengths.

Chapter 3 derives the statistical parameters for demand created by ductile link elements. Experimental data on links obtained from the literature are analysed. The factors contributing to the overstrength are investigated and two models are proposed to compute the overstrength factors resulting from strain hardening of the link. Similarly, using the steel coupon data available from Schmidt (2000), a model is proposed for overstrength due to higher-than-nominal yield strengths.

Chapter 4 derives the reliability formulation, using the First-Order-Second-Moment based approach, which is the basis of the load and resistance factors in S16-09 (CSA, 2009) and the AISC Seismic Provisions for Structural Steel Buildings (AISC, 2005). Statistical parameters for the demand created by the ductile link elements are derived and tabulated. Two sets of statistical parameters for resistances are derived for: a) resistances

computed using the CSA S16-09 procedure and b) resistances computed using the Proposed Design Equation in Chapter 3. Reliability indices, β, are computed for various values of the resistance factor, ϕ, and plotted against key parameters. A sensitivity analysis is carried out and the resistance factor is re-calibrated.

Chapter 5 presents the summary and conclusions of the study.

CHAPTER 2: LITERATURE REVIEW

2.1 INTRODUCTION

In this chapter, a detailed literature review of the various factors affecting the Capacity-Based Design of Eccentrically Braced Frame (EBF) compression brace elements is presented. Figure 2.1 shows the key concepts involved in this review. Literature pertaining to each rectangle shown in the figure is summarized in various sub-sections of this chapter.

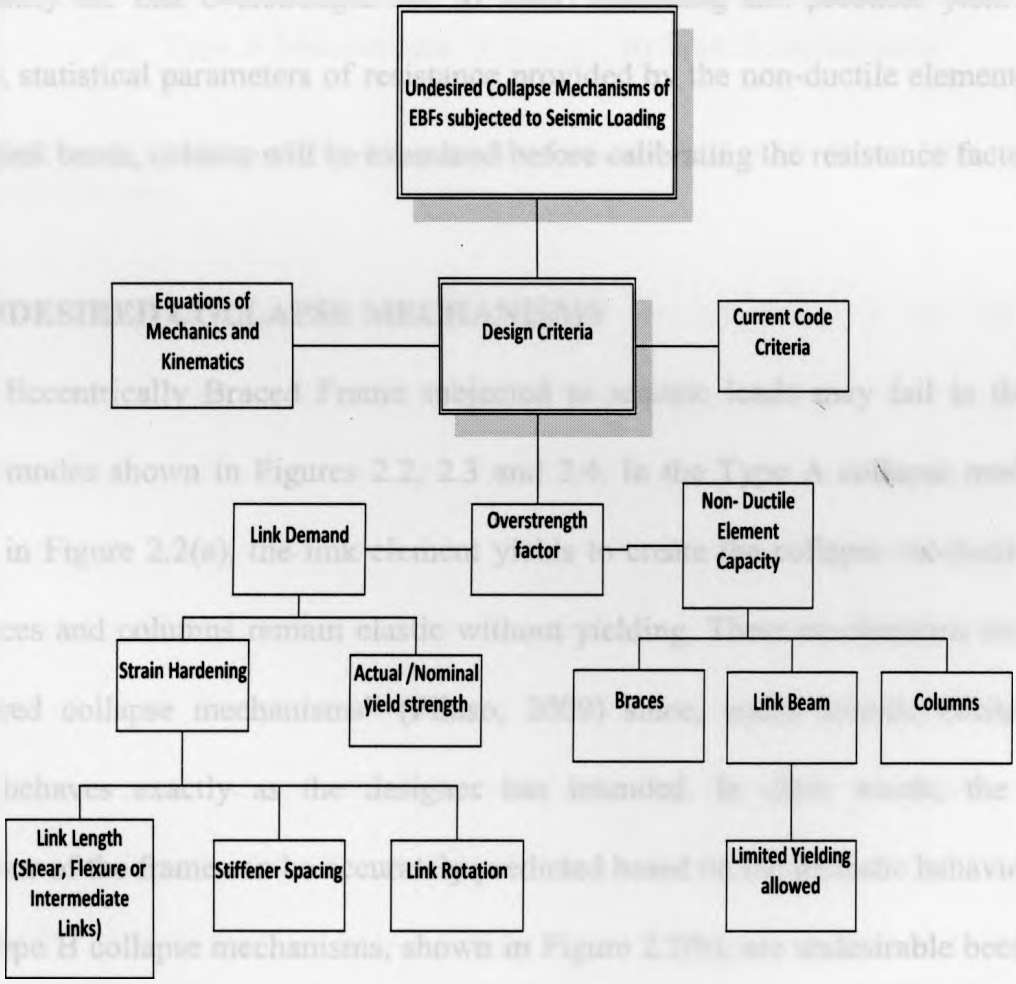

Fig. 2.1: Block diagram for Capacity-Based Design of EBF compression braces elements

The block diagram in Figure 2.1 indicates that undesired collapse mechanisms of EBFs can be avoided by using appropriate design criteria. To understand the current design criteria for EBFs in CSA S16-09 (CSA, 2009), it is essential to establish the equations of mechanics and kinematics of Eccentrically Braced Frames (EBFs). Using these equations, forces in the ductile link elements and other non-ductile members can be computed.

The overstrength factor prescribed in the CSA S16-09 for EBFs is based on the maximum expected capacity of the link. A review of the available literature is essential to quantify the link overstrength due to strain hardening and probable yield strength. Finally, statistical parameters of resistance provided by the non-ductile elements, i.e. the brace, link beam, column will be examined before calibrating the resistance factors.

2.2 UNDESIRED COLLAPSE MECHANISMS

An Eccentrically Braced Frame subjected to seismic loads may fail in the typical failure modes shown in Figures 2.2, 2.3 and 2.4. In the Type A collapse mechanisms, shown in Figure 2.2(a), the link element yields to create the collapse mechanism while the braces and columns remain elastic without yielding. These mechanisms are deemed "preferred collapse mechanisms" (Piluso, 2009) since, under seismic excitation, the frame behaves exactly as the designer has intended. In other words, the inelastic behaviour of the frame can be accurately predicted based on the inelastic behaviour of the link. Type B collapse mechanisms, shown in Figure 2.2(b), are undesirable because they involve yielding of the brace and link beam and, since these elements are typically not specifically designed and detailed to dissipate energy, a premature failure occurs.

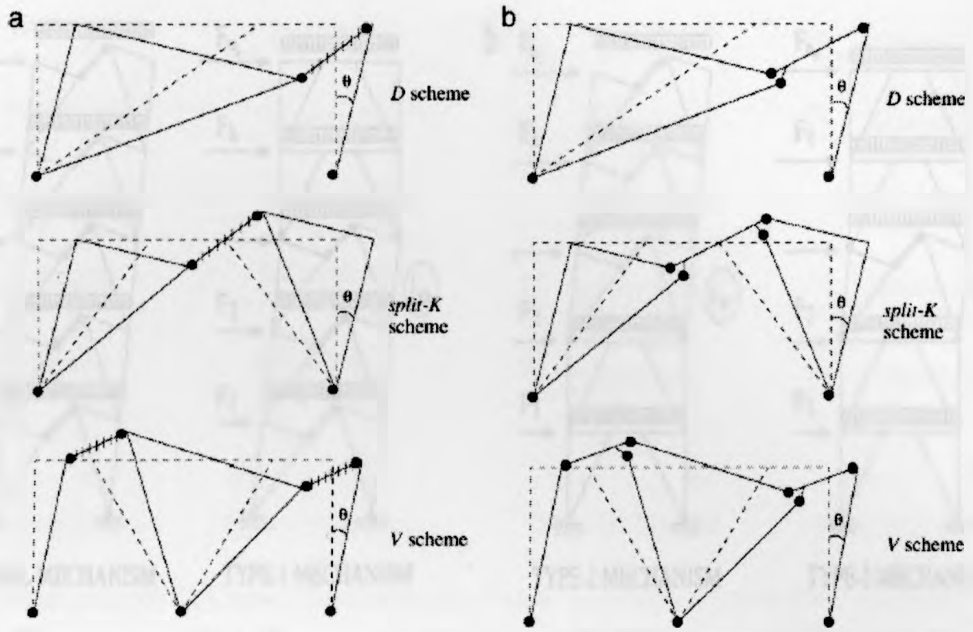

a) Type A Mechanisms b) Type B mechanisms

Fig. 2.2: Type A Mechanisms and Type B mechanisms in an EBF (From Piluso, 2009 used by permission)

Figure 2.3(a) shows various possible collapse mechanisms in a five-storey frame where the link in each storey yields and the base sections of first storey columns also yield. The Type-1 mechanism, and the Type-2 and Type-3 mechanisms shown in Figure 2.3(b), although deemed "allowable" by Piluso (2009), are not preferred because they involve yielding of the link beam or the columns above grade and so dissipate less energy at the link elements. The global mechanism, a particular combination of the Type 1 and 2 mechanisms, is preferred because all the links yield and the energy dissipated is greatest. However, the Type-1, Type-2 and Type-3 mechanisms are allowed by CSA S16-09 (CSA, 2009) since limited link beam yielding can be resisted by the frame. In some cases limited link beam yielding is beneficial (Jain et al., 1996). For example, in flexural links, limited yielding of the link beam contributes to the energy dissipation capacity while still retaining its load carrying capacity (Engelhardt et al., 1992).

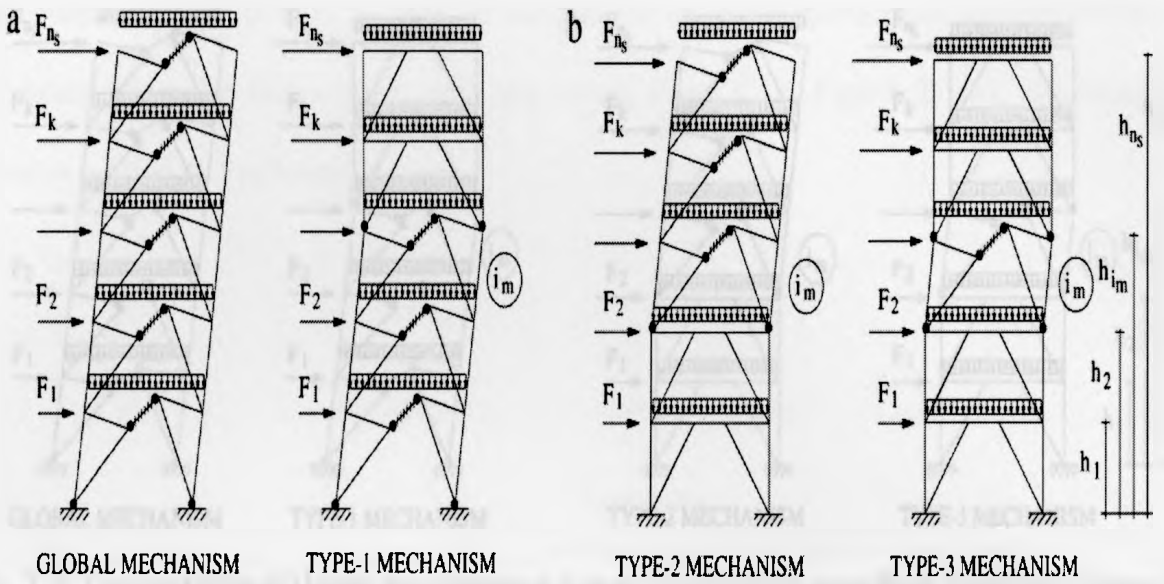

(a) Columns yield at foundation (b) Columns yield above foundation

Fig. 2.3: Possible collapse mechanisms in a 5-storey EBF (From Piluso, 2009, used by permission)

Undesired collapse mechanisms identified by Piluso (2009) are shown in Figure 2.4. In each case, the brace, link beam or column yields before the link yields. Clearly, these failure modes violate Capacity-Based Design principles and must be avoided. They may lead to "increased risk of failure under destructive ground motions" (Piluso, 2009) because the link beams and columns are not designed to dissipate energy through plastic deformations.

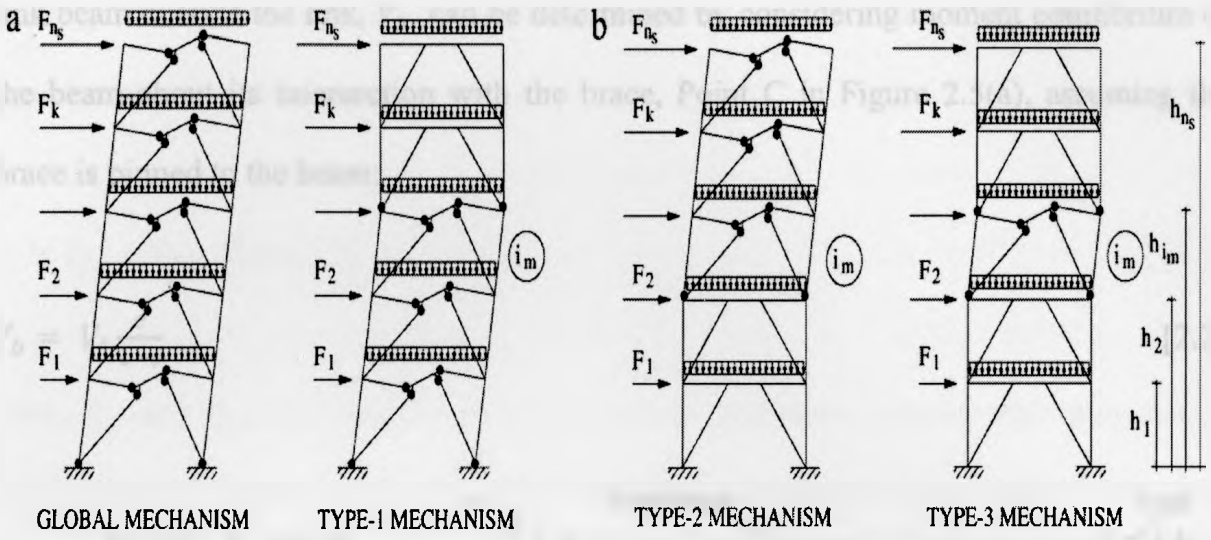

Fig. 2.4: Undesirable collapse mechanisms due to yielding of non-fuse elements (From Piluso, 2009, used by permission)

2.3 STATICS OF AN ECCENTRICALLY BRACED FRAME

Figure 2.5 shows the free body diagram necessary to derive the link shear in an EBF due to seismic forces. Brace members are subjected to mostly axial forces and hence are assumed to be pin-connected at both ends. The link beam can also be assumed to be pin-joined to the columns if it is "continuous over the braces" (Charleson, 2008). Hence, Equations [2.1] to [2.6] are derived (e.g., Han, 1998) as simple applications of force and moment equilibrium of a plane frame.

Moment equilibrium about Point A requires the shear force in the link to be:

$$V_f = \frac{h}{L} V_c \qquad [2.1]$$

where V_c is the factored horizontal storey shear force due to seismic loads, h is the storey height and L is the frame span length as shown in Figure 2.5(a). The shear force in the

link beam outside the link, V_b, can be determined by considering moment equilibrium of the beam about its intersection with the brace, Point C in Figure 2.5(a), assuming the brace is pinned to the beam:

$$V_b = V_f \frac{e}{L-e} \quad [2.2]$$

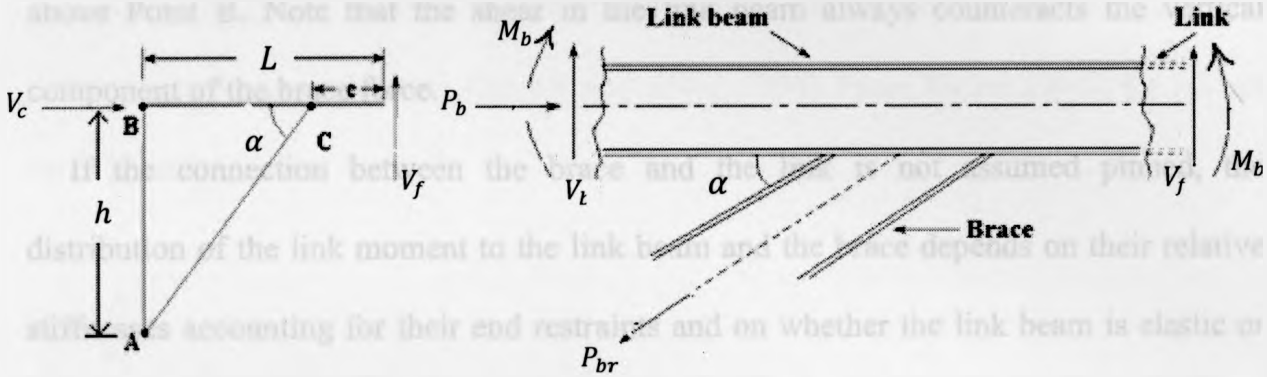

(a) (b)

Fig. 2.5: Statics of an EBF (a) Shear force in link (b) Forces at link-brace-link beam joint

The axial force in the brace, P_{br}, is obtained considering vertical force equilibrium at Point C in Figure 2.5(a):

$$P_{br} = \frac{V_b + V_f}{\sin \alpha} \quad [2.3]$$

where α is angle between the brace and the link beam as shown. The axial force in the link beam, P_b, can be computed considering horizontal force equilibrium of Point C:

$$P_b = P_{br} cos\ \alpha = V_c \quad [2.4]$$

Finally, the axial force in Column A-B, P_c, is computed considering vertical force equilibrium at Point B:

$$P_c = P_{cu} - P_{bru} \sin \alpha + V_b \quad [2.5]$$

Here, P_{cu} and P_{bru} are axial forces in the column and brace, respectively, immediately above Point B. Note that the shear in the link beam always counteracts the vertical component of the brace force.

If the connection between the brace and the link is not assumed pinned, the distribution of the link moment to the link beam and the brace depends on their relative stiffnesses accounting for their end restraints and on whether the link beam is elastic or plastic at its connection with the brace and link. The link end moment not carried by the link-beam must be resisted by the brace:

$$M_{br} = M_e - M_b \quad [2.6]$$

where $M_e = V_f.e$ is the total moment at the end of the link and M_{br} and M_b are the moments transferred in the brace and the link-beam, respectively. The brace is designed to resist the combined effects of P_{br} and M_{br} and may be a Class 1 or 2 W-shape. Engelhardt (1986) used further assumptions to propose simplified equations for EBF member design.

2.4 KINEMATICS OF AN ECCENTRICALLY BRACED FRAME

CSA S16-09 (CSA, 2009) requires the inelastic link rotation be limited to ensure the rotation capacity of the ductile link is not exceeded. This requirement also limits the ductility demand on the frame. Figures 2.6(a) and (b) show a rigid-plastic sway mechanism in an unsymmetric K-braced frame. Assuming a rigid – perfectly plastic material response with rotations confined to the plastic hinges at each end of the link, the link rotation angle, θ, between link and the link beam can be determined from the lateral deflection and frame geometry (Becker and Ishler, 1996). From Figure 2.6(b), the overall sway geometry gives:

$$\theta_1 = \frac{\delta}{h_1} \qquad [2.7a]$$

$$\theta_2 = \frac{\delta}{h_2} \qquad [2.7b]$$

where δ is the design drift for the EBF, h_1 and h_2 are the respective column heights, and θ_1 and θ_2 are the rigid-body rotations of the left and right sides of the frame, respectively.

The vertical link beam deflections at the ends of the link are:

$$\delta_1 = \theta_1 a_1 \qquad [2.8a]$$

$$\delta_2 = \theta_2 a_2 \qquad [2.8b]$$

where a_1 and a_2 are the lengths of the respective link beams. From the deformed shape at the left end of the link:

$$\theta = \theta_1 + \frac{\delta_1}{e} + \frac{\delta_2}{e} \qquad [2.9]$$

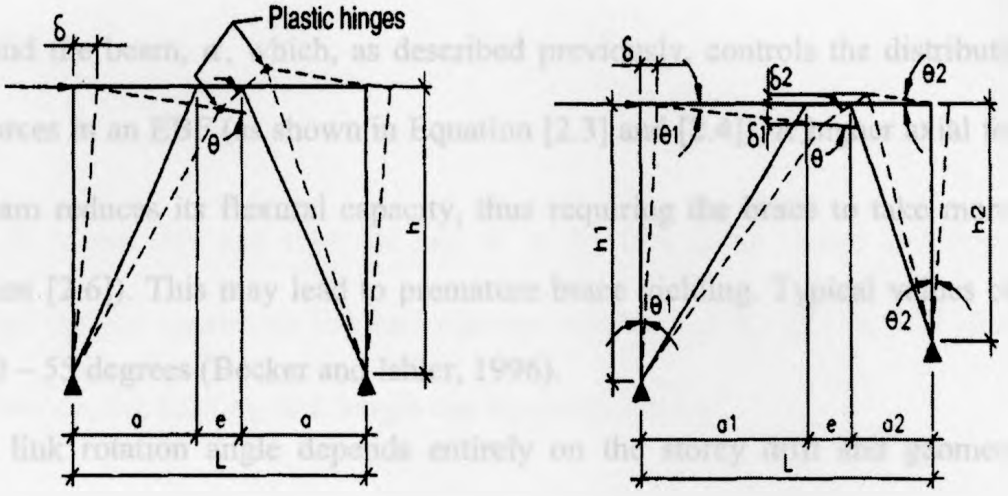

(a) Deformed shape; plastic hinges (b) the angles between the members

Fig 2.6: Rigid-plastic mechanism in a K-braced frame (From Becker and Ishler, 1996, used by permission).

Using [2.7a], [2.7b], [2.8a] and [2.8b] to eliminate δ_1 and δ_2 from [2.9]:

$$\theta = \theta_1 + \frac{\delta a_1}{h_1 e} + \frac{\delta a_2}{h_2 e} \qquad [2.10]$$

For a symmetric configuration, i.e. $a_1 = a_2 = a$ and $h_1 = h_2 = h$, Equation [2.10] reduces to

$$\theta = \frac{\delta}{h}\left(1 + \frac{2a}{e}\right) = \frac{\delta}{h}\left(\frac{e + 2a}{e}\right) = \frac{\delta}{h}\frac{L}{e} \qquad [2.11]$$

2.4.1 EFFECT OF FRAME GEOMETRY

The frame geometry is essentially dictated by three factors, the inter-storey height, h the link length, e and the span length, L. These three factors define the angle between the brace and the beam, α, which, as described previously, controls the distribution of the axial forces in an EBF (as shown in Equation [2.3] and [2.4]). A higher axial force in the link beam reduces its flexural capacity, thus requiring the brace to take more moment (Equation [2.6]). This may lead to premature brace yielding. Typical values of α range from 30 – 55 degrees (Becker and Ishler, 1996).

The link rotation angle depends entirely on the storey drift and geometry of the structure as shown in Equation [2.11]. Figures 2.2 to 2.4 show the kinematically admissible collapse mechanisms. From Equation [2.11] it can be inferred that the link rotation angle, θ is inversely related to the link length, e. Short links, with smaller normalized link lengths, e/L, undergo large rotations and thereby exhibit greater overstrength due to strain hardening, compared to long links. Typically, while the height and span of the frame is decided by practical considerations, the designer can choose a suitable link length, e, to control the link rotation angle. For example, as the span L increases, the length of the link beam, a also increases. For a given frame height, h and frame drift, δ, a longer link length e may be selected to limit the link rotation angle, θ.

2.5 LINK BEHAVIOUR

Links can be sub-classified as shear-yielding or flexural-yielding, based on the normalized link length, $e/(M_p/V_p)$, where M_p and V_p are the plastic moment and shear capacities, respectively, of the link cross section. Using the shear-moment interaction

diagram of a wide flange beam and applying static equilibrium of a link, Malley and Popov (1984) obtained:

$$e = \frac{2M}{V} \qquad [2.12]$$

where M is the link end moment and V is the link shear. Kasai and Popov (1986) estimated that the maximum link end moment reaches 1.2 M_p and the link shear reaches 1.5 V_p. Hence, the limiting link length can be computed as:

$$e = \frac{2M}{V} = \frac{2(1.2M_p)}{(1.5V_p)} = 1.6\frac{M_p}{V_p} \qquad [2.13]$$

A shear-yielding link therefore has $e/(M_p/V_p) \leq 1.6$ and dissipates energy primarily by developing the plastic shear capacity of the web of the link while undergoing a plastic rotation up to 0.08 rad. Short links provide large inelastic rotations under cyclic load and these rotations can be accurately predicted (Equation [2.11]). They fail by web fracture or severe web buckling (Arce et al. 2003). A flexure-yielding link, with $e/(M_p/V_p) \geq 2.6$ develops large moments and plastic hinges at its ends, while undergoing smaller plastic rotations in the order of 0.02 rad. In accordance with CSA S16-09 (CSA, 2009), the link resistance, V_m, in ductile eccentrically braced frames is given by the smaller of the shear forces associated with the shear yielding and flexural-yielding mechanisms:

$$V_m = \min(\phi V_p', 2\phi\frac{M_p'}{e}) \qquad [2.14]$$

where ϕ is the resistance factor for steel. The shear capacity of the link accounting for applied axial force, $V_p{}'$, is:

$$V_p{}' = V_p\sqrt{1 - (\frac{P_f}{A.F_y})^2} \quad [2.15]$$

where P_f is the applied tensile or compressive force in the link due to the factored applied loads, A is the gross area of the link and F_y is the specified minimum steel yield strength. The moment capacity of the link accounting for any applied axial force, $M_p{}'$ is

$$M_p{}' = \frac{1}{0.85} M_p \left(1 - \frac{P_f}{A.F_y}\right) \leq M_p \quad [2.16]$$

where M_p is the plastic moment capacity of the link when no axial force is present.

The plastic shear capacity of the link, V_p, is computed as:

$$V_p = 0.55\, w\, d\, F_y \quad [2.17]$$

where w is the web width and d is the overall depth of the cross section. Krawlinker (1978) states Equation [2.17] was derived for plastic design by multiplying the yield stress in pure shear (according to the von Mises criterion), $F_y/\sqrt{3}$ or $0.58F_y$, by the effective web shear area, $0.95wd$. The definition of V_p in AISC 341-05 (AISC, 2005) is different:

$$V_p = 0.6\, w\, (d - 2t)\, F_y \qquad [2.18]$$

where t is the thickness of the flange. Hence, the design equation for the link is:

$$V_m \geq V_f \qquad [2.19]$$

where V_f is the shear demand on the link due to factored seismic loads.

Three different stages characterize the link behaviour (Hjelmstad and Popov, 1984): "elastic, inelastic pre-buckling and post-buckling. The inelastic pre-buckling response is characterized by the cyclic stability of the hysteresis loop and so represents the stage where the link functions most effectively as an energy dissipating element. After web buckling, the link continues to dissipate energy but the predominant load-carrying mechanism and associated means to dissipate energy changes. Failure of a link, defined as its complete inability to sustain load, is caused by low-cycle fatigue in highly localized regions that experience extreme strain reversals due to cyclic changing of the buckled mode shape."

Engelhardt and Popov (1989) show that the interaction of shear and moment does not exist at the yield limit state and thus can be neglected when predicting the inelastic behaviour of the link. This makes it easier to predict the behaviour of intermediate links with $1.6 \leq e/(M_p/V_p) \leq 2.6$. Figures 2.7(a), 2.7(b) and 2.7(c) show the axial force, shear force and bending moments in the link, link beam and brace respectively. As shown in Figure 2.7(a) a link usually behaves as a short beam subjected to uniform shear force. For normalized link length $e \leq 1.6(M_p/V_p)$, the post-elastic deformation is controlled by

shear yielding. As the normalized link length increases beyond $1.6(M_p/V_p)$, flexural yielding at the end of the link begins. The optimal link shape usually "provides the minimum required shear area *(dw)* and is the deepest possible that satisfies the criteria for compact webs (maximum *d/w*)" (Becker and Ishler, 1996). Also the link must have compact flanges with sufficient bending capacity to ensure shear yielding of the section at ultimate load levels, i.e. before the plastic moment capacity of the link is reached. Wherever architectural constraints permit, short links are preferred over long links (Chao and Goel, 2006), because of the excellent ductility of shear yielding. Mechanisms involving plastic hinge deformations in long links are less ductile (Chao and Goel, 2006).

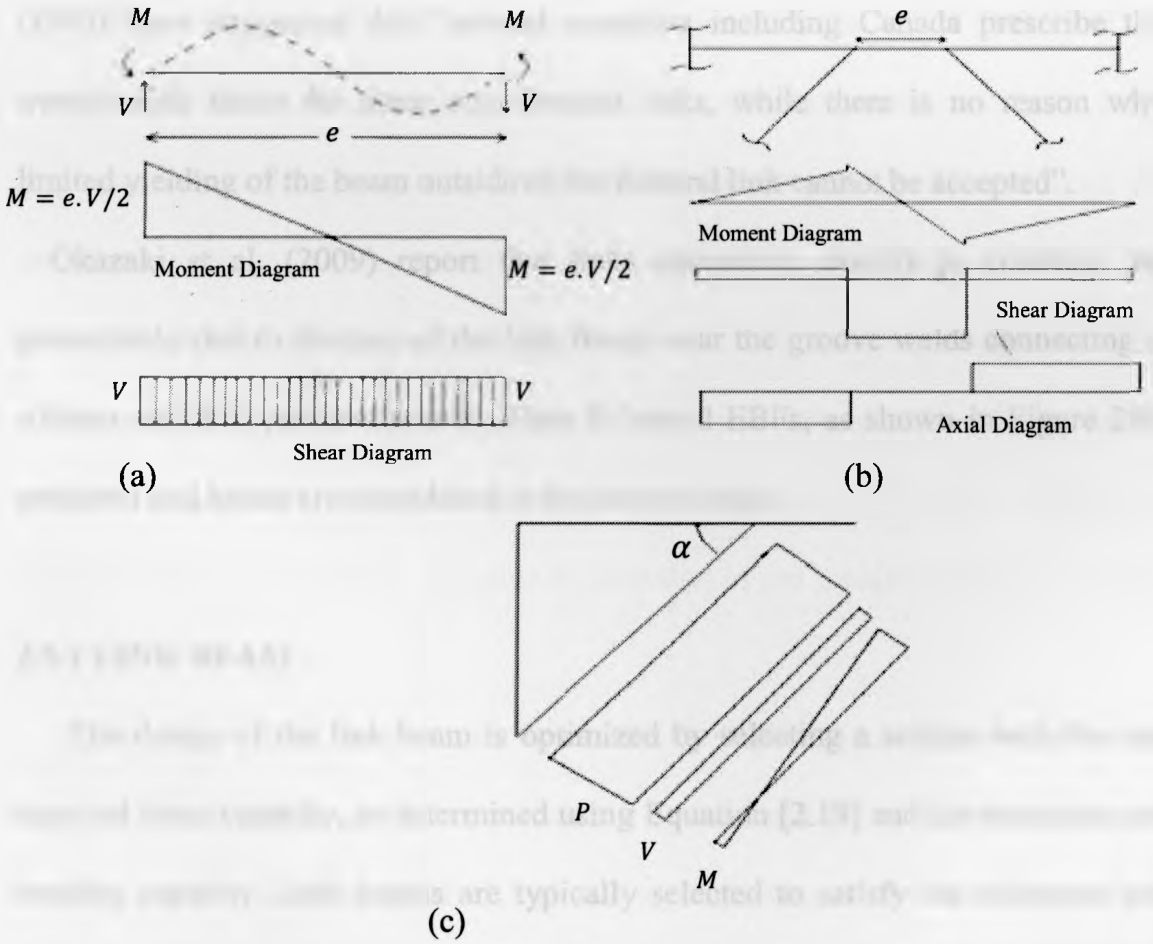

Fig. 2.7: Moment, shear and axial force diagrams: (a) Link (b) Link beam, and (c) Brace

For EBFs with long links, the link beam and brace can experience limited yielding in flexure and hence a loss of strength. Tests conducted in 1988 at UC Berkeley by Engelhardt et al. suggest, however, that "limited yielding" is acceptable and may be beneficial since it contributes to "energy dissipation and reducing inelastic deformation demands on the link" (Engelhardt and Popov, 1992). In reality, "the design goal of maintaining an elastic beam is difficult to achieve in many cases" (Engelhardt and Popov, 1987) because several parameters, e.g. the link-web area, link stiffness, brace beam angle, influence the axial force and bending moment transferred to the link beam. Hence, as long as the EBF design can ensure the occurrence of the preferred collapse mechanisms shown in Figure 2.3(a), limited yielding in the beam and brace may be allowed. Jain et al. (1996) have suggested that "several countries including Canada prescribe the same overstrength factor for shear and flexural links, while there is no reason why some limited yielding of the beam outside of the flexural link cannot be accepted".

Okazaki et al. (2009) report that links connected directly to columns, may fail prematurely due to fracture of the link flange near the groove welds connecting it to the column and thus perform poorly. Thus K-braced EBFs, as shown in Figure 2.6(a), are preferred and hence are considered in the current study.

2.5.1 LINK BEAM

The design of the link beam is optimized by selecting a section with the minimum required shear capacity, as determined using Equation [2.19] and the maximum available bending capacity. Link beams are typically selected to satisfy the minimum web area

required to resist the shear from an eccentric brace. However for ease of design and in actual practice, the link beam is usually chosen to have the same cross section as the link.

The beam-column interaction equation controls the design of the link beam. Limited yielding of the link beam at its connection with the link may be unavoidable and, if lateral bracing exists, may be acceptable. Typically in Canadian practice, the link beam connection to the column is a full moment connection (Han, 1998). However, this connection is assumed as pinned for ease of analysis in the present study.

2.6 EBF DESIGN PRINCIPLES IN CLAUSE 27 OF CSA S16-09

CSA S16-09 (CSA, 2009) requires the links to be designed to have shear resistances that just exceed the factored seismic demand required by the NBCC (NRC, 2010). Since the links define the demand that the rest of the frame must resist elastically, they should not be excessively strong. The links are detailed to provide the estimated necessary ductility, primarily by limiting width-to-thickness ratios to satisfy requirements for a Class 1 section to prevent the premature local buckling of the web and flanges and by providing web stiffeners to further preclude web buckling. Undesirable failure modes such as instability of the beam, brace or column members or failure of the connection are avoided by ensuring that the resistances of these elements exceed that of the yielding link, accounting for its probable overstrength.

Definitions of the overstrength factor are similar in the codes of several countries. They depend on the link member strength to be used and the resistance factor applied for design of other members. Table 2.1 shows a comparison of the overstrength factor and resistance factors adopted in Canada, USA and New Zealand. All three define the link

demand for capacity based design of the non-fuse elements in terms of factors to account for overstrength due to strain hardening of the link material, R_{str}, and additional overstrength due to the actual yield strength being greater than the nominal yield strength, R_y. The central factors of safety values shown are computed as $(R_{str}R_y)/\phi$, and are quite consistent for the three standards. Leslie et al. (2009) have noted that the NZ factors range from being "significantly over conservative" in flexural earthquake design and are "under conservative" when applied in redistribution design in the seismic design of steel structures.

Table 2.1: Comparison of overstrength factor for EBF in various codes

Country	Canada	USA	New Zealand
Standard	CSA S16-09	AISC-341-05	NZS-3404
Strain Hardening factor (R_{str})	1.3	1.25	1.25
Yield Strength factor (R_y)	1.1	1.1	1.2
Resistance Factor, ϕ	0.9	0.9	0.9
Central Factor of Safety	1.59	1.53	1.67

2.7 OVERSTRENGTH IN LINKS

CSA S16-09 states that for design of the diagonal braces "forces developed in the link shall be taken as $1.30R_y$ times the nominal strength of the link" The factor 1.30 is an overstrength factor, R_{str}, intended to capture how strain hardening increases the plastic strength of the link, V_{ult}, at the target link deformation angle to the yield strength, V_y, computed using the nominal steel yield strength, F_{yn}.

$$R_{str} = \frac{V_{ult}}{V_y} \qquad [2.20]$$

The R_y factor accounts for the actual yield strength, F_{ya}, being greater than the nominal yield strength:

$$R_y = \frac{F_{ya}}{F_{yn}} \qquad [2.21]$$

Designs based on high estimates of the overstrength factor can result in uneconomical structures. Designs based on low values can result in undesirable collapse mechanisms, since they can underestimate the capacity of the link and thus lead to the selection of weaker braces and link beams that could yield or fail before the link reaches its full capacity. Literature concerning both sources of link overstrength must therefore be reviewed.

2.7.1 STRAIN HARDENING

Shear yielding in links in EBFs produces very fat and stable hysteresis loops. Figure 2.8 shows strain hardening in an EBF link specimen (Malley and Popov, 1984): a clear yield point is exhibited during the initial cycle of loading and the shear resistance during the final cycle is 50% greater than this value due to strain hardening. Even after the first few cycles, the specimen displays stable loops while undergoing further displacement cycles to dissipate energy. Link overstrength is primarily due to strain hardening.

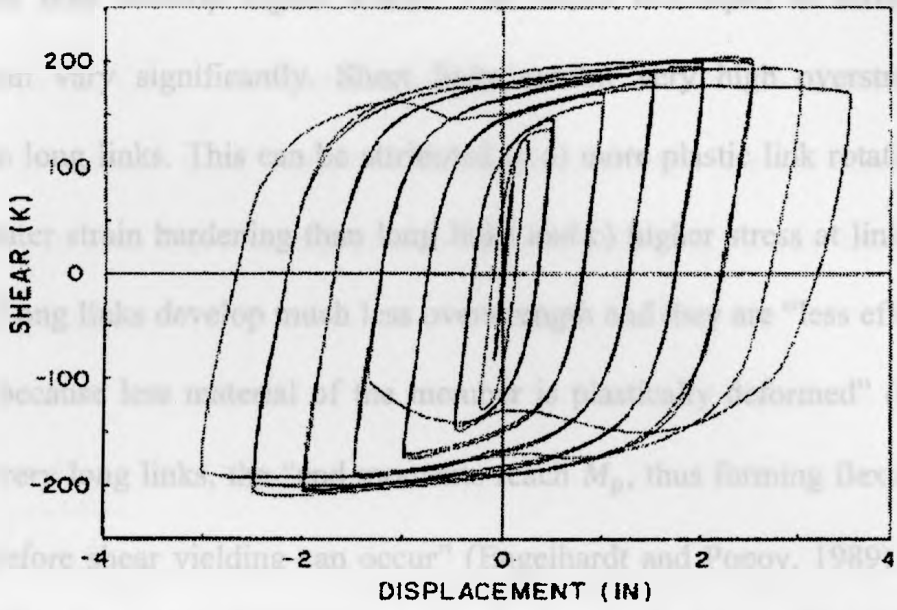

Fig. 2.8: Hysteric loops for link (From Malley and Popov, 1984, used by permission)

Byfield and Davies (2005) present a survey of tensile tests (mill tests) which show that the strain hardening behaviour is independent of material thickness and steel grade. These findings are based on tests of relatively light-weight W-sections W210 x 20 (for beams) with masses less than 20 kg/m and W 150 x 20 (for columns) with masses less than 20 kg/m. They also stated that "It is not clear whether the results are transferable to the heavier sections which are more commonly used in rigidly jointed frames" (e.g. W310 x 33, with masses of 33 kg/m or more). In CSA S16-09 (CSA, 2009) it is assumed that flanges do not contribute to the shear strength of W-sections and hence, the overstrength due to strain hardening is not dependent on flange width or thickness.

Figure 2.9 shows the variation of the total overstrength (i.e. due to both strain hardening and higher-than-nominal yield strengths) with normalized link length, $e/(M_p/V_p)$. Yielding and energy dissipation occur primarily in the links and the hysteric energy is absorbed through the process of strain hardening. Strain-hardened links have higher

capacity and thus develop higher forces. The forces developed in links that strain-hardened can vary significantly. Short links exhibit very high overstrength values compared to long links. This can be attributed to a) more plastic link rotation than long links b) greater strain hardening than long links and c) higher stress at link failure than long links. Long links develop much less overstrength and they are "less efficient energy dissipaters because less material of the member is plastically deformed" (Popov et al., 1987). For very long links, the "end moments reach M_p, thus forming flexural hinges at both ends before shear yielding can occur" (Engelhardt and Popov, 1989). Also, it has been observed that highly concentrated bending strains at the link end cause failure of link flanges at relatively low link rotation values. The current provisions in CSA S16-09 (CSA, 2009) do not relate overstrength to the normalized link length and provide no guidance on the use of different overstrength factors for various link types.

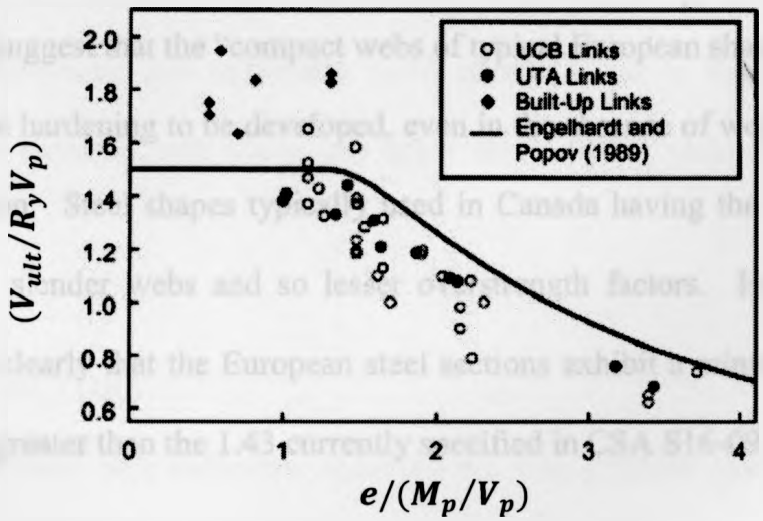

Fig. 2.9: Overstrength in links (From Richards, 2004, used by permission)

Barecchia et al. (2006) used FEM program ABAQUS to estimate overstrength in shear links with $e/(M_p/V_p) \leq 1.6$. Boundary conditions were imposed on various types of shear links to ensure shear deformation and overstrength factors were determined corresponding to peak link rotations of 0.10 rad. The following formula was proposed for the overstrength factor:

$$\frac{V}{V_y} = 1.5 + \frac{b/d}{e/(1.6\frac{M_p}{V_p})} \qquad [2.22]$$

where b is the flange width of the W-shape. Although this equation was derived for European steel shapes at link rotations that are 25% greater than the maximum specified in S16-09, clearly $e/1.6(M_p/V_p)$ and b/d are key parameters. However, both numerical analyses and experimental tests (Barecchia et al., 2006) have demonstrated that European hot-rolled steel shapes possess large overstrength factors due to strain hardening. Barecchia et.al. suggest that the "compact webs of typical European shapes profiles, which allow large strain hardening to be developed, even in the absence of web stiffeners" could be the explanation. Steel shapes typically used in Canada having the similar *b/d* ratios may have more slender webs and so lesser overstrength factors. However, Equation [2.22] indicates clearly that the European steel sections exhibit a minimum overstrength of 1.5, which is greater than the 1.43 currently specified in CSA S16-09.

2.7.2 HIGHER-THAN-SPECIFIED-MINIMUM YIELD STRENGTHS

The second reason for link overstrength is that specified yield strength of steel, F_{yn} is a minimum value and the actual yield strength, F_{y_a}, has a high likelihood

of being greater than this value. Bjorhovde (2005) reported that the most common structural steel specifications in the 1980s in America were ASTM A36 and ASTM A572 Grade 50 with specified minimum yield stresses, F_y, of 36 ksi (248MPa) and 50 ksi (345MPa), respectively. "A36 shapes produced in this period had yield strengths much greater than the minimum specified (SAC, 2000). Some actually satisfied the requirements for both the A36 and A572 Grade 50 specification, since there was no upper bound on the actual yield strength" (Bjorhovde, 2005). This is especially significant because it eliminates any upper bound on the resistance of the link section and so increases the design forces in other members of the frame that are designed based on the capacity of the link.

Dexter et al. (2000) concluded that the tensile yield strengths of 20,003 samples of ASTM A572 grade 50 steel varied from 50 to 65 ksi with mean yield strength of 55.8 ksi (385 MPa) which is 5.8 ksi (40 MPa) greater than the minimum yield strength". Currently A992 steel is now more widely used than ASTM A36 or A592 Grade 50 steel, and has both specified minimum and maximum yield stresses. This is the first time a steel specification has required both lower and upper limits for its yield stress. (Bjorhovde, 2005)

2.7.3 OTHER FACTORS

If the link contains web stiffeners, reducing the web stiffener spacing enhances the energy-dissipating potential of the link because it delays inelastic web buckling. The current stiffener spacing requirements in CSA S16-09 (CSA, 2009) are based on the study by Kasai and Popov (1986b). Figure 2.10 shows the improvement in link

performance obtained by using web stiffeners for a beam with web slenderness, d/w of 56.8. The specimen with the un-stiffened link experiences severe web buckling and shows pinched hysteric loops indicating poor energy-dissipating capacity. The stiffened link exhibits full, stable hysteric loops for more cycles and undergoes large inelastic rotations.

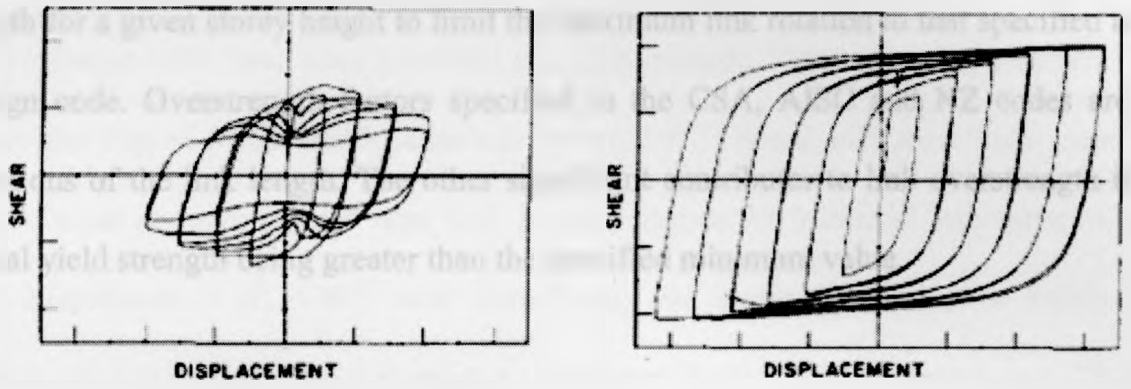

(a) Un-stiffened Link (b) Stiffened Link

Fig. 2.10: Hysteric behaviour of (a) Un-stiffened link and (b) Stiffened link (From Popov et. al. 1987, used with permission from Earthquake Engineering Research Institute)

2.8 SUMMARY

In this chapter, a literature review of the overstrength factors for energy dissipating links in Eccentrically Braced Frames has been presented. The basic mechanics and kinematics of EBFs have been established. Experimental studies conducted since the early 80s have investigated the cyclic behaviour of links and established design guidelines. The code provisions are similar in different countries and a brief overview of the CSA, AISC and the NZ codes is provided. Links are classified, based on their length, as short, intermediate or long. Short links dissipate energy by yielding of the link web in

shear, whereas, long links form plastic hinges at the link ends. Short links are preferred in practice since well-stiffened shear links can achieve greater strain hardening and higher energy dissipation compared to long links. However higher plastic rotations are necessary to do this and so short links have overstrengths due to strain hardening that are markedly greater than those associated with long links. The link rotation angle is inversely proportional to the link length and storey height, so typically a designer chooses a link length for a given storey height to limit the maximum link rotation to that specified in the design code. Overstrength factors specified in the CSA, AISC and NZ codes are not functions of the link length. The other significant contributor to link overstrength is the actual yield strength being greater than the specified minimum value.

CHAPTER 3: STATISTICAL PARAMETERS FOR DEMAND

3.1 INTRODUCTION

The excellent structural characteristics of Eccentrically Braced Frames (EBF) have been verified experimentally, since 1977, by several researchers (e.g. Roeder and Popov, 1977; Popov, 1980; Kasai and Popov, 1986a; Engelhardt and Popov, 1989). A number of useful design rules have been provided (e.g., Engelhardt, 1986). Some researchers (e.g., Kasai and Popov, 1986a and Roeder and Popov, 1977) tested only short links since they are the most commonly used type (e.g. in steel frames for industrial structures). Others (e.g. Engelhardt et al., 1992) have tested long and intermediate links to verify their experimental behavior. Links connected to columns have also been tested (e.g. Okazaki et al., 2006).

It has been noted since the 1980s that the actual link strengths are typically greater than the values prescribed by the AISC (AISC, 1985) steel design codes (Engelhardt and Popov, 1989). A short link tested by Engelhardt with $e/(M_p/V_p) = 1.11$, where e is the length of the link, and M_p and V_p are the plastic moment and shear capacities of the section, had an ultimate shear strength that was 1.9 times its nominal shear capacity determined using the nominal yield strength of the steel (and 1.7 times its actual shear capacity computed using the actual yield strength of the steel). The AISC code (AISC, 1985) specifies the non-fuse elements connected to the link be designed to resist 1.5 times the nominal link shear capacity, and so is clearly unconservative for the design of these elements. On the other hand, specimens with long links, $e/(M_p/V_p) \geq 2.6$, exhibited overstrength factors of 0.9 to 1.2 so the AISC requirements were quite conservative in

such cases. Thus a single link overstrength factor seems inadequate to provide uniform reliability for the design of non-fuse members in Eccentrically Braced Frames.

The objective of this chapter is to accurately quantify the link overstrength, which can then be used to establish consistent design criteria for all lengths of links. As discussed in Chapter 2, test results of W-shapes clearly indicate that the link overstrength depends primarily on the following two factors:

(a) Overstrength due to strain hardening of the links, R_{str}; and,

(b) Overstrength due to actual steel yield strength of the link being greater than the specified minimum, R_y.

The chapter develops overstrength models that independently account for both factors. Firstly, a discussion on the experimental data on W-shape links obtained by other researchers is presented, followed by a regression analysis of experimental data to establish a model for the strain hardening effect. Next, the regression analysis of steel coupon test data obtained by Schmidt (2000) is conducted to quantify R_y and establish a model for its prediction.

3.2 EXPERIMENTAL DATA ON OVERSTRENGTH DUE TO STRAIN HARDENING IN LINKS

Richards (2004) tabulated the results of experiments conducted on 77 links tested between 1983 and 2002, as summarized in Table 3.1. Appendix A-1 shows the complete set of data collected. Hjelmstad and Popov (1984) established the basic equations for stiffener spacing and normalized link lengths. Kasai and Popov (1986b) explored cyclic web buckling in links. Further tests by Engelhardt and Popov (1989) investigated the

behavior of longer links. Arce and Engelhardt (2003) found that the flange slenderness limits prescribed by the AISC steel design code (AISC 1985) were overly conservative. Table 3.1 shows the number of specimens,n, tested by each investigator: the total is less than 77 because the data for built-up test specimens have been excluded. The shape designations are in US customary units: the first number is the nominal depth in inches, and the second number is the weight in lbs/foot. Metric shape designations are shown in parentheses, with the nominal depth in mm and the mass in kg/m. The grades are A36, A572 and A992, with minimum specified yield strengths of 36, 50 and 50 ksi (248, 345 and 345 MPa) respectively. The normalized link lengths range from 1.0 to 3.0 and the associated rotations at failure (γ_p) range from 0.011 to 0.09 radians.

Table 3.1: W-shape Link data tabulated by Richards (2004)

Reference	**Year**	n	**Shape**	**Grade of Steel**	**Normalized link length** $(e/M_p/V_p)$	**Link Rotation at Failure (rad)**
Hjelmstad and Popov	1984	15	W18x40 (W460 x 60)	A36	1.26-2.77	0.047-0.064
Malley and Popov	1984	12	W18x40, W18x60 (W460 x 60, W 460x89)	A36	1.25-1.48	0.05-0.078
Kasai and Popov	1986a	7	W8x10 (W200 x 15)	A36	1.12-1.70	0.019-0.078
Ricles and Popov	1987	8	W12x19 (W310 x 28)	A36	1.50	0.085-.085
Engelhardt and Popov	1989	14	W12x16,W12x22 (W310 x 24, W 310 x 33)	A36	1.34-3.95	0.0115-0.085
Arce and Engelhardt	2003	11	W10x19,W10x33, W 16x36 and W10x68 (W 250 x 38, W 250 x 49, W 410 x 54, W 250x101)	A992	1.0-3.0	0.066-0.079

Overstrength values reported by Richards, not shown in Table 3.1, have to be modified since the formulae used to compute the ultimate shear capacity in the AISC and CSA standards are different as described previously in Chapter 2. Appendix A-2 shows the modified experimental values used in the current study. The overstrength results for the W-shape links were analyzed to determine correlation between geometrical and material properties and link overstrength. Before preliminary scatter plots can be presented, however, it is necessary to define some of the principal parameters involved.

3.2.1 LINK ROTATION CAPACITY AND LOADING PROTOCOL

All investigators report the link rotation angle, γ, as the relative vertical displacement between the two ends of the link divided by the link length. The inelastic rotation capacity, γ_p, is usually defined as that which occurred during the last complete loading cycle that sustained the nominal link shear strength (AISC, 2005). Figure 3.1(a) and 3.1(b) (Richards and Uang, 2005) show a commonly used method to measure plastic rotation. The peak rotation, γ_{ult}, which is not known a-priori by the designer, corresponds to the maximum shear resisted by the link, V_{ult}. The plastic rotation, γ_p, may be determined by constructing a backbone curve as shown in Fig 3.1(a). From the set of hysteresis loops obtained during the cyclic loading of a link specimen, a backbone curve is created by joining the peak points in each cycle. The plastic rotation, γ_p, is assumed by Richards and Uang to correspond to a post-peak shear of 80% of V_{ult}, because he defines link failure or unacceptable degradation of strength as "strength loss below 80% of the maximum shear". The value of plastic rotation determined by this method is called the "experimentally determined" value.

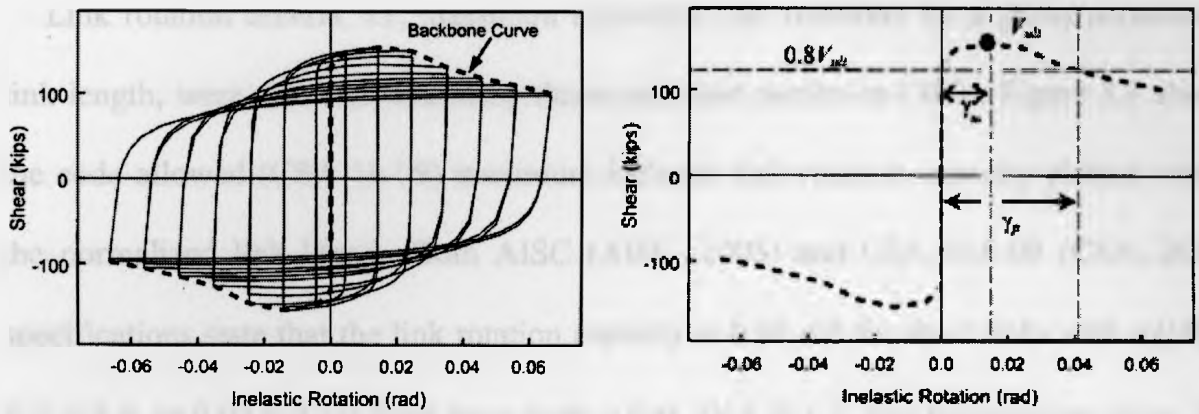

(a) (b)

Fig. 3.1: (a) Obtaining backbone curve and (b) Computing inelastic rotation capacity (From Richards and Uang, 2005, used by permission)

Figure 3.2 shows the definition of plastic rotation capacity, γ_p, adopted in the current study. Here, the γ_p of the link specimens is defined as the maximum plastic rotation sustained for at least one full cycle of loading prior to failure. Here, 'failure' is defined as the complete inability of the link to carry further applied load.

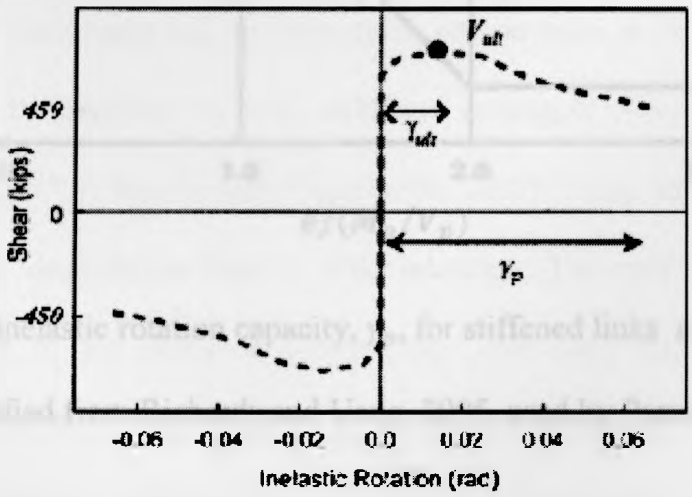

Fig 3.2: Shear capacity of link versus link rotation (modified from Richards and Uang, 2005, used by permission)

Link rotation criteria, i.e. maximum allowable link rotations for a given normalized link length, were also established by these early test results in 1980s. Figure 3.3 shows the code allowed (CSA 16-09) maximum inelastic link rotation capacity plotted versus the normalized link length. Both AISC (AISC, 2005) and CSA S16-09 (CSA, 2009) specifications state that the link rotation capacity is 0.08 rad for short links with $e/(M_p/V_p) \leq 1.6$ or 0.02 rad for long links with $e/(M_p/V_p) \geq 1.6$. For intermediate links, the link rotation capacity is, using linear interpolation:

$$\gamma_p = 0.08 - 0.06(e/(M_p/V_p) - 1.6) \qquad [3.1]$$

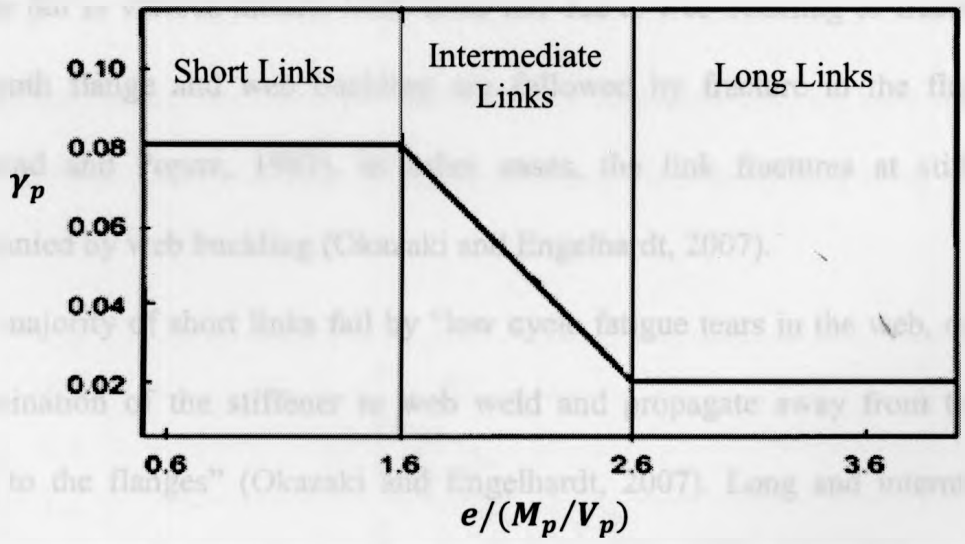

Fig. 3.3: Design inelastic rotation capacity, γ_p, for stiffened links as per CSA S16-09 (modified from Richards and Uang, 2005, used by Permission)

The loading protocol for testing links was standardized in the 1997 AISC seismic provisions and previously adopted procedures have been deemed "arbitrary" by Richards and Uang (2006). A Revised Loading Protocol (RLP) has been proposed by Richards and

Uang (2006) based on EBF analysis, as they consider the 1997 AISC loading protocol conservative because it imposes more severe cycles of rotation at the beginning of the test. Tests conducted by Okazaki et al. (2006) to check the impact of the RLP on the shear capacity and inelastic rotation capacity concluded that links tested with the RLP exhibited a 47% increase in inelastic rotation capacity. However, the shear capacities observed were similar to the values obtained by the 1997 AISC loading provisions. Thus the design rotation capacity of 0.08 rad is stated (Okazaki et al. 2007) to be "overly conservative".

3.2.2 LINK FAILURE MODES

Links fail in various modes. Most links fail due to web buckling or fracture. In some cases, both flange and web buckling are followed by fracture in the flange or web (Hjelmstad and Popov, 1983). In other cases, the link fractures at stiffener welds accompanied by web buckling (Okazaki and Engelhardt, 2007).

The majority of short links fail by "low cycle fatigue tears in the web, originating at the termination of the stiffener to web weld and propagate away from the stiffeners parallel to the flanges" (Okazaki and Engelhardt, 2007). Long and intermediate links experience strength degradation due to web buckling. The role of connections, for connecting the link to the brace or column, has also been discussed. While some researchers investigated welded connections, others investigated bolted connections. Bolted connections have performed better as welded connections have often failed at their connection to the flange (Ghobarah and Ramadan, 1994).

3.3 OVERSTRENGTH DUE TO STRAIN HARDENING

3.3.1 IDENTIFICATION OF KEY PARAMETERS

Before proceeding with the statistical analysis, it is essential to identify the key parameters and eliminate any redundant parameters. Key parameters can be identified by plotting the overstrength data against the geometric and material properties of links, which are available from the 77 modified test results tabulated in Appendix A-2. For example, Figure 3.4 shows the relationship between link overstrength and normalized link length for the test data used in the current study. As discussed in Chapter 2, longer links exhibit lower overstrength values and very short links ($e/(M_p/V_p) \leq 1.2$) exhibit very high overstrengths. Richards (2004) proposed that higher-than-expected overstrength in very short links ($e/(M_p/V_p) \leq 1.2$) can be attributed to the contribution of the flanges to the shear strength. He therefore suggested that, for very short links, the flange contribution may be taken into consideration while computing shear strength.

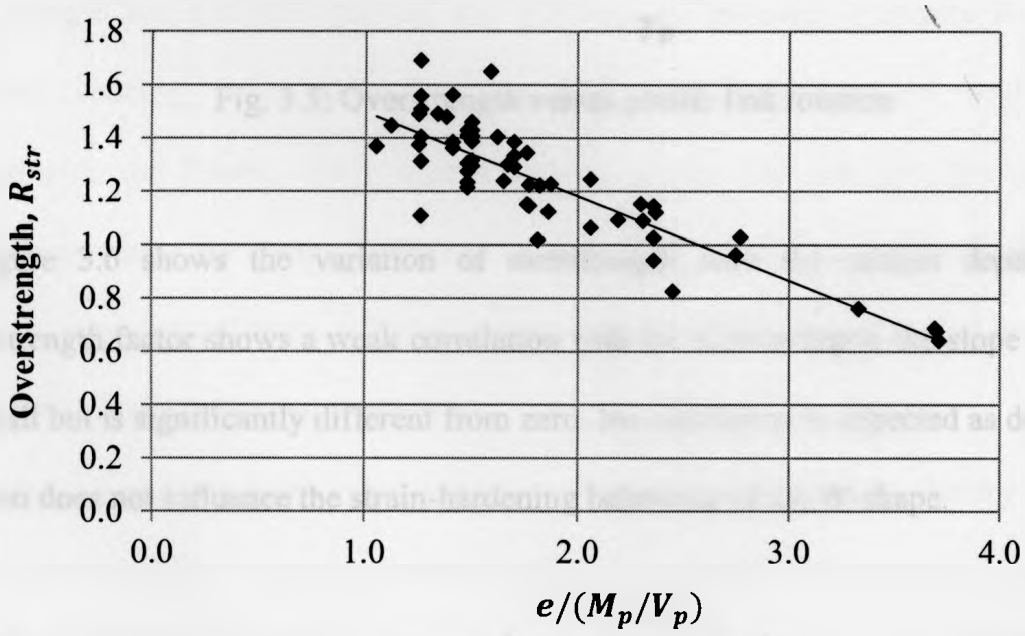

Fig. 3.4: Plot showing a variation of link overstrength with normalized link length

Figure 3.5 shows an almost linear variation of overstrength with plastic link rotation, γ_p. Higher values of link rotation result in larger hysteresis loops causing greater energy dissipation. The large link rotations cause strain hardening after initial yielding and thus lead to higher values of link overstrength.

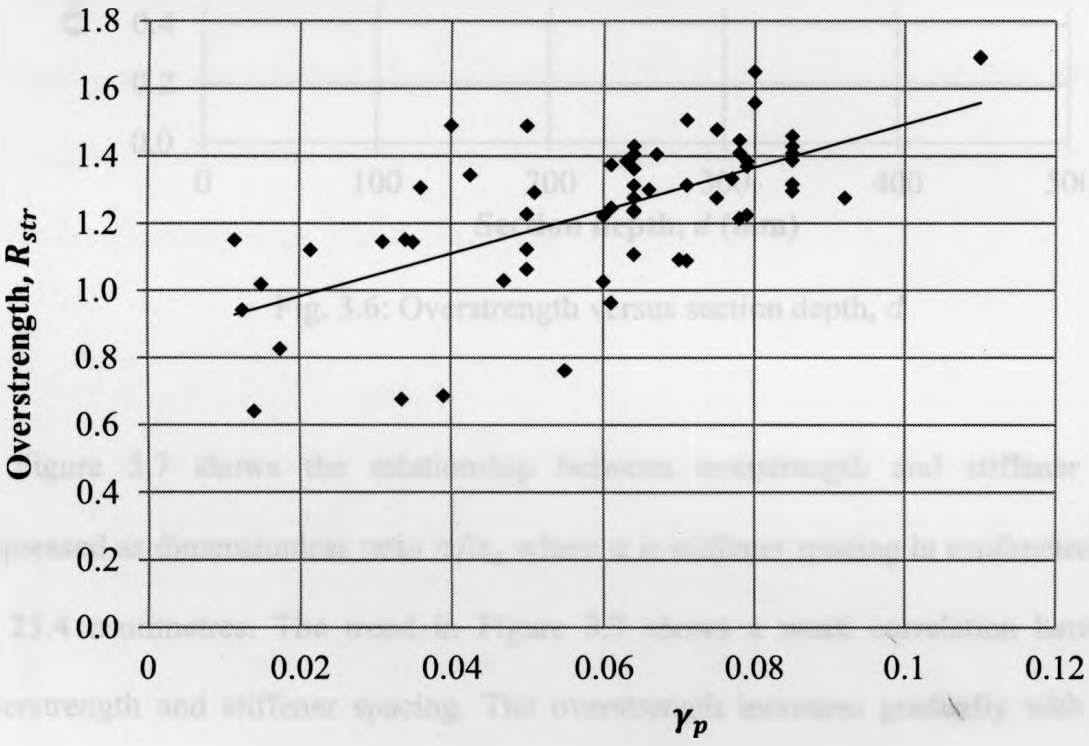

Fig. 3.5: Overstrength versus plastic link rotation

Figure 3.6 shows the variation of overstrength with the section depth, d. The overstrength factor shows a weak correlation with the section depth: the slope of the line is small but is significantly different from zero. No correlation is expected as depth of the section does not influence the strain-hardening behaviour of the W-shape.

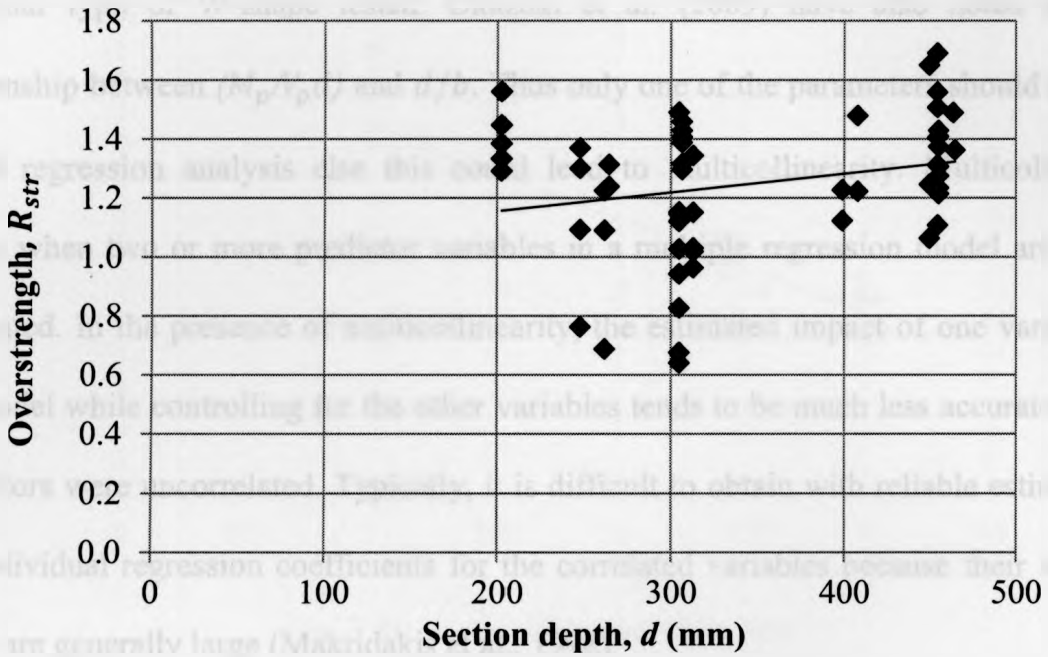

Fig. 3.6: Overstrength versus section depth, d

Figure 3.7 shows the relationship between overstrength and stiffener spacing expressed as dimensionless ratio a/a_o where a is stiffener spacing in centimetres and a_o is 25.4 centimetres. The trend in Figure 3.7 shows a weak correlation between the overstrength and stiffener spacing. The overstrength increases gradually with reduced stiffener spacing. Reduced stiffener spacing causes stable, fatter hysteric loops (Engelhardt and Popov, 1987), thus leading to greater link rotation. The greater link rotation increases the strain hardening beyond yield and so causes the link to exhibit greater overstrength. Hence, stiffener spacing could be a key parameter and hence will be considered in the regression analysis.

Figure 3.8 shows a linear relationship between $(M_p/V_p d)$ and d/b, thereby suggesting that only one of these two parameters should be considered in the regression analysis. In this figure, a number of data points overlap because the d/b ratios are constant for a

particular type of W-shape tested. Okazaki et al. (2009) have also noted a linear relationship between $(M_p/V_p d)$ and d/b. Thus only one of the parameters should be used in the regression analysis else this could lead to multicollinearity. Multicollinearity occurs when two or more predictor variables in a multiple regression model are highly correlated. In the presence of multicollinearity, the estimated impact of one variable on the model while controlling for the other variables tends to be much less accurate than if predictors were uncorrelated. Typically, it is difficult to obtain with reliable estimates of the individual regression coefficients for the correlated variables because their standard errors are generally large (Makridakis et al., 1998).

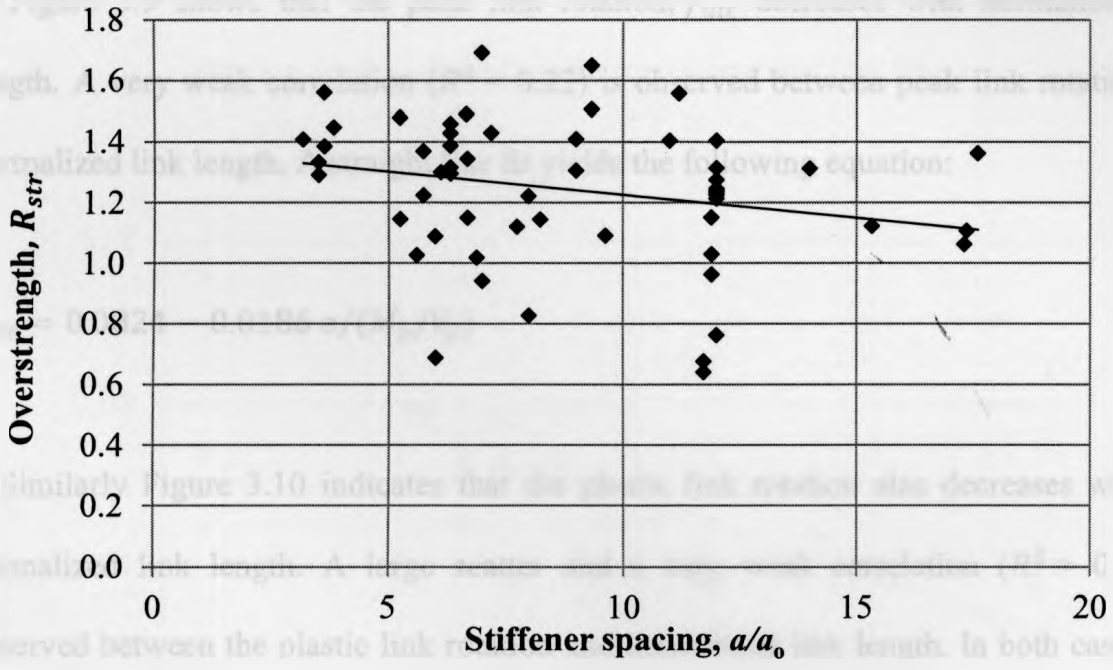

Fig. 3.7: Overstrength versus stiffener spacing, a/a_o

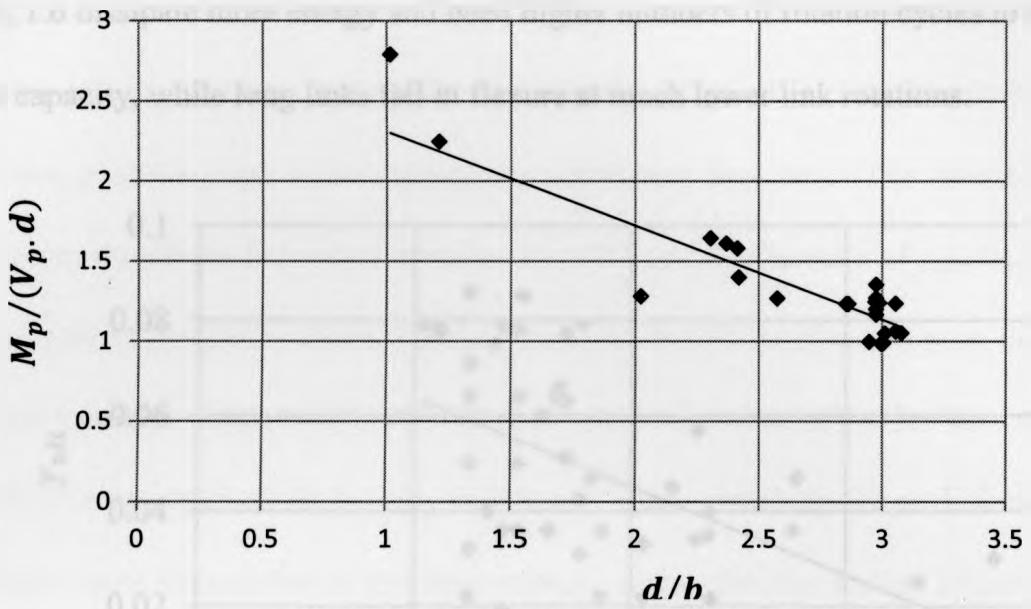

Fig. 3.8: $M_p/(V_p.d)$ versus d/b ratio

Figure 3.9 shows that the peak link rotation, γ_{ult} decreases with normalized link length. A very weak correlation (R^2 = 0.22) is observed between peak link rotation and normalized link length. A straight line fit yields the following equation:

$$\gamma_{ult} = 0.0824 - 0.0186\, e/(M_p/V_p) \qquad [3.2]$$

Similarly Figure 3.10 indicates that the plastic link rotation also decreases with the normalized link length. A large scatter and a very weak correlation (R^2 = 0.21) is observed between the plastic link rotation and normalized link length. In both cases, the link rotation decreases linearly with the normalized link length. As observed when discussing Figure 3.3, experimental tests on EBF links have established that link rotation capacity is a function of normalized link length, $e/(M_p/V_p)$. Short links with $e/(M_p/$

$V_p) \leq 1.6$ dissipate more energy and need higher numbers of rotation cycles to reach their shear capacity, while long links fail in flexure at much lower link rotations.

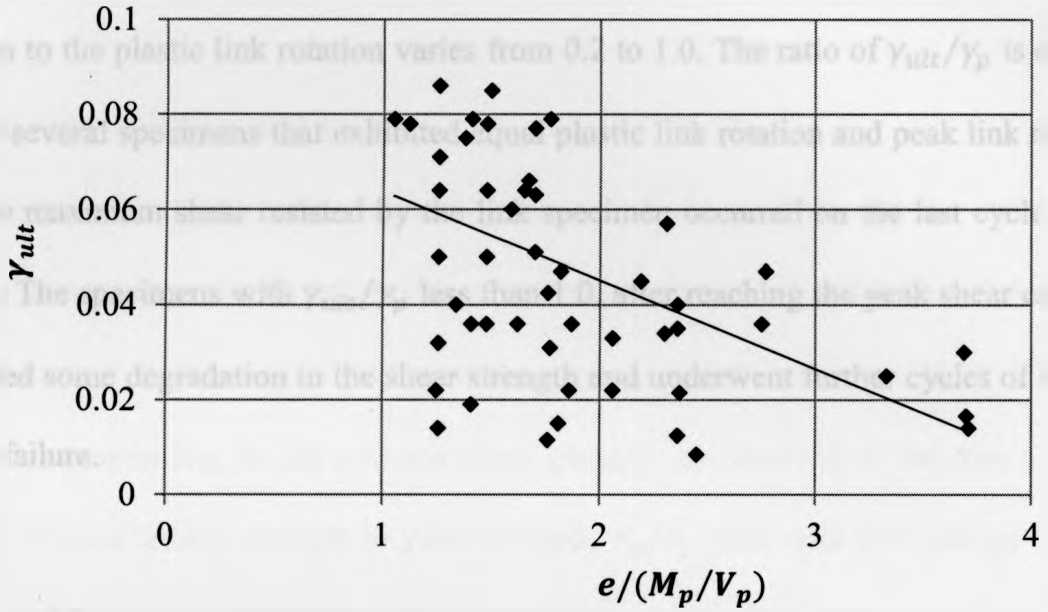

Fig. 3.9: Peak link rotation versus normalized link length

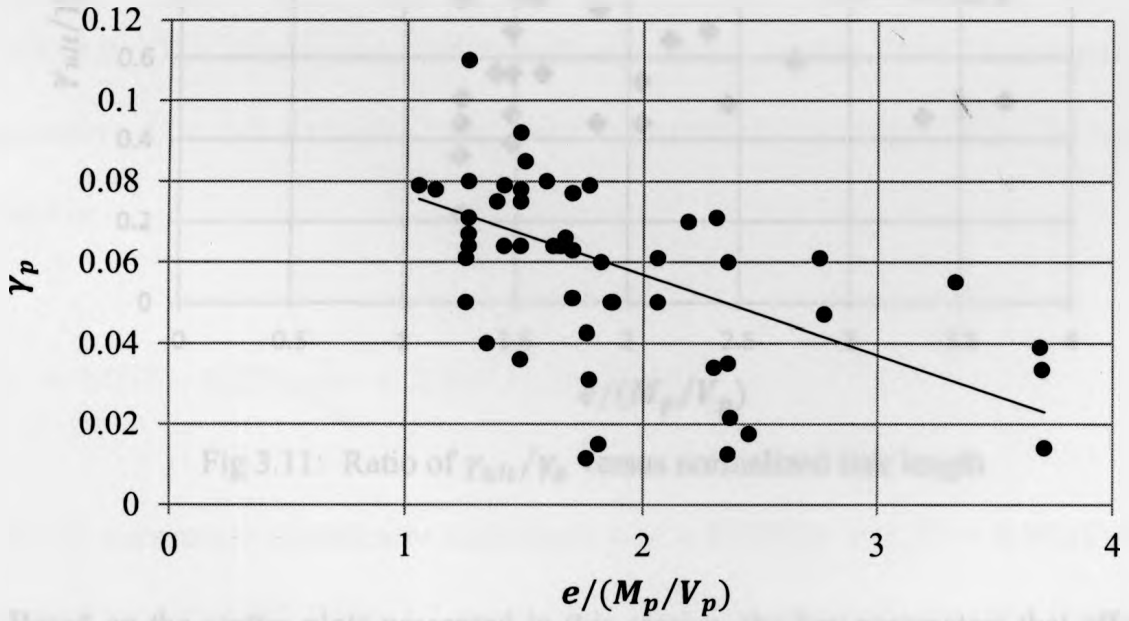

Fig 3.10: Plastic link rotation versus normalized link length

Figure 3.11 shows the variation of the ratio of the peak link rotation to the plastic link rotation, γ_{ult}/γ_p, versus normalized link length, $e/(M_p/V_p)$. No discernable trend is observed, and the slope is not statistically significant from zero. The ratio of peak link rotation to the plastic link rotation varies from 0.2 to 1.0. The ratio of γ_{ult}/γ_p is equal to 1.0 for several specimens that exhibited equal plastic link rotation and peak link rotation, i.e., the maximum shear resisted by the link specimen occurred on the last cycle before failure. The specimens with γ_{ult}/γ_p less than 1.0, after reaching the peak shear capacity, exhibited some degradation in the shear strength and underwent further cycles of rotation before failure.

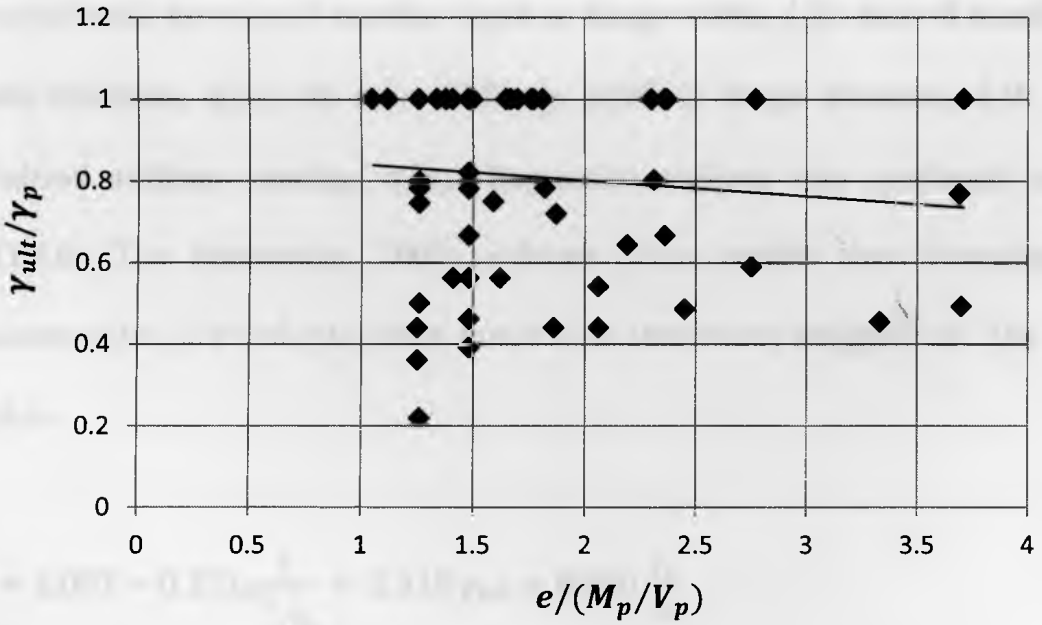

Fig 3.11: Ratio of γ_{ult}/γ_p versus normalized link length

Based on the scatter plots presented in this section, the key parameters that affect the link overstrength are: normalized link length, $/(M_p/V_p)$; link rotation, γ_p ; the ratio of the flange width to section depth, b/d ; and the stiffener spacing ratio, a/a_o. Also a

linear relationship was observed between (M_p/V_p d) and d/b, indicating that only one of these two parameters should be used in the regression analysis to prevent multicollinearity.

3.3.2 REGRESSION ANALYSIS

A multiple linear regression analysis was carried out to determine the influence of various parameters on the observed overstrength factor, V_{ult}/V_p. The independent variables considered in the analysis were: the normalized link length, $e/(M_p/V_p)$; the link rotation corresponding to the ultimate shear capacity as observed in the test, γ_{ult}; the ratio of ultimate tensile strength to yield strength, F_u/F_y (only data from flange coupons are considered); the ratio of member depth to flange width, d/b; ratio of member depth to web thickness, d/w; the ratio of flange width to flange thickness, b/t; and, the normalized stiffener spacing, a/a_o. Regression analysis was conducted using the MATLAB (The Mathworks, 2009) software. Four models were investigated and parameters d/w, b/t and a/a_o were found to be statistically insignificant. The resulting model is:

$$R_{str} = 1.057 - 0.251 \frac{e}{M_p/V_p} + 2.515\,\gamma_{ult} + 0.360\,\frac{F_u}{F_y} \qquad [3.3]$$

with all parameters statistically significant ($p = 0.00001$ and $R^2 = 0.9061$) and a standard error of 0.087. Table 3.2 summarizes the predicted coefficients and their errors: all have p-values much smaller than 0.05 and so are statistically significant. Figure 3.12 shows the excellent fit between the predicted values and the experimental results. The

line on the figure corresponds to the predicted value equaling the experimental value. The coefficient of variation of R_{str} varies due to the constant value of the standard error and a variable mean value of R_{str}. The mean value of R_{str} ranges from 0.737 (for long links) to 1.481 (for short links) and the corresponding CoV values range from 0.045 to 0.112.

Table 3.2: Results from the regression analysis for the generic model

	Constant	F_u / F_y	γ_{ult}	$e/(M_p/V_p)$
Coefficient	1.057	0.3598	2.5149	0.2510
Error in Coeff.	0.1854	0.0232	0.5724	0.1066
***p*-value**	10^{-4}	10^{-4}	0.0013	10^{-4}

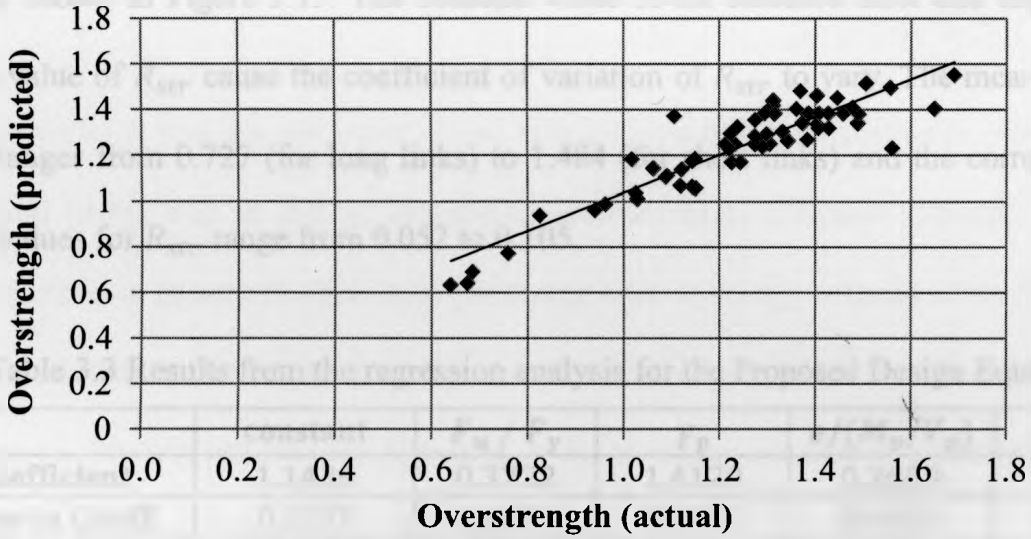

Fig. 3.12: Fit between test results and predicted results (Equation [3.3])

In practice, structural designers have to design the link for the code-prescribed values of plastic rotation shown in Figure 3.3. Hence, they cannot use Equation [3.3] because the peak values of the link rotation, γ_{ult}, can be determined only from experimental testing. Hence, the available data were reanalyzed including the code specified value of γ_p, known a priori by the designer, as an input parameter. As noted previously, γ_p = 0.08 rad

or = 0.02 rad for short or long links, respectively and can be computed using Equation [3.1] for intermediate links. The resulting model, the Proposed Design Equation is:

$$R_{str} = 1.143 + 0.372\left(\frac{F_u}{F_y}\right) + 1.413\,\gamma_p - 0.269\frac{e}{M_p/V_p} - 0.0044\frac{a}{a_o} \qquad [3.4]$$

with R^2= 0.910 and a standard error of 0.093. The parameter estimates and their errors are shown in Table 3.3: all have p-values smaller than 0.05 and so are statistically significant. The excellent fit is further illustrated by the graph of observed and predicted values shown in Figure 3.13. The constant value of the standard error and the variable mean value of R_{str} cause the coefficient of variation of R_{str} to vary. The mean value of R_{str} ranges from 0.727 (for long links) to 1.484 (for short links) and the corresponding CoV values for R_{str} range from 0.052 to 0.105.

Table 3.3 Results from the regression analysis for the Proposed Design Equation

	constant	F_u / F_y	γ_p	$e/(M_p/V_p)$	a/a_o
Coefficient	1.1426	0.3722	1.4129	0.2688	0.0044
Error in Coeff.	0.1857	0.0234	0.1132	0.4465	0.0022
***p*-value**	10^{-4}	10^{-4}	0.0017	0.0024	0.0460

CSA S16-09 (CSA, 2009) prescribes values for normalized link length, link rotation and stiffener spacing. Depending on the grade of steel used, it also suggests nominal values for F_u/F_y. The A992 steel flange coupon data reported by Schmidt (2000) have a mean value of $\overline{F_u / F_y}$ = 1.43 that can be substituted into Equation [3.4] to estimate the value of overstrength. The standard deviation of F_u/F_y, $\sigma_{\frac{F_u}{F_y}}$, for the A992 steel flange coupon data is determined to be 0.054.

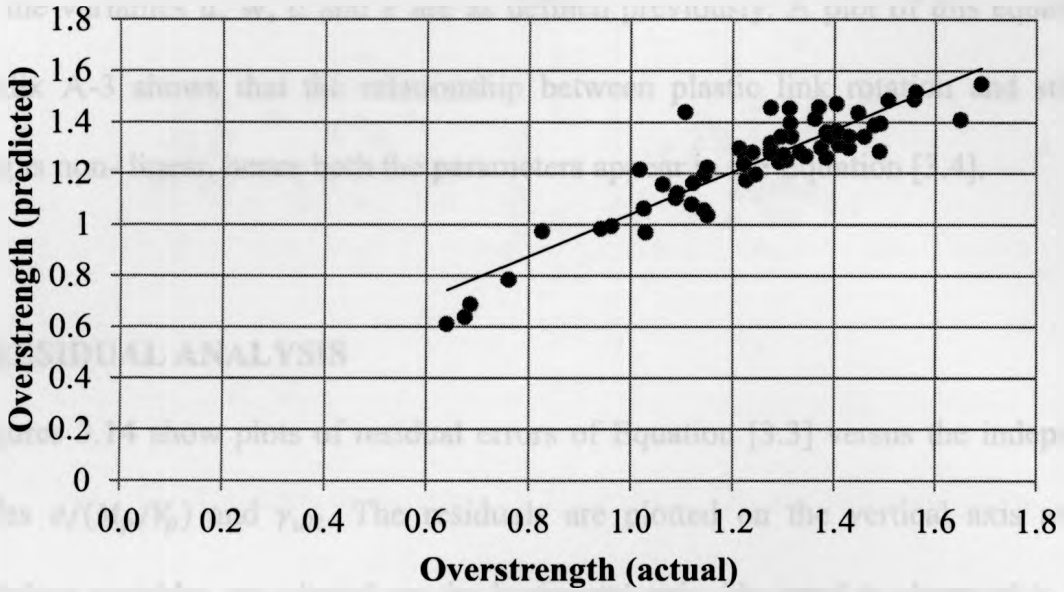

Fig. 3.13: Fit between predicted and actual overstrength values (Equation [3.4])

The stiffener spacing parameter, a/a_o was not found to be statistically significant in Equation [3.3]. This is not an expected outcome: larger stiffener spacing, a, would correspond to a greater likelihood of premature web buckling, reduced strain hardening, and so a lesser overstrength. The experimental data on peak link rotation and stiffener spacing are linearly related (see Appendix A-4), so, it is reasonable to infer that only one of these variables should appear in Equation [3.3].

However, the stiffener spacing parameter, a/a_o was found to be statistically significant in Equation [3.4]. Indeed, Itani et.al (2003) have shown that the plastic link rotation, γ_p is approximately inversely proportional to the stiffener spacing:

$$\gamma_p = \frac{0.05(d/w)}{203(2a/e)^{1.125}} \qquad [3.5]$$

where the variables d, w, a and e are as defined previously. A plot of this equation in Appendix A-3 shows that the relationship between plastic link rotation and stiffener spacing is non- linear, hence both the parameters appear in the Equation [3.4].

3.3.3 RESIDUAL ANALYSIS

Figures 3.14 show plots of residual errors of Equation [3.3] versus the independent variables $e/(M_p/V_p)$ and γ_{ult}. The residuals are plotted on the vertical axis and the independent variables are plotted on the horizontal axis. No trend is observed in either figure.

A similar analysis for the Proposed Design Equation, Equation [3.4], was conducted. In Figure 3.15, the residuals are plotted versus the significant variables F_u/F_y and γ_p: again no trends are observed. More plots displaying the variation of the residuals with other variables are provided in Appendix A-3 and no trends are observed. Hence it is concluded that the computed models, Equations [3.3] and [3.4], are adequate for predicting overstrength.

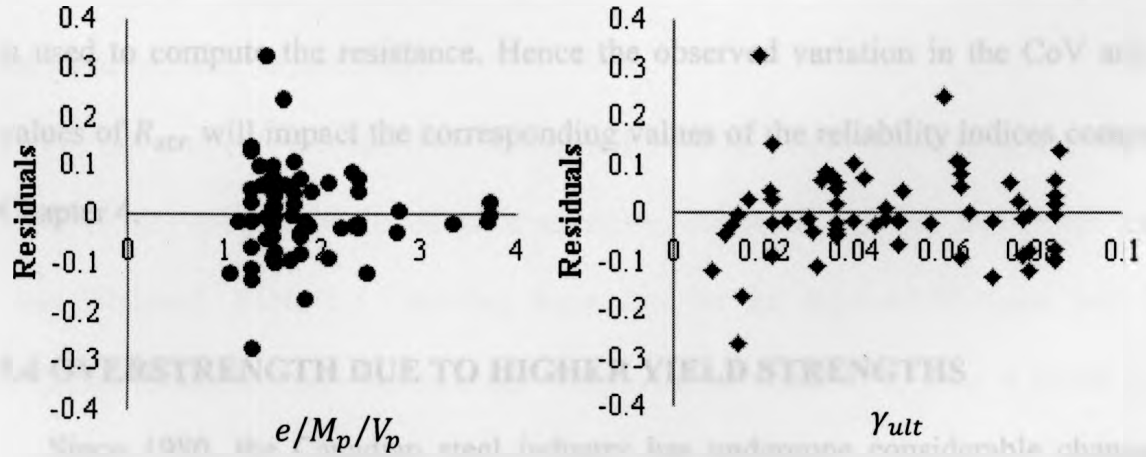

Fig. 3.14: Residuals of Equation [3.3] versus $e/(M_p/V_p)$ and γ_{ult}

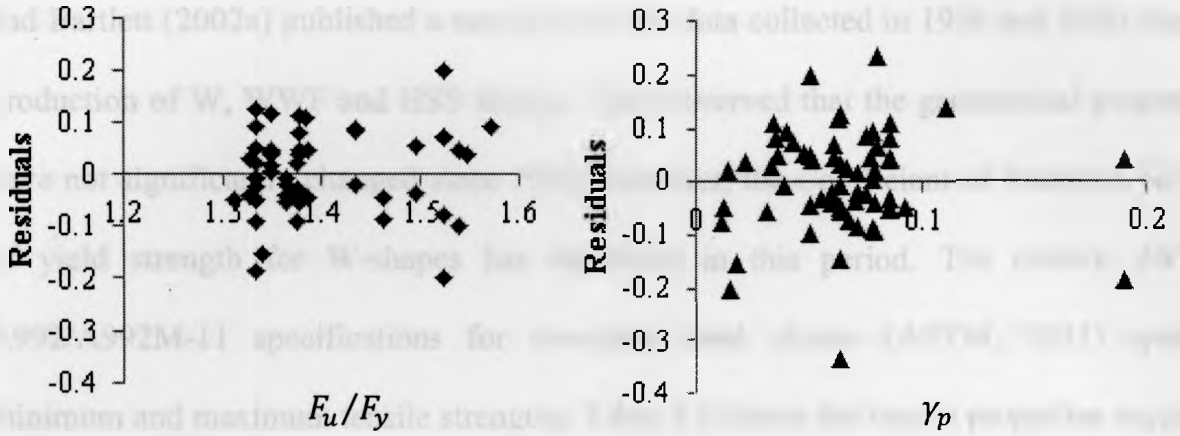

Fig 3.15: Residuals of Equation [3.4] versus F_u/F_y and link rotation, γ_p

3.3.4 COEFFICIENT OF VARIATION OF R_{str} FOR RELIABILITY ANALYSIS

In Section 3.3 it is observed that the CoV values for R_{str} computed using the Generic Equation range from 0.045 for short links to 0.112 for long links. Similarly, the CoV values for R_{str} computed using the Proposed Design Equation range from 0.052 for short links to 0.105 for long links. Also, the coefficient of variation of test/predicted ratios for the mean value of overstrength factor of test results is 0.169, while it is 0.071 for the Generic Equation [3.3] and is 0.072 for the Proposed Design Equation [3.4]. In Chapter 4, the Generic Equation is used to quantify the demand while the Proposed Design Equation is used to compute the resistance. Hence the observed variation in the CoV and mean values of R_{str} will impact the corresponding values of the reliability indices computed in Chapter 4.

3.4 OVERSTRENGTH DUE TO HIGHER YIELD STRENGTHS

Since 1980, the Canadian steel industry has undergone considerable changes that have affected the material and geometric properties of structural steel shapes. Schmidt

and Bartlett (2002a) published a summary of the data collected in 1999 and 2000 during production of W, WWF and HSS shapes. They observed that the geometrical properties have not significantly changed since 1980. However, the Coefficient of Variation (CoV) of yield strength for W-shapes has increased in this period. The current ASTM A992/A992M-11 specifications for structural steel shapes (ASTM, 2011) specify minimum and maximum tensile strengths. Table 3.4 shows the tensile properties required for the various specifications. A992 steel includes a maximum limit on the yield strength, and the yield-to-ultimate strength ratio must be less than 0.85. So, as materials and production practices have changed, the statistical distributions of tensile properties need to be re-examined. The objective of the analysis presented in this section is to develop an empirical equation for the actual yield strength given the specified minimum value. In the CSA S16-09 (CSA, 2009), this overstrength is represented by:

$$R_y = \frac{F_{ya}}{F_{yn}} \qquad [2.21]$$

where F_{ya} and F_{yn} are the actual and the nominal (i.e., specified minimum) yield strengths of steel, respectively.

For this purpose, a re-analysis of Schmidt's (2000) steel coupon data was conducted. Over 13,000 coupon test-based yield strengths, conducted on web and flange samples, were analyzed. Table 3.5 classifies these data by the class of W-shape and coupon location. Structural steel sections are designated as Class 1, 2, 3 or 4 based on their susceptibility to local buckling. Class 1 sections are plastic design sections that can sustain the full plastic moment over large plastic rotations. Class 2 sections are compact

sections that can achieve the plastic moment capacity. Class 3 sections are non-compact sections that can attain the yield moment but buckle locally before achieving the plastic moment capacity. Class 4 sections are slender sections that fail by local buckling before the yield moment is reached.

Schmidt (2000) reported that the bias coefficients for the yield strength of specimens obtained from the flanges of W-shapes rolled by different producers, varied from 1.04 to 1.17 with CoV values ranging from 0.037 to 0.056. The values of 1.11 and 0.063 were adopted to represent the current production. However, these values are calculated for all classes of W-shapes, and hence are not appropriate for links which are typically Class 1 sections. Hence, additional analysis is required to compute the bias coefficients and CoV values for flange coupons taken from Class 1 W-sections.

CSA G40.20 (CSA, 2009a) requires coupons to be taken from the flange if the total flange width exceeds 150mm. For smaller flange widths the coupons are taken from the web. Scatter plots were created to identify potentially significant parameters. Although a US specification, A992 steel includes all steel currently used in Canada because it is written to satisfy the requirements of CSA G40.21-Grade 350W (CSA, 2005).

Table 3.4: Tensile properties for various grades of structural steel (Dexter et al. 2002)

ASTM Specification	**F_y ksi (MPa)**	**F_u ksi (MPa)**
A 992	50-65 (250-350)	65 min(450)
A 36	36 min (250)	58-80(400-550)
A 572 Grade 50	50 min(250)	65 min(450)
A 572 Grade 60	60 min(415)	75 min(520)
A 572 Grade 65	65 min(450)	80 min(550)
A 913 Grade 50	50 min(250)	65 min(450)
A 913 Grade 65	65 min(450)	80 min(550)

Table 3.5: Classification of coupon data

Class of Shape	No. of Web Coupons	No. of Flange Coupons	Total Number
1	1721	5996	7717
2	1235	2824	4059
3	239	1122	1361
4	110	711	821

3.4.1 PLOTS OF R_y VERSUS VARIOUS PARAMETERS

Typically Class 1 W-shapes are used for link sections. A total of 7717 coupon test results are available, with 1721 web coupons and 5996 flange coupons with R_y values ranging from 0.968 to 1.588. For each strength test result the following parameters are known: the nominal depth, d; and mass, m, of the shape; the coupon thickness, w_c; and, whether the coupon was obtained from the web or the flange.

Scatter plots showing the variation of R_y with these variables were prepared. No discernable trends were noted except that R_y is slightly greater if the coupon is obtained from the web of the shape instead of the flange. This is consistent with the long-known observation that the yield strength of the web is in the order of 5% greater than the yield strength of the flange (e.g. Kennedy and Gad Aly, 1980). Figure 3.16 shows the variation of R_y with the mass of the shape: no trend is discernable.

Regression analysis yielded the fitted equation:

$$R_y = 1.136 + 0.045 * Z_w \qquad [3.6]$$

where Z_w is an indicator variable (e.g. Montgomery, Peck and Vining, 2006) set equal to 1 if the coupon is obtained from the web or 0 if it is obtained from the flange. The coupon

location is statistically significant ($p \leq 0.02$) and Equation [3.6] has a standard error of 0.0617. As links typically have flanges of sufficient width that the coupon will be taken from the flange, the associated factor for actual-to-nominal strength has a mean value of 1.136. However, as described in Chapter 2, short links dissipate energy by web yielding. Web sections in W-shapes are typically 4-5% stronger than flange sections: this factor is accounted for in the overstrength values (R_{str}) which are reported with respect to coupons taken from the flange. The residual errors of Equation [3.7] were found to be independent of parameters, d, m, w_c and approximately normally distributed. Thus Equation [3.6] is considered adequate.

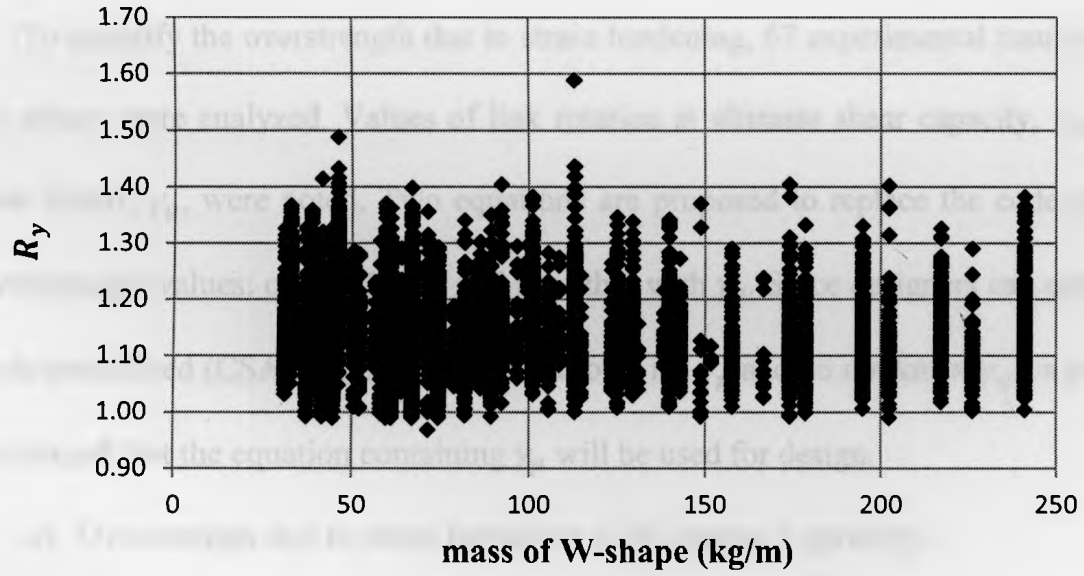

Fig. 3.16: R_y versus mass of W-shape (kg/m)

In CSA-S16-09, the value of R_y is taken equal to 1.1. Equation [3.6] which is derived using yield strength data for Class-1 W-shapes, indicates that the mean value of R_y is higher and equals 1.136, with a CoV value of 0.0617. The strength of both the brace and

the link section is affected by the variation in probable yield strength. Chapter 4 discusses the effect of the statistical parameters of R_y on the demand and the resistance equations in greater detail.

3.5 SUMMARY

In summary, overstrength exhibited by energy-dissipating links in eccentrically braced frames has been quantified in terms of two factors:

a) Overstrength due to strain hardening in W-shape links and

b) Overstrength due to the actual yield strength exceeding the specified minimum value

To quantify the overstrength due to strain hardening, 67 experimental results obtained by others were analyzed. Values of link rotation at ultimate shear capacity, γ_{ult}, and at link failure, γ_p, were noted. Two equations are proposed to replace the code-prescribed overstrength values: one with γ_{ult} and the other with γ_p. Since designers can compute the code-prescribed (CSA S16-09) plastic rotations, i.e. γ_p and do not know γ_{ult} a-priori, it is envisaged that the equation containing γ_p will be used for design.

a) Overstrength due to strain hardening in W-shapes is given by:

$$R_{str} = 1.057 - 0.251 \frac{e}{M_p / V_p} + 2.515\,\gamma_{ult} + 0.360\,\frac{F_u}{F_y} \qquad [3.3]$$

For this equation, $R^2 = 0.9061$, the p-value is 10^{-5} and the standard error is 0.087. The Coefficient of Variation for R_{str} was observed to vary with link length: it varies from 0.045 for very short links to 0.112 for long links.

b) For design practice, the Proposed Design Equation is:

$$R_{str} = 0.9515 + 0.563\left(\frac{F_u}{F_y}\right) + 1.629\,\gamma_p - 0.288\,\frac{e}{M_p/V_p} - 0.0064\,\frac{a}{a_o} \qquad [3.4]$$

For this equation, R^2 = 0.910, the p-value is 10^{-5} and the standard error is 0.093. The CoV of R_{str} was again observed to vary: it is 0.052 for very short links to 0.105 for long links. By substituting the values for normalized link length and stiffener spacing, both of which are chosen by the designer, the value of plastic link rotation computed using Equation [3.1] and the mean value of F_u/F_y, 1.43, the designer can get an estimate of R_{str} for the specific design.

The coefficient of variation of test/predicted ratios for the mean value of overstrength factor of test results is 0.169, while it is 0.071 for the generic Equation [3.3] and is 0.072 for the Proposed Design Equation [3.4].

To model overstrength due to higher yield strengths, 7717 steel coupon data for Class-1 shapes reported by Schmidt (2000) were analyzed. Only the coupon location, i.e. whether it is obtained from the web or flange of the W-section, was found to be a statistically significant parameter. In this case, the fitted equation is:

$$R_y = 1.136 + 0.045\,Z_w \qquad [3.6]$$

where Z_w is an indicator variable set equal to 0 for flange or 1 for web coupons. The p-value for this model is 10^{-6} and the standard error is 0.0617. Clearly, the value of R_y obtained from this equation is 3.3% higher than the R_y value (= 1.1) specified in CSA

S16-09. The fit indicates that web coupons are on average 3.96% stronger than flange coupons.

CHAPTER 4: RELIABILITY INDICES AND CALIBRATION OF RESISTANCE FACTOR

4.1 INTRODUCTION

Reliability indices for the Canadian steel design code CSA S16-09 (CSA, 2009) provisions for Capacity-Based Design of Eccentrically Braced Frames (EBF) have not been derived previously. Steel design in Canada at Ultimate Limit States is generally based on the limit states design equation:

$$\phi R \geq \Sigma \alpha_i S_i \qquad [1.1]$$

where ϕ is the resistance factor, R is the nominal resistance computed for tabulated section properties and specified minimum material strengths, α_i is the load factor and S_i is the nominal load effect for applied load type i. The summation on the right hand side recognizes that the critical load combination is the sum of load effects caused by different types of loads. Values of load and resistance factor are determined by calibration to ensure that target reliability indices are achieved. These can be obtained by various methods (e.g. Madsen, Krenk and Lind, 1986) but for code calibration has historically been determined using a first-order second-moment method as:

$$\beta = \frac{\ln\left(\frac{m_R}{m_S}\right)}{\sqrt{{v_R}^2 + {v_S}^2}} \qquad [4.1]$$

where, m_R represents the mean value of the resistance, m_S represents the mean value of

the total load effect, v_R and v_S represent the coefficients of variation of the resistance and the total load effect, respectively, and β is the reliability index. Typical values of reliability index used for design are presented in guidelines such as CSA S408 (CSA, 1981) and were reviewed in Bartlett et al. (2003). A target value of the 50-year reliability index of 3.0 was deemed sufficient for ductile failure and could be further increased by 0.5 to 3.5 for brittle failure. Assuming braces have some ductility, a 50-year target reliability index of 3.0 is deemed adequate.

Members and connections designed using Capacity-Based Design are proportioned using the limit state design equation:

$$\phi R \geq R_{min} \qquad [1.2]$$

where R_{min} is the expected capacity of the fuse element. Log-normal distributions for the resistance of non-fuse member or connection, R, and the expected demand of the fuse element, R_{min}, are assumed. To the writer's knowledge, reliability indices for the non-fuse components of eccentrically braced frames designed in accordance with the Canadian steel design code, CSA S16-09 (2009) have not been determined previously. The single overstrength factor specified for EBFs has been shown in Chapter 3 to be insufficient for short links $e/(M_p/V_p) \leq 1.6$, which undergo significant plastic rotations causing marked strain hardening in the link region, and conservative for long links, $e/(M_p/V_p) \geq 2.6$, that undergo lesser plastic rotations and so experience much less strain hardening. Hence a reliability analysis for both the current and the proposed code provisions can quantify this perceived non-uniformity using failure probabilities.

4.1.1 OBJECTIVES

The objective of the research reported in this chapter is to determine the reliability index for compression braces in Eccentrically Braced Frames designed using Capacity-Based Design procedures specified in CSA S16-09. Reliability indices will also be computed using the Proposed Design Equation developed in Chapter 3, which accounts for the dependence of the link overstrength on various parameters including the normalized link length, $e/(M_p/V_p)$. Based on these studies, recommendations will be made on the adoption of the proposed overstrength equation and an associated resistance factor for the next edition of CSA S16.

4.2 STATISTICAL PARAMETERS FOR DEMAND

The general expression for the nominal demand imposed on a compression brace is:

$$R_{min} = K\, R_{str}\, R_y\, V_p \qquad [4.2]$$

where R_{min} is the expected capacity of fuse element, R_{str} is the overstrength due to strain hardening and R_y is the overstrength due to higher than nominal yield strength. K is a geometric factor, assumed to be deterministic, that converts the shear in the link to the axial force in the brace, given by:

$$K = [1+e/(L-e)]/\sin\alpha \qquad [4.3]$$

where e is the length of the link, L is the span length and α is the angle between the brace and the beam. Finally, V_p in Equation [4.2] represents the shear capacity of the link, given by:

$$V_p = 0.55\, wdF_y \qquad [2.17]$$

where d is the depth of the W-shape, w is the width of the web and F_y is the yield strength of the steel.

R_y was determined in Chapter 3 to be:

$$R_y = 1.136 + 0.045\, Z_w \qquad [3.6]$$

where Z_w = 0 for coupons taken from the flange or 1 for coupons taken from the web. When computing the value of R_y in this chapter, Z_w is assumed to be zero because the equations for R_{str} have been derived based on actual yield strengths of flange coupons reported by the original investigators as described in Chapter 3.

4.2.1 OVERSTRENGTH DUE TO STRAIN HARDENING

Determining statistical parameters to quantify R_{str} is somewhat complicated and so will be described in detail. The general equation for R_{str} is:

$$R_{str} = \{A + B\,[e/(M_p/V_p)\,] + C\,\gamma_{ult} + D\,(F_u/F_y)\} + \varepsilon \qquad [4.4]$$

where γ_{ult} is the peak rotation, $e/(M_p/V_p)$ is the normalized link length and F_u/F_y is the ratio of ultimate tensile strength to yield strength. In Chapter 3, Parameters A through D were determined by linear regression and the resulting equation is:

$$R_{str} = 1.051 - 0.251 \frac{e}{M_p/V_p} + 2.515\,\gamma_{ult} + 0.360\,\frac{F_u}{F_y} \qquad [3.3]$$

The model error is represented by ε, which quantifies the imperfect fit of Equation [3.3] to the data. It has a mean value of 0 and a standard deviation of 0.087, as reported in Section 3.3.2.

The statistical parameters for R_{str} must be computed recognizing that some of the variables on the right side of Equation [4.4] are random and others are deterministic. Specifically, $e/(M_p/V_p)$ is deterministic, γ_{ult} is random but dependent on $e/(M_p/V_p)$ and F_u/F_y is random. The mean overstrength factor is therefore:

$$\overline{R_{str}} = A + B\,[e/(M_p/V_p)] + C\,\widehat{\gamma_{ult}} + D\,\overline{(\frac{F_u}{F_y})} \qquad [4.5]$$

where $\widehat{\gamma_{ult}}$ is computed for the assumed $e/(M_p/V_p)$ using Equation [3.2] and $\overline{(\frac{F_u}{F_y})}$ is 1.43 for ASTM A992 steel as determined by the analysis in Chapter 3 of coupon data reported by Schmidt (2000). The variance of the overstrength factor can be determined, recognizing that the random part of Equation [4.5] is given by:

$$X = C\,\gamma_{ult} + D\,\frac{F_u}{F_y} + \varepsilon \qquad [4.6]$$

Assuming constants C and D to be deterministic and the other variables to be statistically independent of each other:

$$\sigma_x^2 = C^2\sigma_{\gamma_{ult}}^2 + D^2\sigma_{\frac{F_u}{F_y}}^2 + \sigma_\varepsilon^2 \qquad [4.7]$$

where $\sigma_{\gamma_{ult}}^2$ is the mean square error of Equation [3.2], used to compute the γ_{ult} values, $(0.0114)^2$, $\sigma_{\frac{F_u}{F_y}}^2$ is the variance of the $\frac{F_u}{F_y}$ values for A992 steel computed in Section 3.3.1, $(0.054)^2$, and σ_ε^2 is the mean square error of the linear regression fit, $(0.087)^2$. Hence the coefficient of variation of R_{str} is:

$$v_{R_{str}} = \frac{\sqrt{\sigma_x^2}}{R_{str}} = \frac{\sqrt{C^2\sigma_{\gamma_{ult}}^2 + D^2\sigma_{\frac{F_u}{F_y}}^2 + \sigma_\varepsilon^2}}{A + B\,[e/(M_p/V_p)] + C\,\overline{\gamma_{ult}} + D(\overline{\frac{F_u}{F_y}})} \qquad [4.8]$$

4.2.2 SUMMARY OF STATISTICAL PARAMETERS FOR DEMAND

Table 4.1 shows the statistical parameters for demand. The mean value and the coefficient of variation of R_{str} are variable as implied by Equations [4.5] and [4.8], respectively. The statistical parameters for R_y are as obtained in the regression analysis presented in Chapter 3. The coefficient of variation of R_y is taken to be zero when computing the nominal resistance, but its true uncertainty must be accounted for in the demand. The von Mises constant and geometry factor, K, are assumed to be deterministic. The statistical parameters for the width and the depth of the W-section are as reported by Schmidt and Bartlett (2002a).

Table 4.1: Statistical Parameters for Demand

Parameters	Mean	CoV
Width, w	δ_w = 1.01	0.014
Depth, d	δ_d = 1.01	0.001
Geometry Constant, K	deterministic (δ = 1)	0
von Mises Constant, 0.55	deterministic (δ = 1)	0
R_{str}	$\overline{R_{str}}$ varies (see Eq.[4.6])	varies (see Eq.[4.9])
R_y	$\overline{R_y}$ = 1.136	0.0617

The mean value of demand, $\overline{R_{min}}$ computed using the bias coefficients shown in Table 4.1 is:

$$\overline{R_{min}} = \delta_w \delta_d \, \overline{R_y} \, \overline{R_{str}} \, R_{min} \qquad [4.9]$$

where the symbol δ is the bias coefficient, or mean-to-nominal value, for the parameter indicated by the subscript and R_{min} is the nominal fuse capacity as given by Equation [4.2].

The coefficient of variation (CoV) for demand, $v_{R_{min}}$, is computed as:

$$v_{R_{min}} = \sqrt{\left(1 + {v_{R_{str}}}^2\right)\left(1 + {v_{R_y}}^2\right)(1 + {v_w}^2)(1 + {v_d}^2) - 1} \qquad [4.10]$$

where the CoV of each parameter is represented by the symbol v with the parameter as the subscript.

4.3 STATISTICAL PARAMETERS FOR RESISTANCE

In general, the resistance of a structural member, R can be computed as:

$$R = R_n GMPD \qquad [4.11]$$

where R_n is the nominal resistance, D is the discretization factor and G, M, and P are the geometric, material and professional factors, respectively. The professional factor, P, is computed using the test- to-predicted ratios, where the predicted value is computed for the known geometric and material properties of each test specimen and so quantifies the accuracy of the equation used to predict the resistance. The discretization factor, D, quantifies the constraint that a cross-section be selected from a discrete number of available shapes that provides a resistance at least equal to that required.

Statistical parameters for geometrical and material factors are available in the literature (e.g., Bartlett et al, 2003; Schmidt and Bartlett, 2002a; 2002b). The statistical parameters used in the present study for the geometric factor, G (in this case representing area of the W-shape, A), professional factor, P, discretization factor, D, and the material factor representing the capacity based on yielding or buckling, M, are as reported by Schmidt (2000). The randomness of the geometric factor is accounted for, although its coefficient of variation is small compared to those of the other parameters in Equation [4.11]. The statistical parameters for the professional factor, P, vary with the dimensionless slenderness parameter λ (Schmidt, 2000):

$$\lambda = \frac{kL}{r}\sqrt{\frac{F_y}{\pi^2 E}} \qquad [4.12]$$

where kL/r is the slenderness ratio, and E is Young's modulus of steel. For a typical brace with $\lambda = 0.8$, $\bar{P} = 1.1$ and $v_p = 0.1$ (Schmidt, 2000).

The statistical parameters of the material parameter, M, differ for yielding, inelastic buckling and elastic buckling failure modes and so also depend on λ. For stocky columns ($\lambda = 0$) they reflect the bias and uncertainty of the yield strength whereas for slender columns ($\lambda = \infty$) they reflect the bias and uncertainty of Young's modulus. Schmidt (2000) accounted for this by defining M as:

$$M = F_y C_\lambda \qquad [4.13]$$

where

$$C_\lambda = (1 + \lambda^{2n})^{\frac{-1}{n}} \qquad [4.14]$$

The parameter,n, depends on the magnitude of residual stress in the section and so depends on the means of manufacturing the shape. For hot rolled W-shapes, n =1.34. For $\lambda = 0.8$ and n =1.34, the nominal value of C_λ is 0.721 with a bias coefficient (Schmidt, 2000) of 1.09 and a coefficient of variation of 0.035.

The nominal resistance, R_n, will be computed using the following two methods:

a) CSA S16-09 Equation, and

b) Proposed Design Equation

As the nominal resistances computed using these two equations are different, the associated reliability indices will be different. In both cases, the values used are nominal

values assumed by the designer and so are deterministic. These two methods are described in detail in Section 4.3.1 and Section 4.3.2.

4.3.1 RESISTANCE STATISTCAL PARAMETERS USING CSA S16-09

The design resistance R_d using CSA S16-09 (CSA, 2009) is:

$$R_d = K\ (1.3)\ 1.1\ V_p \qquad [4.15]$$

where K represents the geometry factor, computed using Equation [4.3], 1.3 accounts for the overstrength due to strain hardening, 1.1 accounts for the overstrength due to higher-than-nominal yield strength and V_p is the nominal shear capacity of the link as computed using Equation [2.17]. The nominal resistance is $R_n = R_d/\phi$.

4.3.2 RESISTANCE STATISTICAL PARAMETERS USING PROPOSED DESIGN EQUATION

The design resistance determined using the Proposed Design Equation is:

$$R_d = K\ R_{str}\ R_y\ V_p \qquad [4.16]$$

where R_{str} is computed using:

$$R_{str} = 1.143 + 0.372\left(\frac{F_u}{F_y}\right) + 1.413\gamma_p - 0.269\frac{e}{M_p/V_p} - 0.0044\frac{a}{a_o} \qquad [3.4]$$

where γ_p represents the plastic rotation capacity and a/a_o is the normalized stiffener spacing. All parameters in Equations [3.4] and [4.17] are deterministic because they are selected by the designer to determine a nominal demand. The designer will also assume F_u/F_y to be equal to its mean value of 1.43 (for ASTM A992 steel), and will adopt an appropriate value of a/a_o. In Equation [3.4], the designer will compute γ_p as a function of normalized link length, $e/(M_p/V_p)$ according to CSA S16-09 (CSA, 2009). For short links, $e/(M_p/V_p) \leq 1.6$, γ_p is 0.08 rad and for long links, $e/(M_p/V_p) \geq 2.6$, γ_p is 0.02 rad. For intermediate links, $1.6 \leq e/(M_p/V_p) \leq 2.6$:

$$\gamma_p = 0.08 - 0.06[e/(M_p/V_p) - 1.6] \qquad [3.1]$$

Similarly, R_y in the proposed design equation is computed, using Equation [3.6], to be 1.136 because the test coupon will typically be taken from the flange.

4.3.3 SUMMARY OF STATISTICAL PARAMETERS FOR RESISTANCE

Table 4.2 shows the statistical parameters for resistance. The statistical parameters are the same whether the brace is designed using the CSA S16-09 procedure (Equation [4.15]) or the proposed design equation (Equation [4.16]).

Table 4.2: Statistical Parameters for Brace Resistance

Parameters	Bias Coeff., δ	CoV, ν
Area, *A*	1.03	0.031
Professional, *P*	1.10	0.10
Discretization, *D*	1.05	0.033
Material, *M*	1.09	0.035

If the resistance of the brace is determined using Equation [4.11], its mean resistance is:

$$m_R = \delta_A \, \delta_P \, \delta_D \, \delta_M \, R_d/\phi \qquad [4.17]$$

where R_d is computed using Equation [4.16] in accordance with CSA S16-09 or using Equations [4.16], [3.4] and [3.6] for the Proposed Design Equation. The mean resistance of the brace, m_R is computed using the bias coefficients shown in Table 4.2. Again the various bias coefficients δ correspond to the parameter shown by each subscript. The coefficient of variation (CoV) for resistance, v_R, is:

$$v_R = \sqrt{(1 + v_A{}^2)\,(1 + v_M{}^2)(1 + v_P{}^2)\,(1 + v_D{}^2) - 1} \qquad [4.18]$$

where the various coefficients of variation correspond to the parameter shown by each subscript.

4.4 EXAMPLE CALCULATION OF EBF RELIABILITY INDICES

Figure 4.1 shows the Eccentrically Braced Frame that will be analyzed in this example calculation. The frame height is 3.2 metres and a W 310 x 226 is chosen as the link section. This shape has d = 348mm, w = 22.1 mm, M_p/V_p = 0.83m, and F_y = 345 MPa. For the frame width of 6.0m and link length of 1.25m, the brace angle is 53.4°. From Equation [4.3], K =1.573.

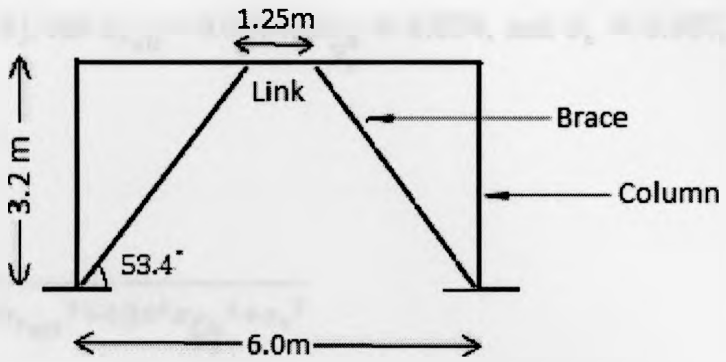

Fig. 4.1: Example Eccentrically Braced Frame.

The nominal shear capacity of the link, V_p, is

$$V_p = 0.55wdF_y = 1460 \text{ kN} \qquad [2.17a]$$

In this case $e/(M_p/V_p) = 1.51$ and, from Equation [3.2], $\widehat{\gamma_{ult}} = 0.0545$. Substituting these values, with $\overline{(\frac{F_u}{F_y})} = 1.43$ for ASTM A992 steel, into Equation [3.3]:

$$\overline{R_{str}} = 1.057 - 0.251(1.5) + 2.515(0.0545) + 0.360(1.43) = 1.332. \qquad [3.3a]$$

For $\overline{R_y} = 1.136$, the mean demand is therefore:

$$\overline{R_{mın}} = \delta_w \, \delta_d \overline{R_y} \; \overline{R_{str}} \, K \, V_p$$

$$= (1.01)\,(1.01)\,(1.136)\,(1.314)\,(1.573*1458) \text{ kN} \qquad [4.9a]$$

$$= (1.523)\,(2294) \text{ kN} = 3490 \text{ kN}$$

From Equation [4.8], for $\sigma_{\gamma_{ult}}$= 0.0114, $\sigma_{\frac{F_u}{F_y}}$ = 0.054, and σ_ε = 0.087, the coefficient of variation of R_{str} is

$$v_{R_{str}} = \frac{\sqrt{2.515^2\sigma_{\gamma_{ult}}{}^2+0.36^2\sigma_{\frac{F_u}{F_y}}{}^2+\sigma_\varepsilon{}^2}}{1.332} \quad [4.8a]$$

$$= 0.070.$$

So from Equation [4.10], the CoV of demand is:

$$v_{R_{min}} = \sqrt{(1+0.0580^2)(1+0.0617^2)(1+0.014^2)(1+0.01^2)-1} \quad [4.10a]$$

$$= 0.0952.$$

The statistics for resistance will be computed for both the S16-09 design criteria and the Proposed Design Equation. In accordance with the S16-09 criteria, the design resistance of the brace is

$$R_d = K\ (1.3)\ 1.1\ V_p = 3280\ \text{kN} \quad [4.15a]$$

The nominal resistance is R_d and, given the bias coefficients given in Table 4.2, the associated mean resistance is

$$m_R = \delta_A\delta_M\delta_D\delta_M R_d/\phi \quad [4.17]$$

$= 1.03\ (1.1)\ 1.05\ (1.09)\ R_d/\phi$

$= 1.297\ R_d/\phi$

Hence,

$$m_R = (1.297)\ 3280/\phi = 4254/\phi \text{ kN} \qquad [4.17a]$$

The design resistance of the brace as per the Proposed Design Method is:

$$R_d = K\ R_{str} R_y\ V_p \qquad [4.16]$$

where R_{str} is computed using Equation [3.4]. The values for the other parameters are $e/(M_p/V_p) = 1.50$, $\gamma_p = 0.08$, $F_u/F_y = 1.43$ and $a/a_o = 8$. Here a is the stiffener spacing in centrimetres and a_o equals 25.4 centimetres. The value of a/a_o in tested links was observed to range from 3.5 to 17.5 and a value of 8 is used in this example.

$$R_{str} = 1.143 + 0.372(1.43) + 1.413(0.08) - 0.269(1.5) - 0.0044(8) = 1.349 \qquad [3.4a]$$

So,

$$R_d = (1.573)\ (1.349)\ (1.136)\ (1458) = 3515 \text{ kN} \qquad [4.16a]$$

Hence,

$$m_R = (1.297)\, R_d/\phi = (1.297)\, 3514/\phi = 4448/\phi \text{ kN} \quad [4.17b]$$

For either case, the CoV is, using CoV values given in Table 4.2:

$$v_R = \sqrt{(1+0.031^2)\,(1+0.1^2)\,(1+0.033^2)(1+0.035^2)-1} \quad [4.18a]$$

$$= 0.115$$

The associated reliabilities are computed using Equation [4.1]. For design in accordance with CSA S16-09, with $\phi = 0.90$:

$$\beta = \frac{\ln {}^{m_R}/_{m_{R_{min}}}}{\sqrt{V_R{}^2 + V_{R_{min}}{}^2}} = \frac{\ln \frac{(4254/0.9)}{(3494)}}{0.150} = \frac{\ln(1.353)}{0.150} = \frac{0.303}{0.150} = 1.94 \quad [4.1a]$$

For design in accordance with the Proposed Design Method, again with $\phi = 0.90$:

$$\beta = \frac{\ln {}^{m_R}/_{m_{R_{min}}}}{\sqrt{V_R{}^2 + V_{R_{min}}{}^2}} = \frac{\ln \frac{(4448/0.9)}{(3494)}}{0.144} = \frac{\ln(1.415)}{0.150} = \frac{0.347}{0.150} = 2.31 \quad [4.1b]$$

4.5 RELIABILITY OF W-SHAPE BRACES

In this section, the sensitivity of reliability indices for W-shape braces in EBFs proportioned using Capacity-Based Design is investigated for varying normalized link length, $e/(M_p/V_p)$, ratio of the ultimate tensile strength to the yield strength, F_u/F_y, peak link rotation, γ_{ult}, plastic link rotation, γ_p and stiffener spacing ratio, a/a_o. Reliability indices for a) Design in accordance with CSA S16-09 and b) Design in accordance with the Proposed Design Method, are computed and plotted versus the key parameters.

4.5.1 RELIABILITY INDICES FOR CSA S16-09

The variation of the reliability index for braces proportioned using CSA S16-09 with F_u/F_y, $e/(M_p/V_p)$ and γ_{ult} are presented in this section. Figure 4.2 shows the variation of the reliability index with F_u/F_y for normalized link lengths of 1.2, 1.5 and 1.8. The reliability index is independent of F_u/F_y because neither the demand nor the resistance equations account for the variation of F_u/F_y. The mean demand is computed for the mean value of F_u/F_y = 1.43 in Equation [4.9]. The resistance is computed using a constant value of 1.3 for R_{str} in Equation [4.15].

It is observed that the reliability indices are higher for longer links compared to short links. Figure 4.2 shows that the reliability index lies below 3.0 for normalized link length, $e/(M_p/V_p)$ ranging from 1.2 to 1.8. From the test data available from Schmidt (2000), the mean value of F_u/F_y for ASTM grade A992 steel is 1.43. The corresponding reliability indices vary from 1.50 to 2.50 and so are lower than the target reliability index of 3.0. For example, the figure shows that the value of the reliability index is 2.0 for short links with $e/(M_p/V_p)$ =1.5.

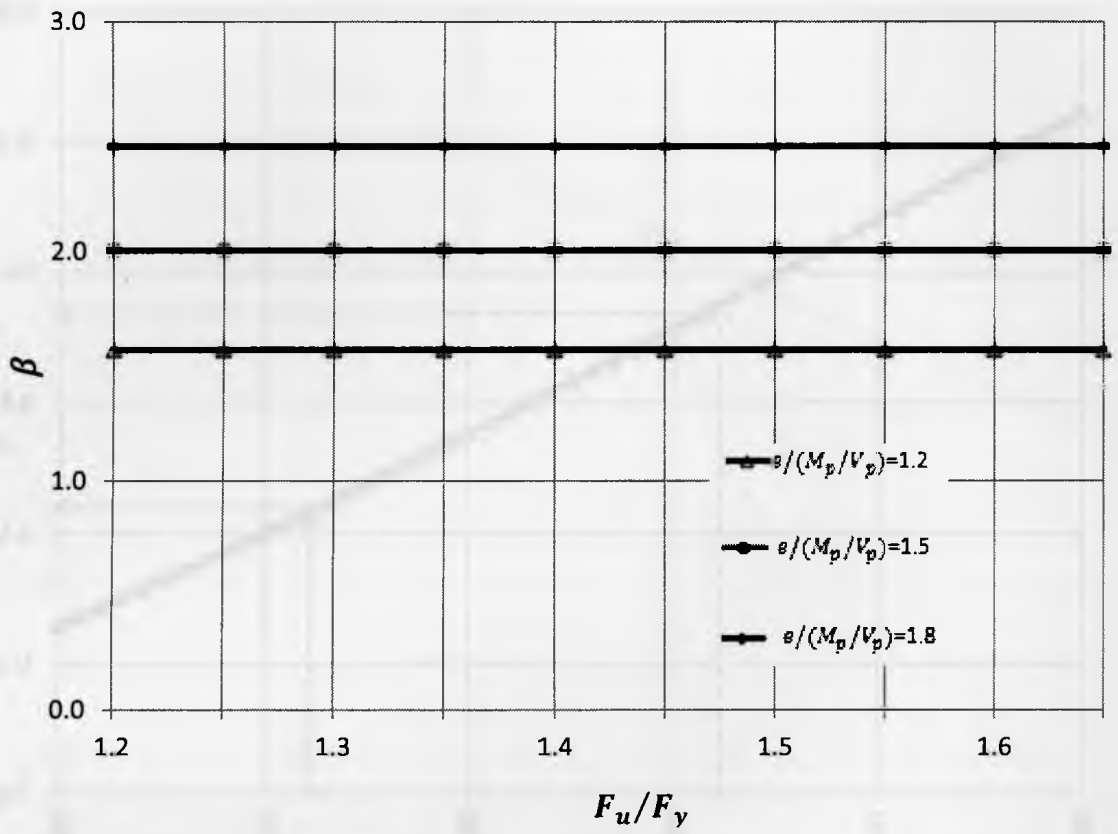

Fig. 4.2: S16-09 Design method: Variation of reliability index with F_u/F_y for $\phi = 0.9$

Figure 4.3 shows variation of reliability index with normalized link length for braces designed according to the provisions of S16-09 with normalized link length for $\phi = 0.9$ and $F_u/F_y = 1.43$. The relationship is almost linear, with short links having small reliability indices and long links having large reliability indices. For short links, $e/(M_p/V_p) \leq 1.6$, the reliability index is between 1.3 and 2.2, which are both much lower than the target value of 3.0. For intermediate links, $1.6 \leq e/(M_p/V_p) \leq 2.6$, the reliability index lies between 2.2 and 3.8 and for long links, $2.6 \leq e/(M_p/V_p)$, it ranges from 3.8 to values above 5.0. This indicates that brace design based on CSA S16-09 is unsafe for short links and overly conservative for long links. Clearly, designs based on S16-09 have non-uniform reliability indices.

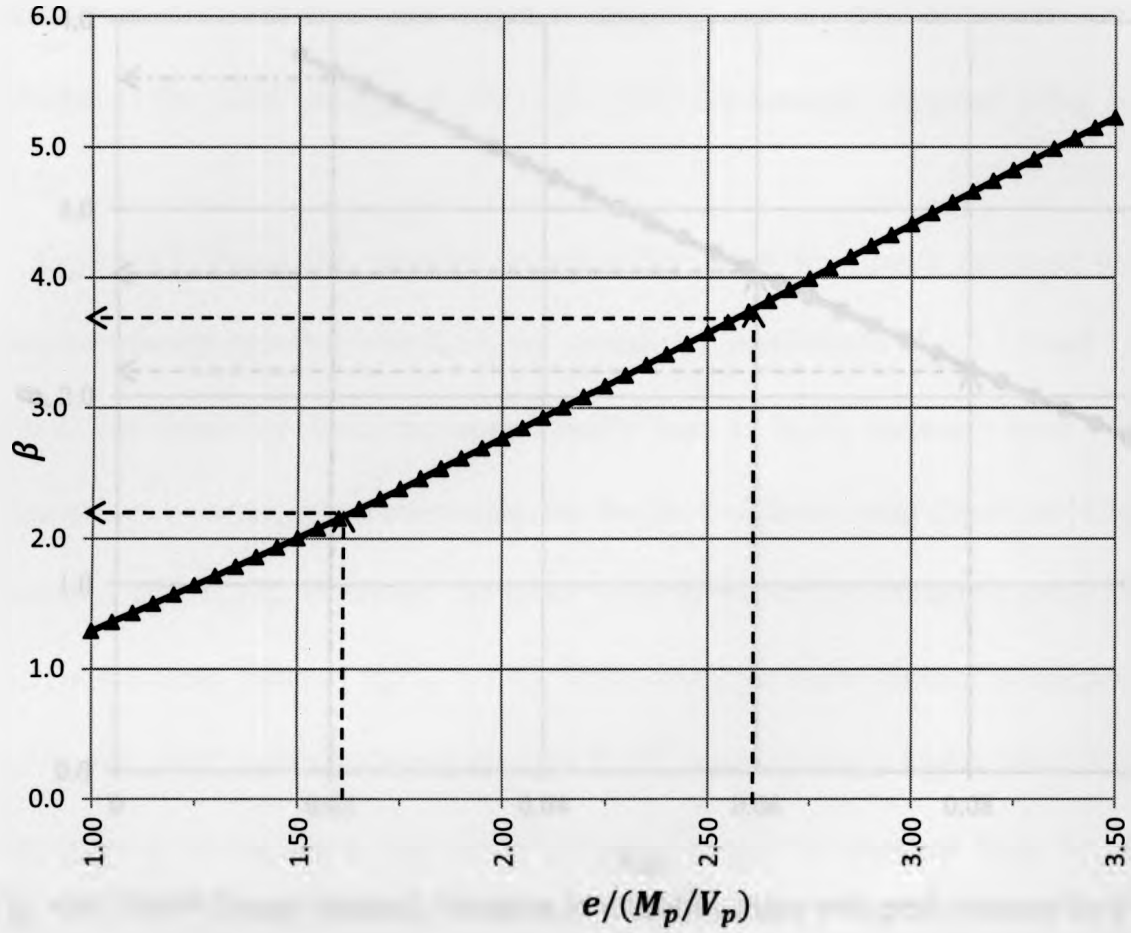

Fig. 4.3: S16-09 Design Method: Variation of reliability index with link length for $\phi = 0.9$

Figure 4.4 shows the variation of the reliability index for braces designed according to S16-09 with peak link rotation, γ_{ult} for $\phi = 0.9$. The reliability index decreases almost linearly with increasing values of peak link rotation. This is entirely consistent with the results shown on Fig. 4.3: short links undergo large peak rotations and long links have small peak rotations. Again clearly the reliability indices are non-uniform and below the target value of 3.0 for the typical range of peak link rotation values, $0.06 \leq \gamma_{ult} \leq 0.08$.

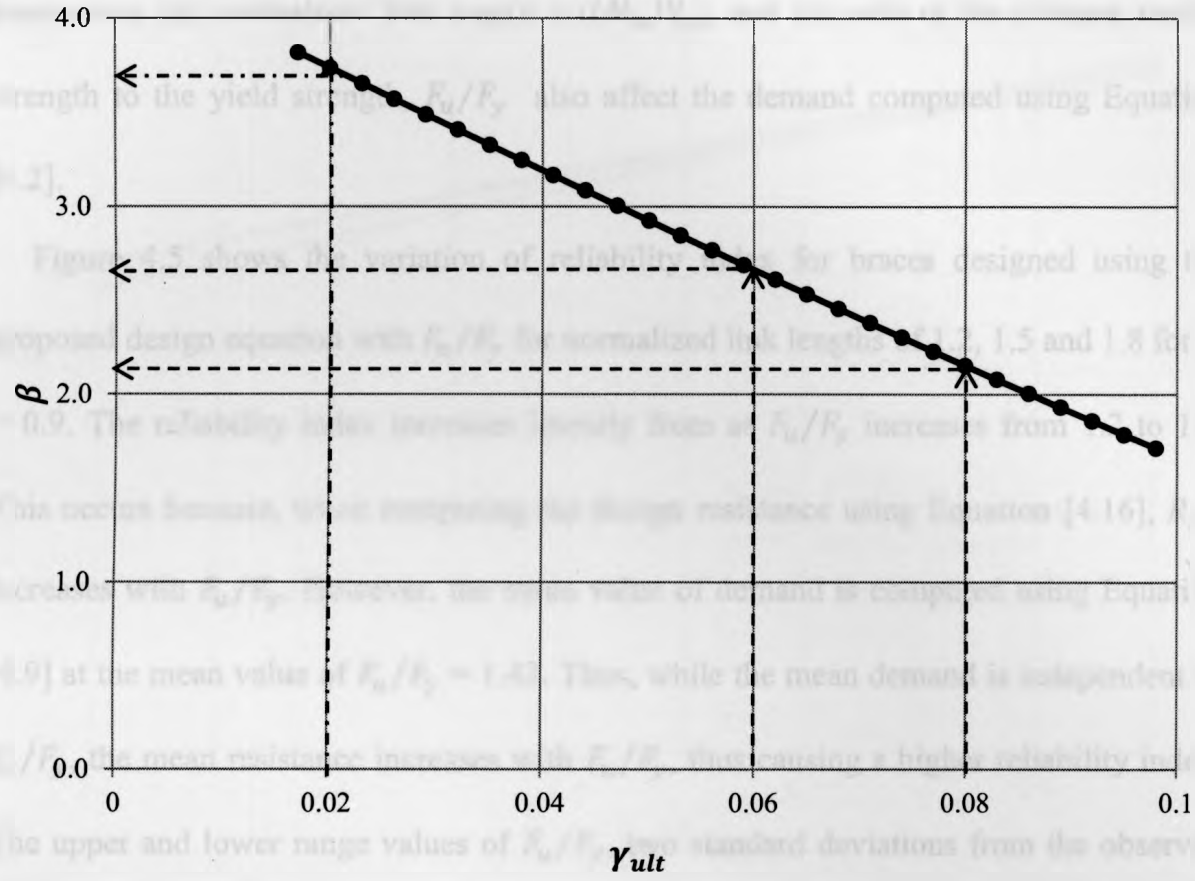

Fig. 4.4: S16-09 Design Method: Variation in reliability index with peak rotation for $\phi = 0.9$

It can be concluded that the reliabilities of compression braces designed using the current criteria in CSA S16-09 are not consistent and often markedly less than those for other load combinations at the Ultimate Limit State.

4.5.2 RELIABILITY INDICES USING PROPOSED DESIGN EQUATION

In this section, the reliability values are presented for braces proportioned using the Proposed Design Equation for four key parameters: normalized link length, $e/(M_p/V_p)$; plastic link rotation, γ_p; ratio of the ultimate tensile strength to the yield strength, F_u/F_y; and, stiffener spacing, a/a_o. These four parameters are selected for investigation because they are used in Equation [3.4] to compute the design resistance. Two of these

parameters, the normalized link length, $e/(M_p/V_p)$, and the ratio of the ultimate tensile strength to the yield strength, F_u/F_y also affect the demand computed using Equation [4.2].

Figure 4.5 shows the variation of reliability index for braces designed using the proposed design equation with F_u/F_y for normalized link lengths of 1.2, 1.5 and 1.8 for ϕ = 0.9. The reliability index increases linearly from as F_u/F_y increases from 1.2 to 1.6. This occurs because, when computing the design resistance using Equation [4.16], R_{str} increases with F_u/F_y. However, the mean value of demand is computed using Equation [4.9] at the mean value of F_u/F_y = 1.43. Thus, while the mean demand is independent of F_u/F_y, the mean resistance increases with F_u/F_y, thus causing a higher reliability index. The upper and lower range values of F_u/F_y, two standard deviations from the observed mean (i.e. mean$\pm 2\sigma$) are 1.545 and 1.329 respectively. The reliability index varies from 2.25 to 2.65 for this range of F_u/F_y.

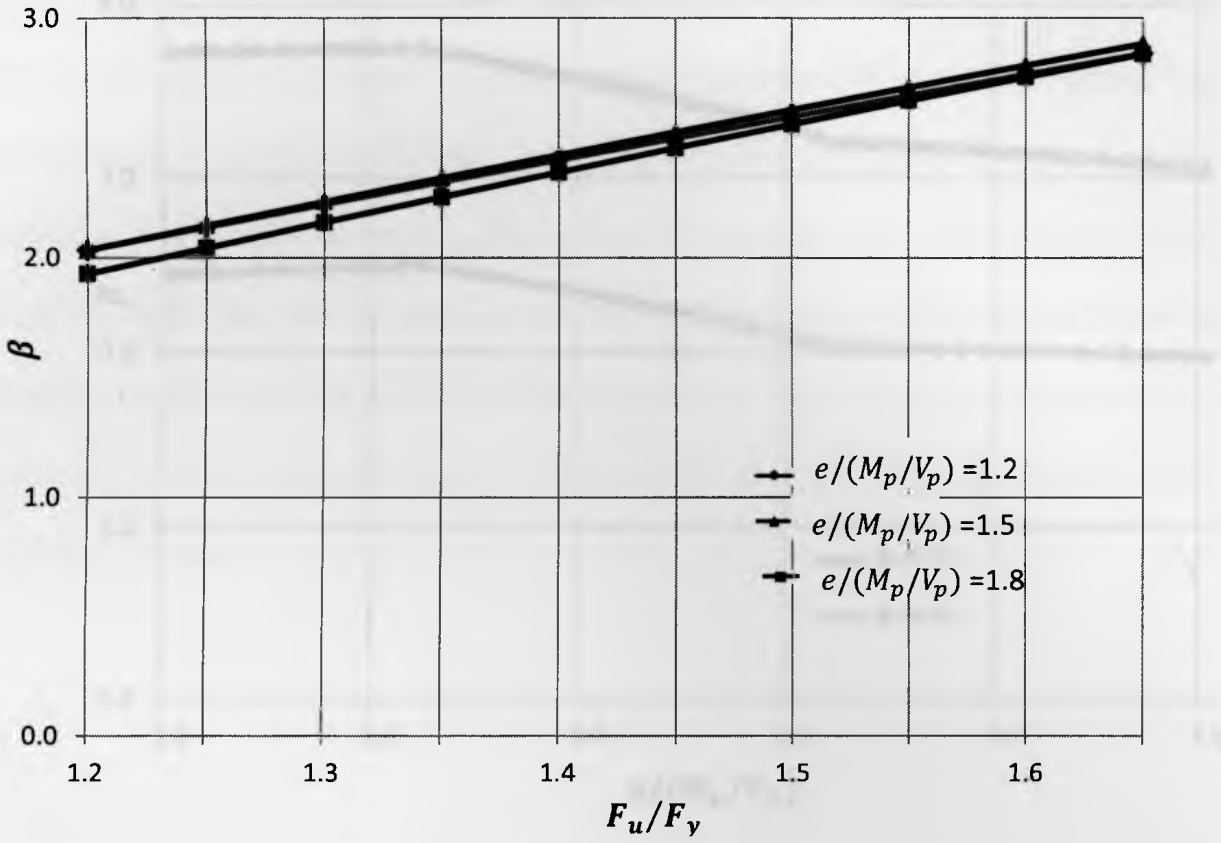

Fig. 4.5: Proposed Design Equation: Variation of the reliability index with F_u/F_y at $\phi = 0.9$

Figure 4.6 shows variation of reliability index for braces designed using the Proposed Design Equation with normalized link length for ϕ = 0.90 and 0.75. The reliability indices range from 2.2 to 2.8 for $\phi = 0.90$ and from 3.0 to 3.7 for $\phi = 0.75$. A slight variation is observed in the plot, which is attributed to the variation in the coefficient of variation (CoV) of R_{str}, Equation [4.8], which varies with the link length and affects the CoV of the demand, Equation [4.10]. Figure 4.7 shows the variation of the CoVs of R_{str} and demand with the normalized link length. The CoV values increase with increasing link length and hence lead to a decrease in the corresponding reliability indices.

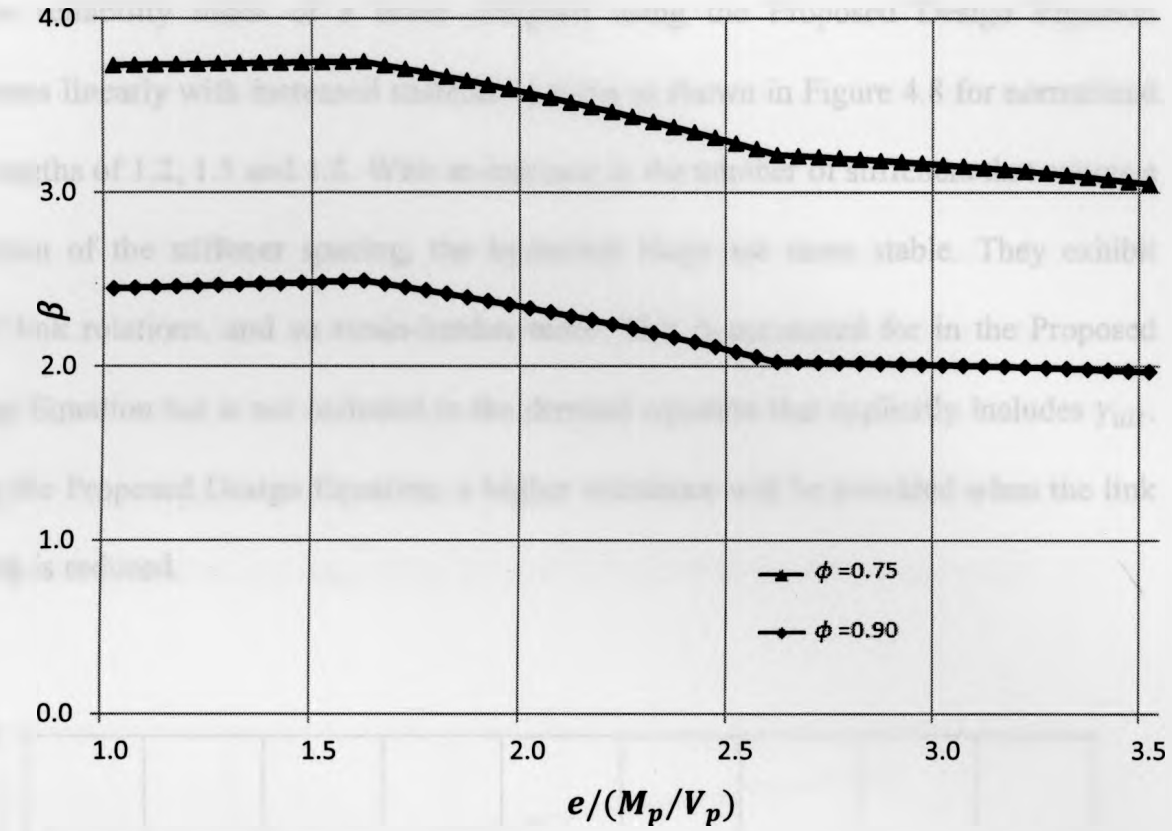

Fig.4.6: Proposed Design Equation: Variation of the reliability index with normalized link length

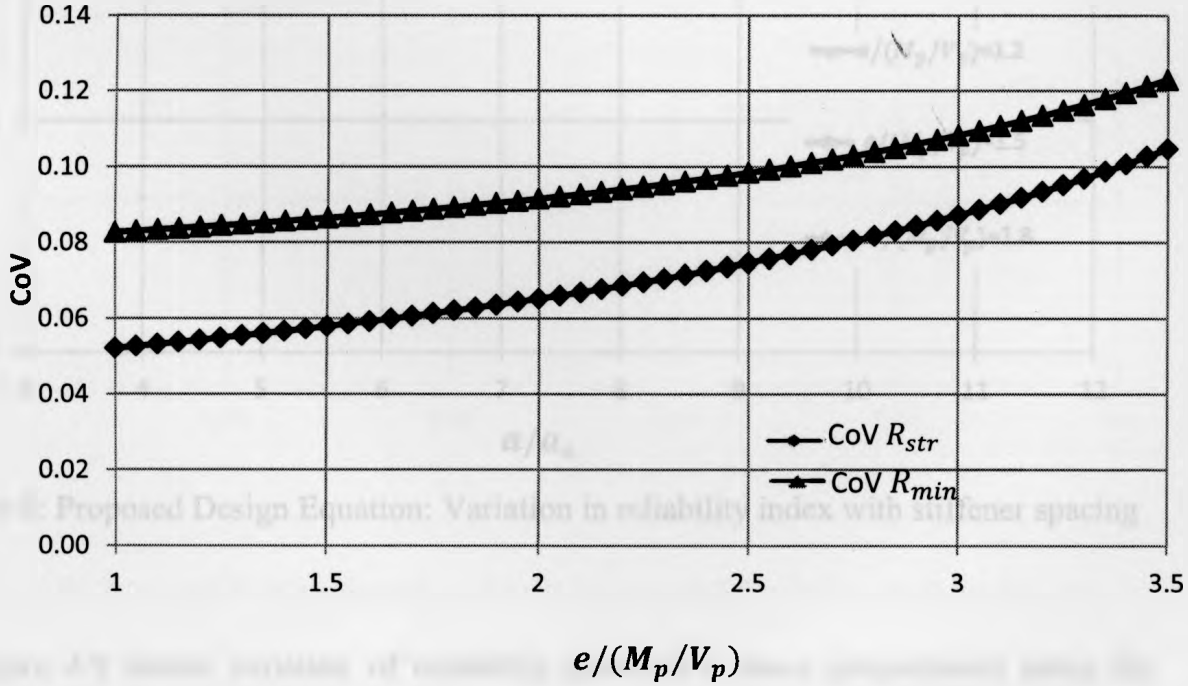

Fig.4.7: Proposed Design Equation: Coefficient of Variation versus normalized link length

The reliability index of a brace designed using the Proposed Design Equation decreases linearly with increased stiffener spacing as shown in Figure 4.8 for normalized link lengths of 1.2, 1.5 and 1.8. With an increase in the number of stiffeners that causes a reduction of the stiffener spacing, the hysteresis loops are more stable. They exhibit larger link rotations, and so strain-harden more. This is accounted for in the Proposed Design Equation but is not included in the demand equation that explicitly includes γ_{ult}. Using the Proposed Design Equation, a higher resistance will be provided when the link spacing is reduced.

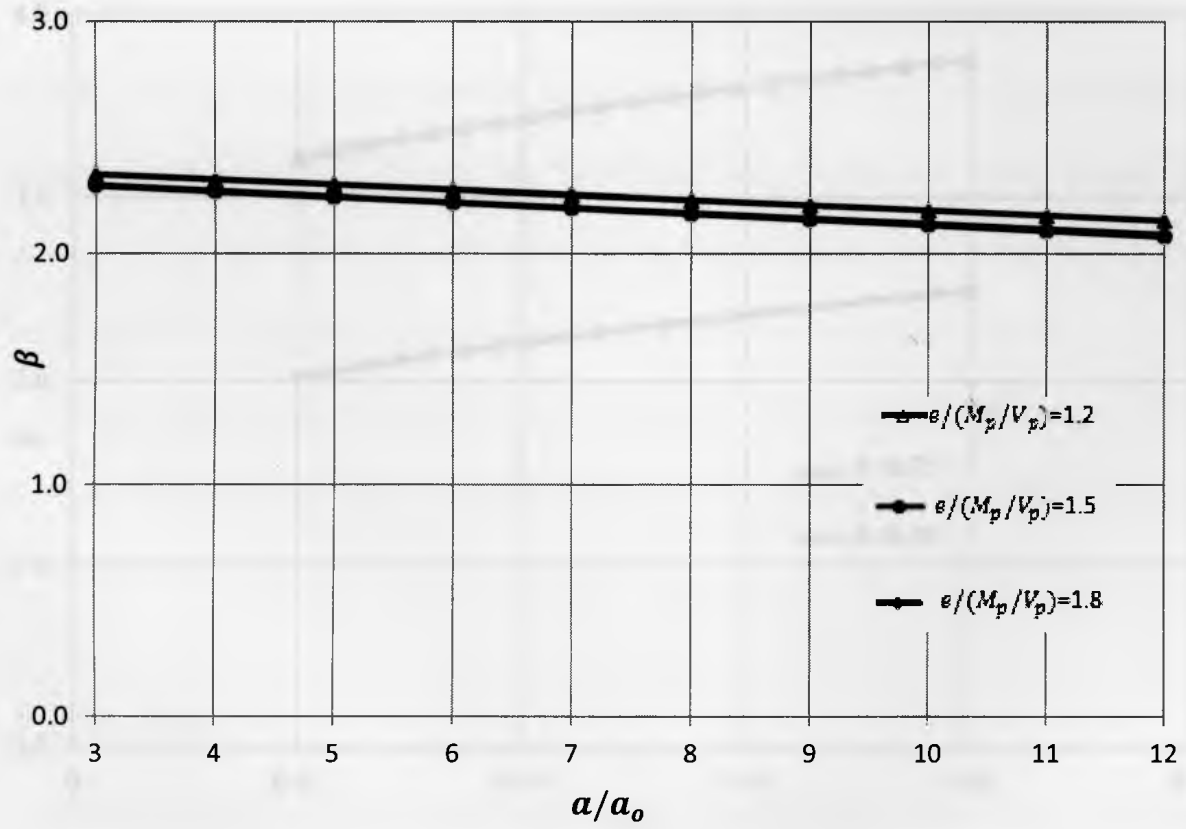

Fig. 4.8: Proposed Design Equation: Variation in reliability index with stiffener spacing

Figure 4.9 shows variation of reliability index of a brace proportioned using the Proposed Design Equation with the plastic link rotation capacity. The reliability indices

increase almost linearly with increasing link rotation values. The coefficient of variation of R_{str}, Equation [4.8], varies with the link length, and hence the plastic rotation capacity, and affects the CoV of the demand, Equation [4.10]. Hence the trend in Figure 4.9 agrees with the trend shown in Figure 4.6. For ϕ = 0.90, the observed value of the reliability index is 2.5 for a plastic link rotation capacity of 0.08 rad which corresponds to a short link. For a plastic link rotation value of 0.02 rad, corresponding to a long link, the reliability index is 2.0. Both values are below 3.0, the target reliability index. For ϕ = 0.75, the reliability indices range from 3.2 and 3.7 and so exceed the target value.

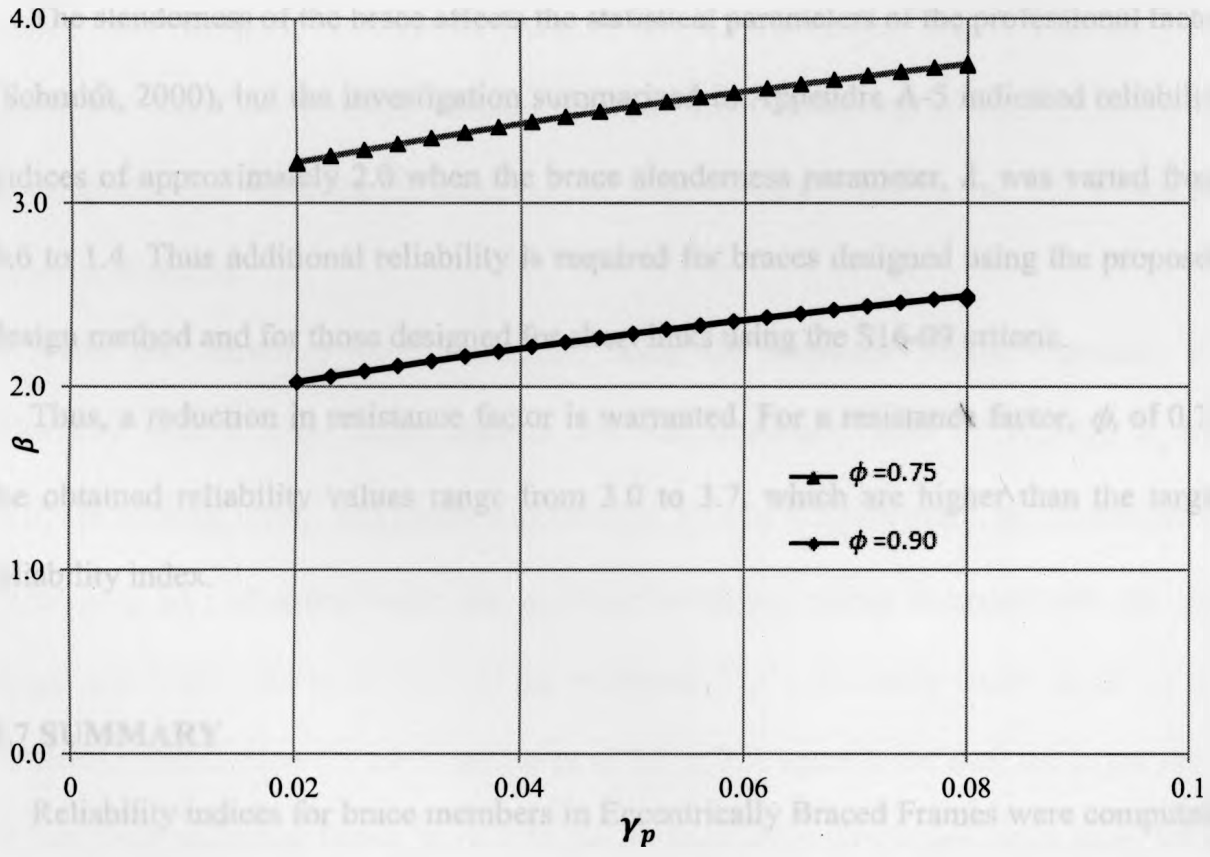

Fig. 4.9: Proposed Design Equation: Variation in reliability index with plastic link rotation

4.6 LOW VALUES OF RELIABILITY INDEX

A value of β of 3.0 for a service life of 50 years was adopted for the derivation of factored load combinations for the 2005 NBCC (Bartlett et al. 2003). Although this value is increased to 3.5 for brittle failures, the braces can be assumed to have some ductility, so a 50-year target reliability index of 3.0 is adequate. In Section 4.5, reliability indices for designs in accordance with the Proposed Design Equation are less than this target value, although they are reasonably insensitive to the feasible range of the design variables considered. For a resistance factor, ϕ, of 0.9 the calculated reliability indices lie in the range of 1.9 to 2.9.

The slenderness of the brace affects the statistical parameters of the professional factor (Schmidt, 2000), but the investigation summarized in Appendix A-5 indicated reliability indices of approximately 2.0 when the brace slenderness parameter, λ, was varied from 0.6 to 1.4. Thus additional reliability is required for braces designed using the proposed design method and for those designed for short links using the S16-09 criteria.

Thus, a reduction in resistance factor is warranted. For a resistance factor, ϕ, of 0.75 the obtained reliability values range from 3.0 to 3.7, which are higher than the target reliability index.

4.7 SUMMARY

Reliability indices for brace members in Eccentrically Braced Frames were computed. Statistical parameters for demand were determined based on the regression analyses presented in Chapter 3. Separate statistical parameters for resistance were computed for cases where the brace is designed using the CSA S16-09 procedure or the Proposed

Design Equation. The coefficients of variation are identical for these two cases but the mean value of the resistances differ. An example calculation was presented to clearly outline the steps involved in the computation of reliability index.

When the resistance was computed using the CSA S16-09 procedure, the reliability indices varied greatly for realistic ranges of the normalized link length, $e/(M_p/V_p)$, and ultimate link rotation, γ_{ult}. They were independent of the ratio of ultimate tensile strength to the yield strength of steel, F_u/F_y, because neither the demand equation nor the resistance equation accounts for this variable, which is not known a priori. The reliability indices were typically less than the target reliability index of 3.0, especially for short links which are most common in practice, where they ranged from 1.3 to 2.2. It is concluded that CSA S16-09 resistance equation leads to variable reliability indices for given parameter variation, especially $e/(M_p/V_p)$, which indicates that this procedure must be modified.

When the resistance was determined using the Proposed Design Equation, the reliability indices were more uniform but varied linearly with $e/(M_p/V_p)$, F_u/F_y, stiffener spacing, a/a_o, and plastic link rotation, γ_p. For this procedure, the coefficient of variation (CoV) of overstrength due to strain hardening, varies inversely with the link length and hence affects the CoV of the resistance. For a resistance factor, ϕ, of 0.9 the obtained reliability indices are in the range of 1.9 to 2.9, again lower than the target value of 3.0. For a resistance factor, ϕ, of 0.75 the obtained reliability values range from 3.0 to 3.7. It is concluded that the proposed design equation leads to uniform reliability indices but still less than the target values. The resistance factor, ϕ, should be reduced to 0.75 to give acceptable reliability values when using the Proposed Design Equation.

CHAPTER 5: SUMMARY AND CONCLUSIONS

This chapter presents a summary of the research conducted on the reliability of compression braces in an Eccentrically Braced Frame (EBF) proportioned by Capacity-Based Design methods. The conclusions and their implications for practice are also presented. Future research is suggested.

5.1 SUMMARY

In Chapter 1, Capacity-Based Design was introduced. It was demonstrated that the use of existing resistance factors to design members using Capacity-Based Design is inappropriate since these factors were originally derived for members subjected to external loads, and the degree of uncertainty is different in the two cases. Thus the basis for re-evaluation of the current resistance factors was established. It was recommended that the calibration be done using the First-Order-Second-Moment method as it is the basis of the load and resistance factors in CSA S16-09 (CSA, 2009). For this calibration, the chosen seismic-load-resisting system is the EBF.

Chapter 2 presented a detailed literature review on EBFs. Equations of statics and kinematics of EBFs were presented. The relation between frame geometry, link rotation and strain hardening was discussed. Links were classified, based on their length, as short, intermediate or long. Short links dissipate energy by shear yielding of the web and long links dissipate energy at flexural plastic hinges at the link ends. Designers have preferred well-stiffened short links in practice since they dissipate more energy than long links. The code provisions for overstrength in EBF links in Canada, USA and New Zealand were compared and found to be similar. Overstrength factors specified in the CSA, AISC and

NZ codes are not functions of the normalized link length even though the overstrength clearly depends on this factor.

Chapter 3 presented the details of EBF tests conducted since the early 1980s. Link overstrength is due to two factors: (a) strain hardening and (b) higher-than-nominal yield strengths. Both factors were quantified by regression analysis of the available data. The overstrength due to strain hardening, R_{str}, was found to be strongly correlated to the normalized link length, $e/(M_p/V_p)$, rotation capacity at peak shear, γ_{ult} and the ratio of the ultimate tensile strength to the yield strength, F_u/F_y. This equation was termed the "generic equation". However as γ_{ult} is not typically known a priori by the designer, a Proposed Design Equation for strain hardening was determined using the plastic link rotation, γ_p, as one of the modeling parameters. In the current study, γ_p is defined as the maximum plastic rotation sustained for at least one full cycle of loading prior to failure. The overstrength factor, R_{str} was found to be strongly correlated to $e/(M_p/V_p)$, F_u/F_y , γ_p and the stiffener spacing ratio, a/a_o.

The overstrength due to higher-than-nominal yield strengths, R_y, was also quantified by analysis of 13,500 steel coupon test results collected by Schmidt (2000). The data were classified according to the local buckling class. The model for Class 1 (Plastic design) data was adopted because links in EBFs are permitted only to be Class-1 W-shapes. The overstrength, R_y, is found to be strongly correlated to the location of the test coupon, i.e. flange or web coupon. Coupons obtained from the web are on an average 4.46% stronger than coupons obtained from the flange.

Chapter 4 presented the reliability indices for EBF compression braces proportioned using Capacity-Based Design. Reliability indices were derived using the First-Order-

Second-Moment (FOSM) Method and plotted against: normalized link length, $e/(M_p/V_p)$; peak link rotation, γ_p; ultimate link rotation, γ_{ult}; stiffener spacing, a/a_o; and the ratio of the ultimate tensile strength to the yield strength, F_u/F_y. Statistical parameters for demand were determined based on the regression analyses presented in Chapter 3. Two sets of statistical parameters for resistance were computed: (1) when the brace is designed using the CSA S16-09 procedure (CSA, 2009); (2) when the brace is designed using the Proposed Design Equation. The coefficients of variation are identical for these two cases but the mean value of the resistances differ. For resistances computed using the CSA S16-09 procedure, the reliability indices vary greatly for realistic ranges of the normalized link length, $e/(M_p/V_p)$, and ultimate link rotation, γ_{ult}. They are independent of the ratio of ultimate tensile strength to the yield strength of steel, F_u/F_y.

The Proposed Design Equation for computing link overstrength was presented. It depends on four primary variables, the normalized link length, $e/(M_p/V_p)$, plastic link rotation, γ_p, stiffener spacing, a/a_o and the ratio of ultimate tensile strength to the yield strength, i.e. F_u/F_y. The residual analysis shows no trends between the errors and the parameters involved in the proposed overstrength equation, thus validating the Proposed Design Equation.

5.2 CONCLUSIONS

The conclusions of the present investigation are as follows:

1) The current code criteria, CSA S16-09, for overstrength in links are unconservative for short links and over-conservative for long links. The reliability indices for resistance factor $\phi = 0.90$ lie in the range of 1.3 to 2.2 for short links and range from 3.8 to values

above 5.0 for long links. The reliability indices, β, varied greatly when plotted against realistic ranges of the key parameters, especially the normalized link length, $e/(M_p/V_p)$, and the ultimate link rotation, γ_{ult}. The reliability indices were low compared to target reliability indices, especially for short links which are most common in practice.

2) Using the Proposed Design Equation, with ϕ = 0.90, reliability indices are more uniform and lie in the range of 1.9 to 2.9, which is lower than the target value of 3.0. For ϕ = 0.75, the reliability indices lie above the target β value of 3.0. The computed reliability indices are more uniform but vary approximately linearly with variations of $e/(M_p/V_p)$, F_u/F_y, stiffener spacing, a/a_o, and plastic link rotation, γ_p.

3) The Proposed Design Equation should be used with $\phi = 0.75$ to replace the CSA S16-09 overstrength criteria. Reducing the reduction factor increases the target reliability indices to the range 3.2 - 3.7.

4) The proposed reduced resistance factor implies that much stronger compression braces need to be designed in EBFs, requiring, heavier shapes and thereby leading to an increased cost of steel EBFs.

5.3 FUTURE RESEARCH

The following future research is suggested:

a) The link data analyzed in this study are pre-2003. The revised loading protocol (RLP) proposed by Richards and Uang (2006) must be considered in future studies as it

will increase the inelastic rotation capacity of links. The existing loading protocol is severe and understates the link rotation capacity, especially in short links. Using the RLP, in certain cases, short links have exhibited 10%-40% greater link rotation capacity than expected by the CSA–S16-09 (CSA, 2009) though such an increase has not been observed for intermediate and long links. However, the link overstrength values observed using the RLP lie in the same range as those obtained using the existing loading protocol. It is anticipated that the new loading protocol will be adopted in the future. Hence, further tests on all types of links (short, long and intermediate) using the new loading protocol are warranted. Once more test results are available, a review of the proposed overstrength models would be beneficial before finalizing the calibration of the resistance factor.

b) Reliability indices for columns and connections in eccentrically braced frames must be examined because the current study focused only on compression braces connected to links. Data on link-to-column connections and link-to-beam connections are now available. For example, several experimental studies have been done (e.g. Okazaki, 2006) to verify the suitability of link-to-column connections in EBFs. Also AISC 341-05 (AISC, 2005) states that until further research is available, it may be advantageous to avoid link-to-column connections. Hence, reliability analysis of columns in an EBF is necessary.

REFERENCES

American Institute of Steel Construction (AISC) (2005): "AISC Seismic Provisions for Structural Steel Buildings", ANSI/AISC 341-05, American Institute of Steel Construction, Chicago, Illinois, 309 pp.

Arce, G., Okazaki, T. and Engelhardt, M.D. (2003): "Experimental behaviour of shear and flexural yielding links of ASTM 992 steel", STESSA 2003: proceedings of the Conference on Behaviour of Steel Structures, pp. 107-114.

ASTM Standard A992/A992M-11 (2011): "Standard Specification for Structural Steel Shapes" ASTM International, West Conshohocken, PA, DOI: 10.1520/A0992_A0992M-11, www.astm.org.

Barecchia, E, Corte, D.G. and Mazzolani F.M. (2006): "Plastic over-strength of short and intermediate links" Fifth International Conference on the Behaviour of Steel Structures in Seismic Areas (STESSA), Yokohoma, Japan.

Bartlett, F.M. (2007): Proposal to SSEF- CISC, "Resistance Factors for Components Proportioned using Capacity Design".

Bartlett, F.M., Hong, H.P. and Zhou, W. (2003): "Load Factor Calibration for NBCC 2004: Statistics of Loads and Load Effects", Canadian Journal of Civil Engineering, Vol. 30, No.2, pp. 429-439.

Becker, R. and Ishler, M., (1996): "Seismic Design Practice for Eccentrically Braced Frames", Steel TIPS, Structural steel Education Council, USA.

Bjorhovde, R. (2005): "Realistic Performance Requirements for Steel in Structures", Advances in Structural Engineering, Vol. 8, No.3, pp. 203-215.

Byfield, M.P., Davies, J.M. and Dhanalakshmi, M.(2005): "Calculation of the strain hardening behaviour of steel structures based on mill tests", Journal of Constructional Steel Research, Vol. 61, pp. 133–150.

Chao, S.H. and Goel, S. C. (2006): "Performance-Based Design of Eccentrically Braced Frames Using Target Drift and Yield Mechanism", Engineering Journal, 3rd Quarter, pp. 173-200.

Charleson, A. (2008): "Seismic Design for Architects", Architectural Press, Elsevier, Hungary, 296 pp.

Canadian Standards Association (CSA) (1981): "Guidelines for Development of Limit States Design (CSA S408-81)", Canadian Standards Association, Toronto, Ontario.

Canadian Standards Association (CSA) (2009): "Design of Steel Structures (CSA S16-09)", Canadian Standards Association, Toronto, Ontario.

Canadian Standards Association (CSA) (2004): "General requirements for Rolled or Welded Structural Quality Steel/ Structural Quality Steel (CSA G40.21-04)", Canadian Standards Association, Toronto, Ontario.

Dexter, R. J., Graeser, M., Saari, W.K., Pascoe, C., Gardiner, C.A. and Galambos, T.V. (2000): "Structural Shape Material Property Survey. Technical Report for Structural Shape Producers Council", University of Minnesota, Minneapolis.

El Damatty, A. (2006): Lecture Notes on Design of Structures for Lateral loads, Department of Civil and Environmental Engineering, University of Western Ontario, London, Canada.

Engelhardt, M.D. (2006): Memorandum to Tom Schafly, AISC, presenting Recommendations of AISC TC9/CPRP Ad Hoc Committee on Capacity Design Factors.

Engelhardt, M.D. and Popov, E.P. (1986): "Long Links in Eccentrically Braced Frames: A Preliminary Assessment", CE 299 Report, Department of Civil Engineering, University of California Berkeley, Berkeley, CA.

Engelhardt, M.D. and Popov, E.P. (1987): "Advances in Design of Eccentrically Braced Frames", Earthquake Spectra, Vol. 3, pp. 43-55.

Engelhardt, M.D. and Popov, E.P. (1989): "Behaviour of Long links in Eccentrically Braced Frames", Report No. UCB/EERC-89/01, Earthquake Engineering Research Center, University of California at Berkeley, Richmond, CA.

Engelhardt, M.D. and Popov, E.P. (1992): "Experimental performance of Long Links in Eccentrically Braced Frames", Journal of Structural Engineering, Vol.118, pp. 3067-3088

Engelhardt, M.D., Tsai, K.C. and Popov, E.P. (1992): "Stability of beams in Eccentrically Braced Frames," Chapter in: Stability and Ductility of Steel Structures under Cyclic Loading, Y.Fukumoto and G.C.Lee, Editors. CRC Press, pp. 99-112

Ghobarah, A. and Ramadan, T. (1994): "Bolted link-column joints in eccentrically braced frames", Engineering Structures, Vol.16, pp. 33-41.

Han, X.M. (1998): "Design and Behaviour of Eccentrically Braced Frames in Moderate Seismic Zones" M.Sc. thesis, Department of Civil Engineering and Applied Mechanics, McGill University, 113 pp.

Hjelmstad, K.D. and Popov, E.P. (1983): "Cyclic Behavior and Design of Link Beams", Journal of Structural Engineering, ASCE, Vol.109, No.10, pp. 2387-2403.

Hjelmstad, K.D. and Popov, E.P. (1984): "Characteristics of Eccentrically Braced Frames", Journal of Structural Engineering, Vol. 110. No.2, pp. 340-353.

Itani, A.M., Lanaud, C. and Dusicka, P. (2003): "Analytical Evaluation of Built-up Shear Links under Large Deformations", Computers and Structures, Vol. 81, pp. 681-696.

Jain, A.K , Koboevic, S. and Redwood, R. (1996): "Design and Behavior of Eccentrically Braced Frame with flexural links", Conference Proceedings of Advances in Steel Structures (ICASS-96), Vol.1, pp. 233-238.

Kasai, K. and Popov, E.P. (1986a): "Cyclic Web Buckling Control for Shear link Beams", Journal of Structural Engineering, ASCE, Vol. 112, No.3, pp. 505-523.

Kasai, K. and Popov, E.P. (1986b): "General Behavior of WF Steel Shear Link Beams", Journal of Structural Engineering, Vol. 112, No.3, pp. 362-382.

Kennedy, D.J.L. and Gad Aly, M. (1980): "Limit States Design of Steel Structures-Performance Factors", Canadian Journal of Civil Engineering, Vol. 7, pp. 45-77.

Krawlinker, H. (1978): "Shear in beam-column joints in seismic design of steel frames", AISC Engineering Journal, Vol. 15, No.3, pp. 82-91.

Leslie, S.R., MacRae, G.A., Staiger, M.P, Hyland, C. and Clifton, G.C. (2009): "Overstrength Factors for Seismic Design of Steel Structures", New Zealand Society for Earthquake Engineering, Annual NZSEE Technical Conference.

Madsen, H.O., Krenk, S. and Lind, N.C. (1986): "Methods of Structural Safety", Prentice-Hall Inc., Englewood Cliffs, N.J, USA.

Makridakis, S., Wheelwright, S.C. and Hyndman, R.J. (1998): "Forecasting: Methods and Applications", John Wiley and Sons, New York, USA, 642 pp.

The MathWorks Inc. (2010): MATLAB version 7.1, Natick, Massachusetts.

Montgomery, Peck and Vining (2006): "Introduction to Linear Regression Analysis", Wiley-Interscience, Hoboken, NJ, USA.

Malley, J.O., Popov, E.P. (1984): "Shear Links in Eccentrically Braced Frames" Journal of Structural Engineering, ASCE, Vol. 110, No.9, pp. 2275-2295.

National Research Council (NRC) (2010): "National Building Code of Canada (NBCC) 2010", Ottawa, Canada.

Okazaki T. and Engelhardt M.D. (2005): "Experimental Study of Local Buckling, Overstrength, and Fracture of Links in Eccentrically Braced Frames", Journal of Structural Engineering, Vol. 131, No.10, pp. 1526-1535.

Okazaki T., Engelhardt, M.D., Nakashima, M. and Suita, K. (2006): "Experimental performance of link-to-column connections in Eccentrically Braced Frames", Journal of Structural Engineering, Vol. 132, No.8, pp. 1201-1211.

Okazaki T. and Engelhardt M.D. (2007): "Cyclic Loading Behavior of EBF links constructed of ASTM A992 steel", Journal of Constructional Steel Research, Vol. 63, No.6, pp. 751-765.

Okazaki T., Engelhardt, M.D., Drolios, A., Schell, E., Hong, J.K. and Uang, C.M. (2009): "Experimental investigation of link-to-column connections in Eccentrically Braced Frames", Journal of Constructional Steel Research, Vol. 65, No.7, pp. 1401-1412.

Popov, E.P. (1980): "An Update on Eccentric Seismic Bracing"; Journal of American Institute of Steel Construction, Third Quarter, 1980.

Popov, E.P., Kasai, K. and Engelhardt, M.D. (1987): "Advances in Design of Eccentrically Braced Frames" Earthquake Spectra, Vol. 3, No.1, pp. 43-55.

Piluso, V. (2009): "Plastic Design of Eccentrically Braced Frames, II: Failure Mode Control", Journal of Constructional Steel Research, Vol. 65, pp. 1015-1028.

Ricles, J. and Popov, E. P. (1987): "Dynamic Analysis of Seismically Resistant EBFs", Report No. UCB/EERC-87/07, Earthquake Engineering Research Center, Berkeley, CA.

Richards, P.W. (2004): "Cyclic stability and Capacity Design of Steel Eccentrically Braced Frames", PhD Dissertation, University of California, San Diego, CA.

Richards, P.W. and Uang, C.M. (2005): "Effect of flange width-thickness ratio on Eccentrically Braced Frames link cyclic rotation capacity", Journal of Structural Engineering, Vol. 131, No. 10, pp. 1546-1552.

Richards, P.W. and Uang, C.M. (2006): "Testing Protocol for short links in Eccentrically Braced Frames", Journal of Structural Engineering, Vol. 132, No. 8, pp. 1183-1191.

Richards, P.W., Okazaki, T., Engelhardt, M. and Uang, C.M. (2007): "Impact of Recent Research Findings on Eccentrically Braced Frame Design", Engineering Journal, Vol. 44, No. 1, pp. 41-53.

Roeder, C.W. and Popov, E.P. (1977): "Inelastic Behaviour of Eccentrically Braced Frames under Cyclic Loading", Report No. EERC-77/18, Earthquake Engineering Research Center, University of California, Berkeley, USA.

SAC (2000b): "Recommended Seismic Evaluation and Upgrade Criteria for Existing Welded Steel Moment-Frame Buildings", prepared by the SAC Joint Venture for the Federal Emergency Management Agency, Report No. FEMA-351, Washington D.C.

Schmidt, B.J. (2000): "Review of the Resistance Factor for Steel", M.E.Sc Thesis, University of Western Ontario, London.

Schmidt, B.J. and Bartlett, F.M. (2002a): "Review of Resistance Factor for Steel: Data Collection", Canadian Journal of Civil Engineering, Vol. 29, No.1, pp. 98-108.

Schmidt, B.J. and Bartlett, F.M. (2002b): "Review of Resistance Factor for Steel: Resistance Distributions and Resistance Factor Calibration", Canadian Journal of Civil Engineering, Vol. 29, No.1, pp. 109-118.

Wangsdinata, W. (1999): "Capacity Design: A Concept to Ensure Seismic Resistance of Building Structures", First National Conference on Earthquake Engineering, Institut Teknologi Bandung, Indonesia.

APPENDICES

APPENDIX A-1:

AISC LINK TEST DATA

No.	Overstrength (AISC)	Normalized Link Length ($e/M_p/V_p$)	F_u/F_y	Peak Link Rotation γ_{ult}	Plastic Link Rotation γ_p	Stiffener spacing ratio, a/a_o
1	1.08	1.26	1.38	0.014	0.064	17.36
2	1.28	1.26	1.38	0.032	0.064	14
3	1.47	1.26	1.38	0.071	0.071	9.33
4	1.65	1.26	1.38	0.086	0.11	7
5	1.37	1.26	1.38	0.05	0.067	11
6	1.52	1.26	1.38	0.064	0.08	11.2
7	1.58	1.59	1.38	0.06	0.08	9.33
8	1.35	1.41	1.33	0.036	0.064	17.6
9	1.37	1.62	1.31	0.036	0.064	12
10	1.08	1.86	1.43	0.022	0.05	15.34
11	1.05	2.06	1.38	0.022	0.05	17.31
12	1.3	2.75	1.33	0.036	0.061	11.9
13	1.18	1.87	1.33	0.036	0.05	12
14	1.23	2.06	1.34	0.033	0.061	12
15	1.39	2.77	1.55	0.047	0.047	11.9
16	1.48	1.25	1.57	0.022	0.05	36
17	1.2	1.48	1.36	0.036	0.064	12
18	1.34	1.25	1.52	0.022	0.061	36
19	1.24	1.48	1.52	0.036	0.092	12
20	1.24	1.48	1.52	0.05	0.075	12
21	1.24	1.48	1.36	0.05	0.064	12
22	1.24	1.48	1.36	0.05	0.064	12
23	1.24	1.48	1.36	0.078	0.19	12
24	1.18	1.48	1.38	0.036	0.078	12
25	1.37	1.48	1.38	0.064	0.078	9
26	1.39	1.48	1.38	0.064	0.064	7.2
27	1.27	1.48	1.38	0.036	0.036	9
28	1.5	1.41	1.43	0.019	0.19	3.63
29	1.33	1.41	1.43	0.079	0.079	3.63
30	1.33	1.7	1.46	0.063	0.063	3.63
31	1.28	1.7	1.46	0.077	0.077	3.5
32	1.24	1.7	1.38	0.051	0.051	3.5
33	1.39	1.12	1.38	0.078	0.078	3.83
34	1.35	1.5	1.38	0.085	0.085	6.33

APPENDIX A-1:

AISC LINK TEST DATA (CONTD...)

No.	Overstrength (AISC)	Normalized Link Length ($e/M_p/V_p$)	F_u/F_y	Peak Link Rotation γ_{ult}	Plastic Link Rotation γ_p	Stiffener spacing ratio, a/a_o
35	1.37	1.5	1.38	0.085	0.085	3.17
36	1.26	1.5	1.38	0.085	0.085	6.33
37	1.26	1.5	1.38	0.085	0.085	6.33
38	1.42	1.5	1.38	0.085	0.085	6.33
39	1.39	1.5	1.38	0.085	0.085	6.33
40	1.28	1.5	1.38	0.085	0.085	6.33
41	1.26	1.5	1.38	0.085	0.085	6.33
42	1.16	2.36	1.33	0.04	0.06	5.6
43	1.06	2.36	1.31	0.0125	0.0125	7
44	1.3	2.36	1.43	0.035	0.035	8.25
45	1.27	2.3	1.38	0.034	0.034	11.89
46	1.15	3.71	1.33	0.014	0.014	11.73
47	1.2	3.7	1.33	0.0165	0.0335	11.73
48	0.97	2.45	1.34	0.0085	0.0175	8
49	1.28	2.37	1.55	0.0215	0.0215	7.75
50	1.43	1.34	1.57	0.04	0.04	6.67
51	1.1	1.77	1.36	0.031	0.031	5.25
52	1	1.81	1.52	0.015	0.015	6.88
53	1.13	1.76	1.52	0.0115	0.0115	6.69
54	1.32	1.76	1.52	0.0425	0.0425	6.69
55	1.21	1.77	1.36	0.079	0.079	5.75
56	1.24	2.31	1.36	0.057	0.071	6
57	1.26	3.69	1.36	0.03	0.039	6
58	1.38	1.05	1.38	0.079	0.079	5.75
59	1.31	1.67	1.38	0.066	0.066	6.125
60	1.2	2.19	1.38	0.045	0.07	9.625
61	1.27	3.33	1.38	0.025	0.055	12
62	1.44	1.38	1.43	0.075	0.075	5.25
63	1.19	1.82	1.43	0.047	0.06	8
64	1.41	1.26	1.46	0.071	0.071	12
65	1.33	1.65	1.46	0.064	0.064	12

APPENDIX A-2:

DATA USED TO MODEL STRAIN HARDENING

No.	Overstrength (CSA)	Normalized Link Length $(e/M_p/V_p)$	F_u/F_y	Peak Link Rotation γ_{ult}	Plastic Link Rotation γ_p	Stiffener spacing ratio, a/a_o
1	1.107	1.26	1.67	0.014	0.064	17.36
2	1.312	1.26	1.67	0.032	0.064	14
3	1.507	1.26	1.67	0.071	0.071	9.33
4	1.691	1.26	1.67	0.086	0.11	7
5	1.404	1.26	1.67	0.05	0.067	11
6	1.558	1.26	1.67	0.064	0.08	11.2
7	1.650	1.59	1.67	0.06	0.08	9.33
8	1.362	1.41	1.71	0.036	0.064	17.6
9	1.404	1.62	1.67	0.036	0.064	12
10	1.122	1.86	1.39	0.022	0.05	15.34
11	1.063	2.06	1.54	0.022	0.05	17.31
12	0.962	2.75	1.50	0.036	0.061	11.9
13	1.226	1.87	1.39	0.036	0.05	12
14	1.245	2.06	1.54	0.033	0.061	12
15	1.029	2.77	1.50	0.047	0.047	11.9
16	1.489	1.25	1.52	0.022	0.05	36
17	1.233	1.48	1.33	0.036	0.064	12
18	1.374	1.25	1.52	0.022	0.061	36
19	1.275	1.48	1.33	0.036	0.092	12
20	1.275	1.48	1.33	0.05	0.075	12
21	1.275	1.48	1.33	0.05	0.064	12
22	1.275	1.48	1.33	0.05	0.064	12
23	1.275	1.48	1.33	0.078	0.19	12
24	1.213	1.48	1.33	0.036	0.078	12
25	1.408	1.48	1.33	0.064	0.078	9
26	1.429	1.48	1.33	0.064	0.064	7.2
27	1.305	1.48	1.33	0.036	0.036	9
28	1.561	1.41	1.35	0.019	0.19	3.63
29	1.384	1.41	1.35	0.079	0.079	3.63
30	1.384	1.7	1.35	0.063	0.063	3.63
31	1.332	1.7	1.35	0.077	0.077	3.5
32	1.291	1.7	1.35	0.051	0.051	3.5
33	1.447	1.12	1.35	0.078	0.078	3.83
34	1.387	1.5	1.38	0.085	0.085	6.33

APPENDIX A-2:

DATA USED TO MODEL STRAIN HARDENING (CONTD...)

No.	Overstrength (CSA)	Normalized Link Length $(e/M_p/V_p)$	F_u/F_y	Peak Link Rotation γ_{ult}	Plastic Link Rotation γ_p	Stiffener spacing ratio, a/a_o
35	1.408	1.5	1.38	0.085	0.085	3.17
36	1.295	1.5	1.38	0.085	0.085	6.33
37	1.295	1.5	1.38	0.085	0.085	6.33
38	1.459	1.5	1.38	0.085	0.085	6.33
39	1.428	1.5	1.38	0.085	0.085	6.33
40	1.315	1.5	1.38	0.085	0.085	6.33
41	1.295	1.5	1.38	0.085	0.085	6.33
42	1.026	2.36	1.33	0.04	0.06	5.6
43	0.941	2.36	1.31	0.0125	0.0125	7
44	1.144	2.36	1.43	0.035	0.035	8.25
45	1.151	2.3	1.38	0.034	0.034	11.89
46	0.640	3.71	1.33	0.014	0.014	11.73
47	0.675	3.7	1.33	0.0165	0.0335	11.73
48	0.826	2.45	1.34	0.0085	0.0175	8
49	1.120	2.37	1.55	0.0215	0.0215	7.75
50	1.491	1.34	1.57	0.04	0.04	6.67
51	1.145	1.77	1.36	0.031	0.031	5.25
52	1.018	1.81	1.52	0.015	0.015	6.88
53	1.150	1.76	1.52	0.0115	0.0115	6.69
54	1.343	1.76	1.52	0.0425	0.0425	6.69
55	1.224	1.77	1.36	0.079	0.079	5.75
56	1.089	2.31	1.36	0.057	0.071	6
57	0.686	3.69	1.36	0.03	0.039	6
58	1.369	1.05	1.38	0.079	0.079	5.75
59	1.300	1.67	1.38	0.066	0.066	6.125
60	1.091	2.19	1.38	0.045	0.07	9.625
61	0.761	3.33	1.38	0.025	0.055	12
62	1.478	1.38	1.43	0.075	0.075	5.25
63	1.222	1.82	1.43	0.047	0.06	8
64	1.313	1.26	1.46	0.071	0.071	12
65	1.238	1.65	1.46	0.064	0.064	12

APPENDIX A-3:

GEOMETRICAL DATA OF THE TEST SPECIMENS

No.	Link Section	Test Name	Section depth, d	Web width, w	Flange thickness t_f	Flange width b	Link length e	Stiffener spacing a
1	W 18X 40	1	17.88	0.314	0.521	5.985	28	17.36
2	W 18X 40	2	17.88	0.314	0.521	5.985	28	14
3	W 18X 40	3	17.88	0.314	0.521	5.985	28	9.33
4	W 18X 40	4	17.88	0.314	0.521	5.985	28	7
5	W 18X 40	5	17.88	0.314	0.521	5.985	28	11
6	W 18X 40	6	17.88	0.314	0.521	5.985	28	11.2
7	W 18X 35	7	17.69	0.324	0.378	6	28	9.33
8	W 18X 60	8	18.28	0.422	0.681	7.555	36	17.6
9	W 18X 40	9	17.88	0.314	0.521	6.015	36	12
10	W 16 x 26	10	15.7	0.263	0.356	5.5	36	15.34
11	W 18 X 40	11	17.69	0.324	0.378	5.906	36	17.31
12	W 12 X 22	12	12.31	0.266	0.415	4.03	36	11.9
13	W 16X 26	13	15.7	0.263	0.356	5.484	36	12
14	W 18X 35	14	17.69	0.324	0.378	5.906	36	12
15	W 12X 22	15	12.31	0.266	0.415	4	36	11.9
16	W 18X 60	16	18.24	0.415	0.695	7.555	36	36
17	W 18 X 40	17	17.9	0.315	0.525	6.015	36	12
18	W 18X 60	18	17.9	0.415	0.695	7.555	36	36
19	W 18 X 40	20	17.9	0.315	0.525	6.015	36	12
20	W 18 X 40	21	17.9	0.315	0.525	6.015	36	12
21	W 18 X 40	22	17.9	0.315	0.525	6.015	36	12
22	W 18 X 40	23	17.9	0.315	0.525	6.015	36	12
23	W 18 X 40	24	17.9	0.315	0.525	6.015	36	12
24	W 18 X 40	25	17.9	0.315	0.525	6.015	36	12
25	W 18 X 40	26	17.9	0.315	0.525	6.015	36	9
26	W 18 X 40	27	17.9	0.315	0.525	6.015	36	7.2
27	W 18 X 40	28	17.9	0.315	0.525	6.015	36	9
28	W 8 X 10	1	7.97	0.17	0.208	3.94	14.5	3.63
29	W 8 X 10	3	7.97	0.17	0.208	3.94	14.5	3.63
30	W 8 X 10	4	7.97	0.17	0.208	3.94	14.5	3.63
31	W 8 X 10	5	7.97	0.17	0.208	3.94	17.5	3.5
32	W 8 X 10	6	7.97	0.17	0.208	3.94	17.5	3.5
33	W 8 X 10	7	7.97	0.17	0.208	3.94	11.5	3.83
34	W 12 X 19	A1	12.06	0.254	0.354	4.005	19	6.33
35	W 12 X 19	B1	12.06	0.254	0.354	4.005	19	3.17
36	W 12 X 19	C1	12.06	0.254	0.354	4.005	19	6.33
37	W 12 X 19	D1	12.06	0.254	0.354	4.005	19	6.33

APPENDIX A-3:

GEOMETRICAL DATA OF THE TEST SPECIMENS (CONTD...)

No.	Link Section	Test Name	Section depth, d	Web width, w	Flange thickness t_f	Flange width b	Link length e	Stiffener spacing a
38	W 12 X 19	A2	12.06	0.254	0.354	4.005	19	6.33
39	W 12 X 19	B2	12.06	0.254	0.354	4.005	19	6.33
40	W 12 X 19	C2	12.06	0.254	0.354	4.005	19	6.33
41	W 12 X 19	D2	12.06	0.254	0.354	4.005	19	6.33
42	W 12 X 16	1	11.99	0.22	0.265	3.99	28	5.6
43	W 12 X 16	2	11.99	0.22	0.265	3.99	28	7
44	W 12 X 22	3	11.99	0.26	0.425	4.03	33	8.25
45	W 12 X 22	4	11.99	0.26	0.425	4.03	33	11.89
46	W 12 X 16	5	11.99	0.22	0.265	3.99	44	11.73
47	W 12 X 16	6	11.99	0.22	0.265	3.99	44	11.73
48	W 12 X 16	7	11.99	0.22	0.265	3.99	29	8
49	W 12 X 22	8	11.99	0.26	0.425	4.03	36	7.75
50	W 12 X 22	9	11.99	0.26	0.425	4.03	20	6.67
51	W 12 X 16	10	11.99	0.22	0.265	3.99	21	5.25
52	W 12 X 22	11	12.31	0.26	0.425	4.03	27.5	6.88
53	W 12 X 22	11R1	12.31	0.26	0.425	4.03	26.75	6.69
54	W 12 X 22	11R2	12.31	0.26	0.425	4.03	26.75	6.69
55	W 10 X 19	1c	10.304	0.265	0.383	4.002	23	5.75
56	W 10 X 19	2	10.304	0.265	0.383	4.002	30	6
57	W 10 X 19	3	10.304	0.265	0.383	4.002	48	6
58	W 10 X 33	4c	9.744	0.319	0.437	8.045	23	5.75
59	W 10 X 33	5	9.744	0.319	0.437	8.045	36.6	6.125
60	W 10 X 33	6b	9.744	0.319	0.437	8.045	48	9.625
61	W 10 X 33	7	9.744	0.319	0.437	8.045	73	12
62	W 16 X 36	8	16.056	0.301	0.487	6.963	36.6	5.25
63	W 16 X 36	9	16.056	0.301	0.487	6.963	48	8
64	W 10 X 68	10	10.4	0.449	0.773	10.26	36.6	12
65	W 10 X 68	11	10.4	0.449	0.773	10.26	48	12

Note: Dimensions in imperial units (inches).

APPENDIX A-4: STIFFENER SPACING VERSUS LINK ROTATION

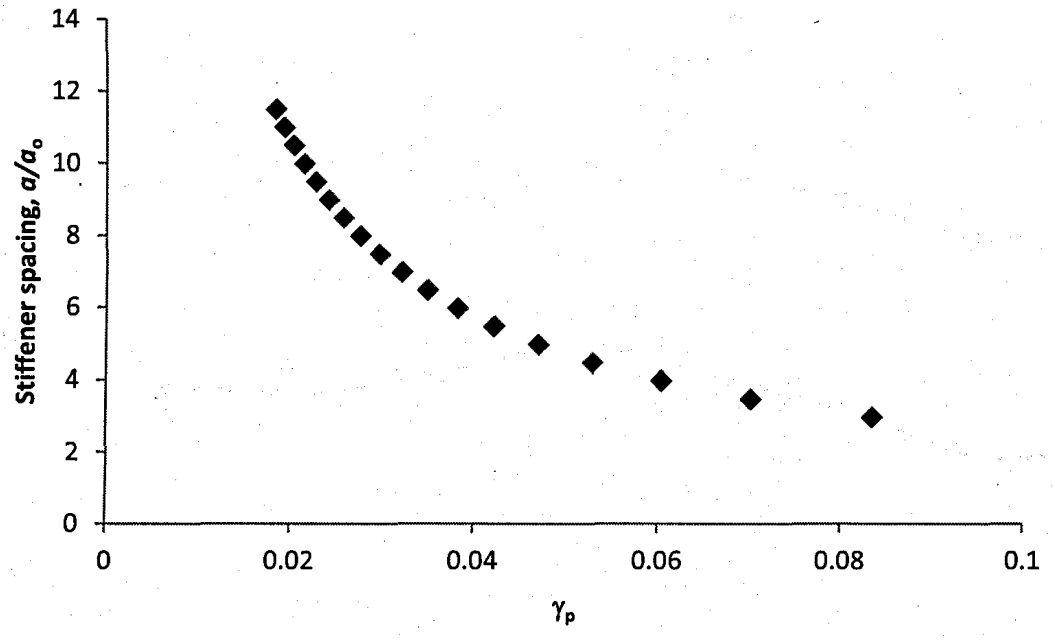

Fig A-1: Stiffener spacing versus plastic rotation (Itani's Equation at $d/w = 60$)

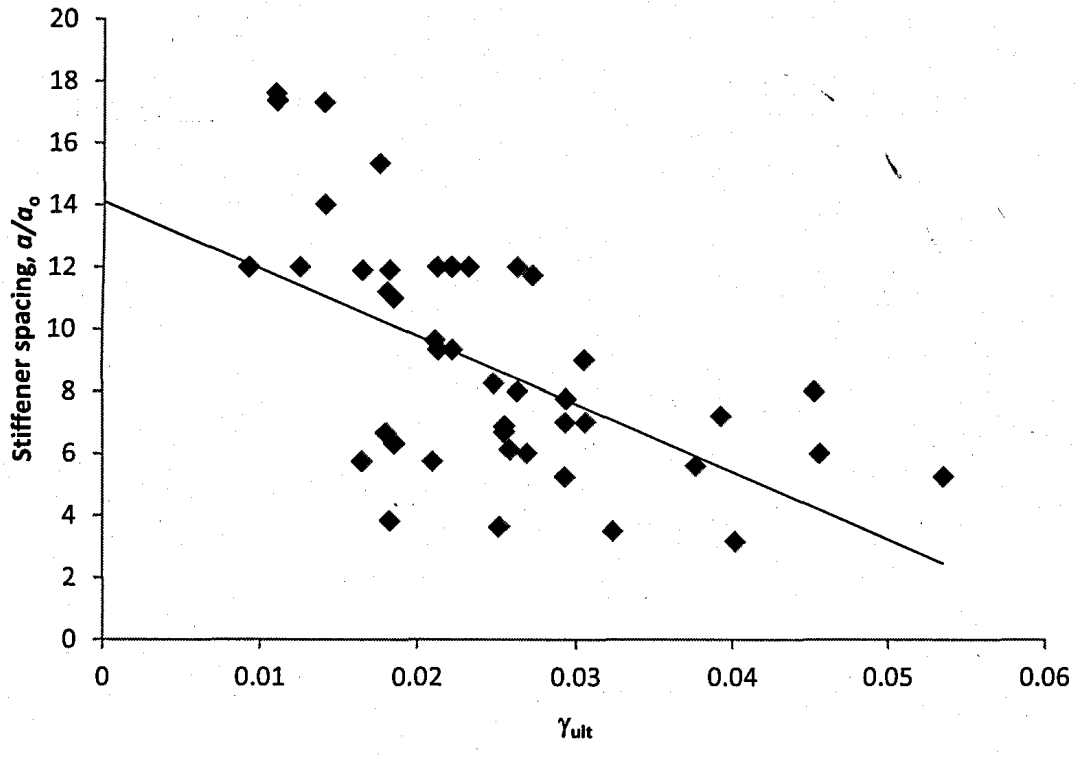

Fig A-2: Stiffener spacing versus peak link rotation (Experimental data)

APPENDIX A-5: RELIABILITY INDICES VERSUS λ

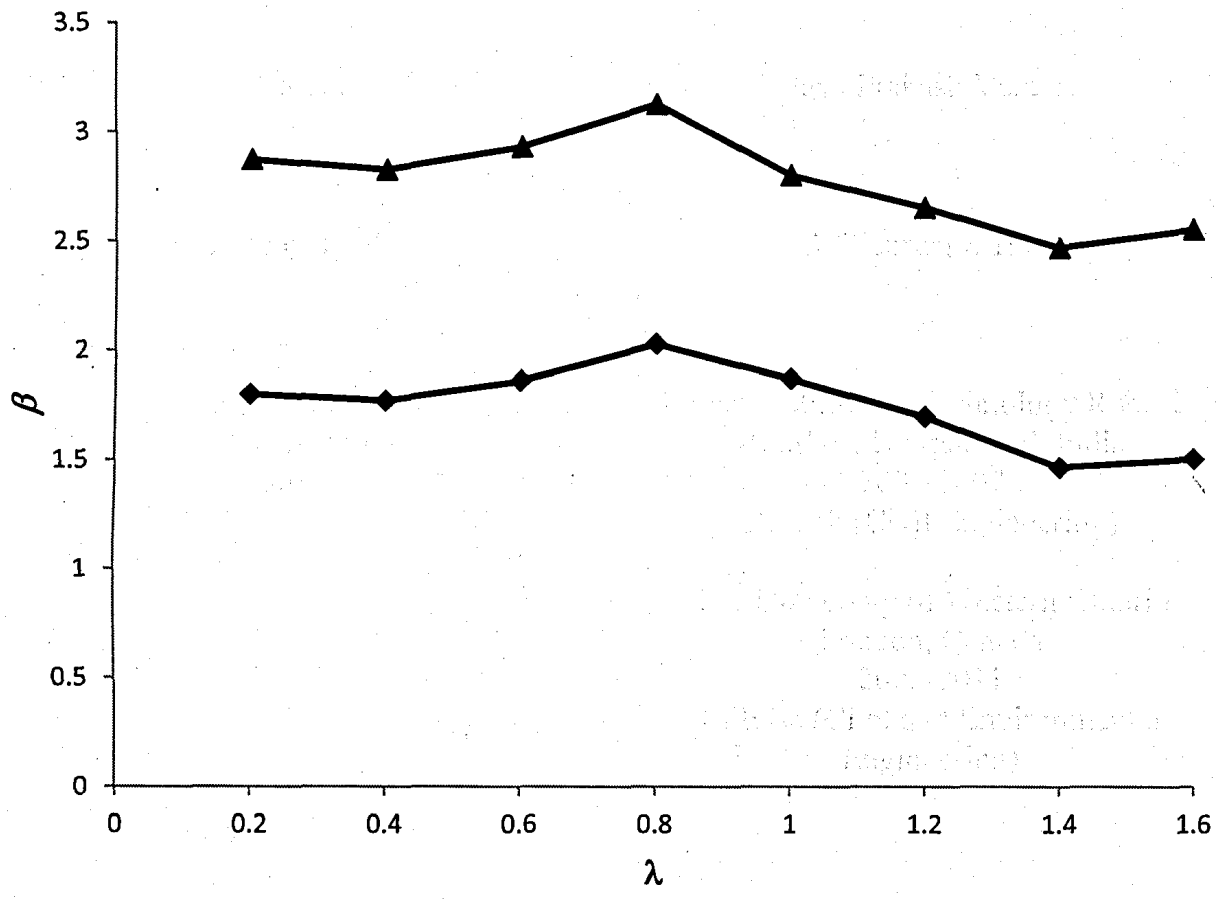

Fig A-3: Variation in reliability index with slenderness parameter λ